NUTRIENT-BASED STRATEGIES TO ENHANCE DOCOSAHEXAENOIC ACID (DHA) UTILIZATION IN THE PIGLET BRAIN

BY

REEBA MATHEW JACOB

THESIS

Submitted in partial fulfillment of the requirements
for the degree of Master of Science in Nutritional Sciences
in the Graduate College of the
University of Illinois at Urbana-Champaign, 2015

Urbana, Illinois

Master's Committee:

Professor Sharon M. Donovan, Chair
Assistant Professor Ryan N. Dilger, Advisor
Associate Professor Manabu T. Nakamura

ABSTRACT

Using the piglet as a model for the human infant, the goal of this study was to compare dietary lipid matrices found in infant formula and maternal milk on post-natal neurodevelopmental patterns. Over a 25-day feeding study, piglets (n=9-10 per treatment, 1.5 ± 0.2 kg initial BW) were either sow-reared (SR) with *ad libitum* intake, or artificially-reared (AR) receiving 1 of 3 milk replacers modified to mimic the nutritional profile and intake pattern of sow's milk. Our AR treatments included: T1, artificially-reared (AR) control formula; T2, T1 + 45% total dietary fat replaced with pre-digested fat (PDF); T3, T2 + 10% lecithin + 0.4% cholesterol. Sow-reared animals were used as a positive control for study outcomes. Piglets were weighed daily, serum samples were collected at d 0, d 14, and d 25 of study, and fecal samples were collected, and pooled from d 13-27. At 3 weeks of age, piglets were subjected to a standardized set of magnetic resonance imaging (MRI) procedures to identify macro- and micro-structural characteristics of the brain. At study conclusion, piglets were euthanized and tissues were collected for further analysis. For the duration of the study, SR piglets exhibited higher BW gain and heavier extracted whole brain weights compared with AR piglets. Analysis of fecal fat suggested greater ($P < 0.05$) excretion of dietary fat with addition of PDF along with lecithin and cholesterol. Serum lipid profiling at d 14 and d 25 of study revealed serum triglycerides (TAG) concentrations to be higher ($P = 0.176$, $P = 0.164$) in T3-fed piglets when compared with T1- and T2-fed piglets. Furthermore, serum cholesterol concentrations were higher ($P < 0.05$) in T3-fed piglets when compared with T1- and T2-fed piglets on d 25 of study. Furthermore, hippocampal tissue analysis revealed neutral lipid (NL) docosahexaenoic acid (DHA) concentrations were greater ($P < 0.05$) in T3-fed pigs compared with T1-fed and SR pigs. Hippocampal phospholipid (PL) DHA concentrations of T2- or T3-fed pigs were intermediate to T1-fed and SR piglets. Diffusion tensor imaging, a MRI sequence that characterizes brain

microstructure, revealed that SR piglets had greater ($P < 0.05$) average whole-brain fractional anisotropy (FA) values compared with AR piglets, suggesting differences in white matter organization. Although global analysis did not reveal differences within AR treatments for DTI outcomes, FA values of the internal capsule were not different between SR and T3-fed piglets, suggesting a modulatory effect of PDF + lecithin + cholesterol fat system on white matter maturation. Higher fecal fat excretion, partnered with higher serum TAG concentrations in T3-fed piglets as compared with other AR treatments, suggested higher bioavailability of the PDF when supplemented with lecithin and cholesterol. Elevated serum cholesterol at d 25 of study, partnered with elevated hippocampal DHA concentrations of T3-fed animals suggested higher bioavailability of the PDF, especially when supplemented with lecithin and cholesterol. Higher FA values in the internal capsule of T3-fed piglets indicate higher myelination of this early maturing white matter rich region as compared with other AR treatments, and may be impacted by elevated serum cholesterol concentrations. As the animal matures in age, the 2-fold elevation of hippocampal DHA seen in T3-fed piglets, as compared with control or SR animals, may produce similar elevations white matter maturation in the hippocampus as seen in the IC. Overall, our results indicate differential patterns of white matter development between AR and SR animals, and replacing part of formula TAG with PDF, and addition of lecithin and cholesterol, may elicit preferential accretion of brain DHA due to compositional manipulations of the dietary lipid matrix.

For my mom

ACKNOWLEDGEMENTS

First and foremost, I acknowledge my advisor, Dr. Ryan Dilger, for providing me with this opportunity to begin my career in the field of Nutritional Neuroscience. This experience, as well as your mentorship, has been invaluable to my growth as a researcher. I thank Dr. Sharon Donovan and Dr. Manabu Nakamura for serving on my M.S. committee, and for providing feedback on this thesis. I also thank our laboratory technician, Laura Bauer, and the staff at the Imported Swine Laboratory for their invaluable assistance.

I extend my sincere thanks to my colleagues in the Dilger Laboratory. Neither the completion of this thesis, nor the preservation of my sanity would have been possible without their collective guidance, well-timed shenanigans, and comradery. I thank my undergraduate mentee, Anna Ryan, for her dedication, work ethic, and for bearing with me as I became a more efficient teacher. I would like to extend a special thanks to Dr. Lindsey Alexander as an informal, yet irreplaceable mentor, and Austin Mudd for his contribution to the MRI component of this thesis. I would also like to acknowledge Caitlyn Getty, Ashley DeGroot, Samuel Rochell, Matthew Panasevich, and Stephen Fleming for their support at various points in my graduate career.

My absolute and unending gratitude is due to my parents for their love, support, and encouragement over the years. It has been through their example that I have learned the most valuable of life lessons: to pursue one's goals with diligence, to be resilient in the face of adversity, and to accept success with humility.

Finally, I am grateful for the deepest of friendships I have experienced as of yet. Although you remain unnamed here, words cannot fully convey your influence in shaping the person I am today.

TABLE OF CONTENTS

Page

Chapter 1: INTRODUCTION 1

Literature Cited 3

Chapter 2: LITERATURE REVIEW 4

Nutrient Composition of Breast Milk 4

Dietary Fat Metabolism in Human Infants 10

The Role of DHA in Neurodevelopment 12

Incorporation of Polyunsaturated Fatty Acids into Neural Tissue 16

Nutritional Influences on Gastrointestinal Development 19

Patterns of Brain Development of the Term Infant 21

Magnetic Resonance Imaging Techniques to Assess Brain Development 24

The Piglet as a Biomedical Model for the Human Infant 29

Summary and Thesis Objectives 31

Literature Cited 34

Figures 45

Chapter 3: IMPACT OF DIETARY LIPID MATRIX ON BRAIN MICRO-STRUCTURE OF THE NEONATAL PIG 48

Abstract 48

Introduction 49

Materials and Methods 51

Results 57

Discussion 59

Literature Cited 67

Tables 72

Figures 79

Chapter 4: COMPARISON OF BRAIN DEVELOPMENT IN SOW-REARED AND ARTIFICIALLY-REARED PIGLETS 81

Abstract 81

Introduction....82
Materials and Methods....84
Results....90
Discussion....93
Literature Cited....100
Tables....103
Figures....115
Chapter 5: SUMMARY AND SIGNIFICANCE 119
Literature Cited....124

Chapter 1

INTRODUCTION

Breast milk is considered the "gold standard" for infant nutrition with its unique nutrient macro and micronutrient composition. Although designed to meet the nutrient requirements of neonate, commercially available infant formulas are frequently reformulated as ongoing research elucidates a more complete characterization of maternal milk. One such area of research focuses on the variability between the dietary lipid matrix found in infant formula, and that of breast milk. There are notable differences in cholesterol and polyunsaturated fatty acid composition as well as structural incorporation of these factors within the dietary triacylglycerol and phospholipids in infant formula when compared with breast milk (1). Lipids constitute 50-60% dry weight of the mammalian brain, with n-3 and n-6 fatty acids accounting for 30-35% of total brain fatty acids (2). Accretion of docosahexaenoic acid (DHA), the most abundant n-3 fatty acid of the central nervous system, has been shown to be 2 fold higher in breast-fed infants when compared with formula-fed infants (3). Consumption of preformed DHA has been reported to be negatively correlated with neurodevelopmental disorders (4), improve structural and functional maturity of neurons (5), and enhanced cognitive abilities in early life (6). As DHA is a natural component of breast milk, a large body of epidemiological literature hypothesizes this n-3 fatty acid drives the differential neurodevelopmental trajectories observed in breast-fed and formula fed infants (1,7,8). Characterization of the role of DHA in infant neural maturation has gained momentum in the recent past, yet few studies have focused on the incorporation, metabolism and bioavailability of long chain polyunsaturated fatty acids in infant formula and maternal milk.

The broad goal of this thesis is to identify nutrient-related strategies to alter the lipid matrix found in infant formula to allow for greater incorporation of DHA in the brain. Due to

ethical concerns surrounding the use of human infants for such research, we employed the neonatal piglet that has previously been established in nutritional neuroscience research (9–11). Clinically relevant magnetic resonance imaging (MRI) techniques were used to assess macro and microstructural maturation of the brain, as well as hippocampal neurochemical concentrations in both formula-reared and sow reared piglets. Characterization of the neurodevelopmental patterns of the sow-reared piglet allowed for the establishment of a conspecific positive control for the artificially-reared piglet model, similar to the relationship of the breast-fed infant to the formula-fed infant. Finally, erythrocyte and hippocampal DHA concentrations, whole body growth performance, maturation of the intestinal epithelium, and circulating lipid profiles were assessed to further understand the impact of modifying the dietary lipid matrix on lipid metabolism of the neonate and incorporation of LCPUFA into neural tissue.

Literature Cited

1. Yum J. The effects of breast milk versus infant formulae on cognitive development. *J Dev Disabil*. 2007;13:525–35.

2. Youdim KA, Martin A, Joseph JA. Essential fatty acids and the brain: possible health implications. *Int J Dev Neurosci*. 2000;18:383–99.

3. Cunnane SC, Francescutti V, Brenna JT, Crawford MA. Breast-fed infants achieve a higher rate of brain and whole body docosahexaenoate accumulation than formula-fed infants not consuming dietary docosahexaenoate. *Lipids*. 2000;35:105–11.

4. Kidd PM. Omega-3 DHA and EPA for cognition, behavior, and mood: clinical findings and structural-functional synergies with cell membrane phospholipids. *Altern Med Rev*. 2007;12:207–27.

5. Luchtman DW, Song C. Cognitive enhancement by omega-3 fatty acids from child-hood to old age: findings from animal and clinical studies. *Neuropharmacology*. Elsevier Ltd; 2013;64:550–65.

6. Kuratko CN, Barrett EC, Nelson EB, Salem N. The relationship of docosahexaenoic acid (DHA) with learning and behavior in healthy children: a review. *Nutrients*. 2013;5:2777–810.

7. McCrory C, Murray A. The effect of breastfeeding on neuro-development in infancy. *Matern Child Health J*. 2013;17:1680–8.

8. Deoni SCL, Dean DC, Piryatinsky I, O'Muircheartaigh J, Waskiewicz N, Lehman K, Han M, Dirks H. Breastfeeding and early white matter development: A cross-sectional study. *Neuroimage*. Elsevier B.V.; 2013;82:77–86.

9. Radlowski EC, Conrad MS, Lezmi S, Dilger RN, Sutton B, Larsen R, Johnson RW. A neonatal piglet model for investigating brain and cognitive development in small for gestational age human infants. *PLoS One*. 2014; 9:e91951.

10. Rytych JL, Elmore MRP, Burton MD, Conrad MS, Donovan SM, Dilger RN, Johnson RW. Early life iron deficiency impairs spatial cognition in neonatal piglets. *J Nutr*. 2012;142:2050–60.

11. Odle J, Lin X, Jacobi SK, Kim SW, Stahl CH. The suckling piglet as an agrimedical model for thestudy of pediatric nutrition and metabolism. *Annu Rev Anim Biosci*. 2014;2:419–44.

Chapter 2

LITERATURE REVIEW

Nutrient Composition of Breast Milk

Breast milk as gold standard for human infant nutrition

Complete with a comprehensive macro- and micro-nutrient panel, and nonnutritive bioactive components, breast milk (BM) is often labeled the 'gold standard' for human infant nutrition. The World Health Organization recommends 6 months of exclusive breast feeding for infants, as it has long been associated with increased survival and optimal growth and development of the infant. Of particular significance are the large body of observational and cognitive studies have correlated exclusive or mixed breast feeding to the optimal development of the infant brain and increased intelligence quotients in adolescence and adulthood (1,2).

Nutritional quality of human BM is highly conserved across different populations with average macronutrient content of term milk approximating at 0.9-1.2 g/dL protein, 3.2-3.6 g/dL fat, and 6.7-7.8 g/dL lactose. Whey and casein primarily make up the protein fraction of BM, along with other components including α-lactalbumin, lactoferrin, secretory immunoglobulin A (IgA), and others. Lactose is the principal sugar present, but is complimented by oligosaccharides that possess a bioactive effect on the developing organism (3). Breast milk is also high in palmitic and oleic acids that are esterified to the sn-2 and sn-1 or 3 positions, respectively, of the glycerol backbone of dietary fat. In addition to the macronutrient components, BM also contains bioactive components and growth factors that aid in the development of multiple organ systems. Some examples of these include epidermal growth factor (EGF), brain derived neurotropic factor (BDNF), and glial cell derived neurotropic factors (GDNF), which aid in growth of the enteral nervous system, and multiple immunological factors

aiding in the transfer of immunity from mother to child (3). Overall, BM allows for the transfer of a plethora of compounds from the mother to child that are not currently present in artificial infant formula.

Lipid Fraction of Human Breast Milk

In recent years, the impact of BM lipids on the development of the neonatal brain has been heavily studied (1,4,5). Maternal milk fat not only provides up to 50% of the infant's caloric intake, but also serves as a building block for the complex and rapid development experienced during infancy (6). Triacylglycerols (TAG) provide approximately 98% of total fat, and is considered the major lipid fraction in BM. Cholesterol, hydrocarbons, sterol esters, diacylglycerols, monoacylglycerols, free fatty acids, sterols and phospholipids constitute the remaining subset of dietary fat found in human BM (7).

Breast milk TAG are unique not only in terms of the lipid composition, but also in the structural integration of n-3 and n-6 poly unsaturated fatty acids (PUFA) and their precursors. The short chain predecessors of these PUFA, α-linolenic acid (ALA; 18:3 *n*-3) and linoleic acid (LA; 18:2 *n*-6), are considered essential fatty acids (EFA), and must be obtained from dietary sources due to mammalian incapacity for endogenous synthesis (8,9). These fatty acids play a vital role in the maturation of the rapidly proliferating central nervous system of the infant. In adults, an intake of EFA at 3-6% of total dietary fat is recommended for normal biological function, with provisions of ALA at 0.5-1% of total fat intake also required for the integrity of neuronal and visual tissues (10). The most common dietary sources of ALA are green leaves, linseed, canola, flaxseed and walnut oils as well as fish such as herring, salmon and tuna. In addition to fatty fish, LA can be acquired from corn, sunflower and safflower oils, pork, walnuts, peanuts, and wheat products (11–13). The most biologically active metabolites of these essential

fatty acids are docosahexaenoic acid (DHA; 22:6 n-3), eicosapentaenoic acid (EPA; 20:5 n-3), and arachidonic acid (ARA; 20:4 n-6) (14). Alpha-linolenic acid and LA serve as precursors to their metabolites through the action of delta-6 desaturase, elongation, delta-5 desaturation and β-oxidation in the PUFA biosynthetic pathway (**Figure 2.1**).

Docosahexaenoic acid has been increasingly promoted as a long-chain (LC) PUFA essential to neural development in infancy. Incorporation of DHA in the infant diet has been associated with increased brain DHA accretion (15), improved development of myelinated white matter (16), visual acuity (17) and cognitive development (18). To assess the impact of DHA on visual and cognitive development, BM and RBC DHA was quantified, and segmented into high, middle and low categories. Of these infants, those possessing the lowest concentration of RBC phosphatidylethanolamine (PE) DHA at 60 days of age, were found to have lower visual acuity at 1 year when compared with subjects with high RBC PE DHA concentration. Language development at 9 and 18 months of age were also altered due to BM DHA status when environmental, maternal and infant variables known to effect development were taken into account (19). Moreover, DHA supplementation during both gestation and lactation elicited higher mental processing scores in children at 4 years of age as assessed by sequential processing, simultaneous processing, and non-verbal abilities (20). Considering the significant rate of brain development that occurs during the perinatal stages, insufficient intake of DHA may lead to alterations in neurogenesis and neurotransmitter metabolism, resulting in suboptimal cognitive performance in the developing infant (21). Feeding a DHA deficient diet during the perinatal period has been shown to be detrimental to cognitive development, including deficits in learning and memory paradigms including the Morris water maze and passive avoidance tasks in mice (22). These DHA-deprived mice were able to partially recover reference and working

memories when supplemented with DHA-rich fish oil. In contrast, control animals fed chow supplemented with DHA showed significant increases in both memory types (22). These data from human and animal research suggest DHA is a key dietary FA required to ensure proper development of the infant brain. In order to further understand the impact of DHA on infant brain development, it is essential to identify and assess the ideal concentration, and structural inclusion of DHA in dietary fat, whether it is provided in infant formula or BM.

Human BM concentrations of DHA correlate with maternal dietary intake of PUFA. Average DHA content of breast milk varies across countries and geographic regions, but North American, European and Australian populations average at DHA concentration of 0.2-0.3 g/100g total FA (14,23,24). Areas of the world, such as Japan, where consumption of seafood rich in DHA is high, BM DHA concentrations average at 1.0 g/100 g total FA (25). Daily average intake of DHA at 200 mg/d during lactation can allow for accretion of BM DHA at 0.30-0.35% of total milk fats (26). To meet these requirements, approximately one 3.5 oz. serving of fatty salmon or 10 non-fatty fish should be consumed on a weekly basis (27). Under circumstances in which breast feeding is not possible, the World Association of Perinatal Medicine recommends 0.2-5% of total fat provisions to be obtained from DHA (26).

Breast-fed infants experience whole body DHA accretion at approximately 10 mg/d in the first 6 months of life. Approximately half of this whole-body gain is represented within the brain at 5.0 mg/d during this time period. Once consumed, there is an estimated 50-60% obligatory loss of consumed DHA to carbon recycling to de novo synthesis of saturated and monounsaturated FA, cholesterol synthesis and oxidation (28). Considering the high amount of obligatory loss, 20 mg of DHA must be consumed daily to maintain accretion status seen with breast fed infants. Assuming average milk intake of 750 mL/d with DHA content at 0.2% of total

FA, breast fed infants consume 60 mg of DHA per day, which is well above the required 20 mg/d (28). Although endogenous synthesis of DHA from ALA is possible, the conversion rates are often lower than what is necessary to obtain DHA accretion similar to that of the breast-fed infant. Baboon infants provided with commercially available formula devoid of DHA, but supplemented with ALA and LA at a ratio of 1:10, experienced conversion rates of ALA to DHA at 9% of human infant requirements (29). In rats, conversion rates are slightly higher at 1.4% or 27% of human infant requirement. These data suggest supplementation of preformed DHA is a viable strategy to manipulate the fat matrix, and may allow for absorption of DHA to be similar to that of maternal milk.

The Impact of Structure and Composition of Dietary Fat Matrix on Absorption

Of the vast array of saturated fatty acids present in human BM, palmitic acid (16:0) composes 20-25% of milk fatty acids. The structural incorporation of palmitic acid into BM TAG is unique in structure and composition (12). Approximately 70% of palmitic acid found in milk TAG is esterified at the sn-2 position. A higher proportion of BM palmitic acid is absorbed compared with cow milk or infant formula which preferentially esterifies palmitic acid at sn-1and sn-3 positions (7,30). Palmitic acid positioned at the latter positions are hydrolyzed by pancreatic lipase, while sn-2 esterified FA remain as 2-monoacylglycerol. This pre-determined hydrolysis pattern dictates the importance of positional distribution of FA for the sake of bioavailability. Alterations of to these specific positional specificity of palmitic acid results in calcium soaps, which subsequently impedes both fat and calcium absorption in the infant gut (31). Palmitic acid has a melting point well above body temperature (63°C), and combines with calcium and other divalent cations at intestinal pH to generate soaps (30). Incorporation of sn-2 esterified palmitic acid in infant formula reduces stool concentration of palmitic acid and

increases stool softness compared with control formulas (30). These data suggest greater absorption of palmitic acid and lower calcium excretion as indicated by softer stool. Similarly, DHA and other LCPUFA are primarily esterified to sn-1 and sn-3 positions in BM (12), and is cleaved by pancreatic lipase to allow for optimal absorption. Overall, the combined activity of lipases and the positional specificity of FA esterification plays a critical role in fat digestion and absorption in infancy.

Although the role of DHA on infant development has obtained notoriety in the literature over recent years, few studies focus on identifying dietary strategies which allow for tissue incorporation of DHA at levels similar to that found in breast fed infants. Presently there are three sources of delivery of DHA in human foods including infant formula: triacylglycerols (TAGs), phospholipids (PL), or ethyl esters (32). These TAG sources of DHA are predominantly generated from microalgae, and PL source extracted from egg yolk. Although the absolute quantity of DHA accretion in tissue is higher with TAG, DHA accretion in the brain has been determined to be more efficacious, when provided in the PL (32). Although the percentage of fat absorption has been reported to be higher with the incorporation of PUFA with PL rather than TAG (33), other studies have shown no differences in DHA absorption between piglets fed DHA in TAG form compared with DHA supplemented as egg-yolk PL (34). Liu et al. found absolute gray matter and synaptosome DHA concentrations to be higher when provided in TAG form, but DHA accretion, as a % of dosage, to be significantly higher when provided as PL (32). Considering this conflicting evidence, it is essential that the role of dietary PL in DHA absorption is characterized to enable to allow for optimal incorporation of DHA in the developing brain.

Dietary Fat Metabolism in Human Infants

Hydrolysis of Dietary Fat

Absorption and post-processing of dietary lipids can be summarized in four steps which include hydrolysis, absorption, intracellular processing, and export of dietary fat into lymphatic circulation. Hydrolysis of milk triglycerides is a highly efficient process carried out through the sequential actions of gastric lipase, colipase-dependent pancreatic lipase (pancreatic lipase), bile salt-dependent lipase (BSDL, i.e., carboxyl esterase lipase), and bile salt-stimulated lipase (BSSL) (35–37). Preferential action of gastric lipase on the sn-3 position of dietary TAG primarily initiates the hydrolysis of dietary fat. The high level of stereo specificity found in human BM dictates that major milk unsaturated fats including oleic acid (18:1 n-9) and linoleic acid (18:2 n-6) are esterified at these outer 1 and 3 positions, generating 1,2-diacylglycerol and 3-monoglyceride (12,38,39). Mediated by pancreatic lipase, hydrolysis of TAG continues in the duodenum to further hydrolyze 1,2-diacylglycerol into 2-monoacylglycerol (2-MAG) and 2 free fatty acids (FFA) (31,40).

Though pancreatic lipase levels are low in infancy in comparison to a fully developed digestive system, the BM-fed infant is able to efficiently metabolize high concentrations of dietary fat (41). This considerable difference in hydrolysis capacity is reinforced through the activity of BSDL derivative, BSSL, that is also present in BM. Bile salts secreted by the liver and dispensed by the gall bladder acts as an emulsifier for the lipid components entering the small intestine, allows for larger surface area for lipase activity and mediates micelle formation to transport monoacylglycerols and FA into the enterocyte.

Absorption and Post Processing

Protein-independent and protein-dependent diffusion models have been proposed as mechanisms of transport of LCFA across the apical membrane of the enterocyte (42). Due to its lipophilic nature, FA are presumed to diffuse through the apical membrane, but multiple proteins of interest have been identified as long chain FA transporters across the plasma membrane of the enterocyte (42,43). First identified in mice, fatty acid translocase (FAT) and the human analog CD36, are known to be a highly expressed protein of interest for FA transport (44). The expression of FAT/CD36 is significant in tissues exposed to large concentrations of FA, and is up regulated in the presence of high dietary fat (45). Another apical membrane protein with high affinity for LCFA transport is fatty acid binding protein (FABP), which has been identified in the brush border membrane. Fatty acid uptake can be inhibited with the use of FABP binding antibodies in mice, thus revealing its role in LCFA absorption into the enterocyte (Stremmel, Lotz, Strohmeyer, & Berk, 1985). The fatty acid transport protein 4 (FATP4) is predominantly expressed in the mammalian gut and has been hypothesized to be responsible for the intracellular trapping of FA by esterification with coenzyme A (CoA) (48,49). Although the mechanism behind FA absorption into the enterocyte is not fully characterized, it is likely that passive diffusion and active transport jointly moderate the high level of fat absorption that occurs in the intestine.

Re-esterification and Transport

Re-esterification of TAG post-absorption into the enterocyte occurs through 2 major pathways, the glycerol-3-phosphate (G-3-P) and 2-MAG pathways, and one minor pathway, the dihydroxyacetone phosphate pathway (**Figure 2.2)**. Sequential acetylation of G-3-P to sn-1, 2 diacylglycerol via the activity of G-3-P acyltransferase and the acylation of sn-2 MAG via the

acyl-CoA:monoacylglycerol acyltransferase (MGAT) activity generates diacylglycerol (DAG). Diacylglycerol is then converted to TAG by acyl CoA:diacylglycerol acyltransferases (12). Of the three pathways that are present, the 2-MAG pathway serves as the primary route of re-synthesis and accounts for 70-80% of TAG regeneration (50).

Following re-esterification, dietary lipids are incorporated into chylomicrons and secreted into the mesenteric lymphatic system. Chylomicrons, being the largest and least dense of the lipoprotein family [less than 0.95g/ml, 100-500 nm in diameter], are composed of a hydrophilic phospholipid monolayer, with a hydrophobic core containing cholesterol esters and TAG (51). Formation of chylomicrons occurs in a two-step process. First, apolipoprotein B48, phospholipids, apolipoprotein A-IV, cholesterol and TAG combine to generate a high density particle called the primordial chylomicron. In the second step, this primordial chylomicron combines with a TAG and cholesterol ester mass (that does not feature Apo B48) to form the pre-chylomicron, which is subsequently transported to the cis-Golgi. During the first step of lipoprotein biogenesis, microsomal triglyceride transfer protein (MTP), possessing lipid transfer activity, adds newly synthesized TAG to the Apo B48 and primordial chylomicron complex (42). Subsequent to addition of Apo A-IV and stabilization of the phospholipid and cholesterol monolayer, prechylomicrons are then exported from the endoplasmic reticulum to the cis-Golgi via prechylomicron transport vesicles (52). The complex is further modified in the golgi, and ultimately undergoes exocytosis into the lymphatic system and is transported to the liver via the thoracic duct and subclavian vein (31).

The Role of DHA in Neurodevelopment

The modulatory effects of DHA on a variety of physiological and disease states have been thoroughly investigated (53–57). Although the molecular basis of these effects have not

been fully characterized, DHA has been shown to play a significant role in eicosanoid production, formation of peroxidation products, conformation and activity of enzymes, transcription of proteins and plasma membrane integrity (58). Of particular interest is the incorporation of DHA in the rapidly proliferating neuronal membrane of the infant cerebrum, and its unique ability to impact structure-induced functions of neurons and resulting alternations in the neuronal integrity and learning potential of developing infants.

Of the many physical properties of membranes affected by PUFA status, the most fundamental impact may be on membrane fluidity, or disorder and rates of molecular reorientation experienced by the plasma membrane. Naturally-occurring DHA-rich membranes, such as neuronal tissue and the outer segment of retinal photoreceptors, are reported to be highly fluid, which begs the question of whether a diet-induced increase in membrane fluidity is possible. Consumption of DHA deficient diets has been shown to cause substantial decreases in DHA incorporation and membrane fluidity (59). Although dietary supplementation of DHA has revealed increased membrane fluidity in animal models consuming fish oil diets high in DHA, others have not been able to reproduce such results (58,60,61). However, increases in fluidity were observed in "modeled" membranes using steady-state fluorescence, with significant increases with the addition of the first double bond and further increases in fluidity up to the addition of four double bonds (62). More sensitive methods have revealed an increase in lateral fluidity, indicating that physiologically-relevant changes in membrane fluidity may be present in the whole animal due to dietary incorporation of DHA. These changes may be more subtle, yet still relevant, in the physiological membrane.

Structure Impacting Function: n-3 PUFA and Modulation of Learning and Memory

Compositional differences in neuronal membranes due to DHA status may not only impact structural components, but also alter functional aspects of the neuron, including signal conduction and transmission and neurochemistry. Diet-induced changes in lipid composition of neuronal membranes can compromise the propagation of electrical signals, and also inhibit chemical signaling between neurons due to depletion of vesicle-stored neurotransmitters. Changes to plasma membrane integrity alters neuronal responses to acetylcholine, a neurochemical responsible for arousal, attention, and learning and memory. Impaired attention and learning behavior have been reported in chronically n-3 PUFA-deficient rodents during shock avoidance tasks, olfactory learning and exploratory behavior. In these animals, hippocampal release of acetylcholine was 34% lower than in control animals, however basal levels of acetylcholine in the hippocampus remained high when compared with control animals (63). Elevated basal levels present in deficient animals have been hypothesized to be a result of the compositional difference in glycerophospholipid incorporation of DHA and a resulting depletion of vesicle-stored neurotransmitters (63).

Dopaminergic neurotransmission, often associated with motivation and attention, have also shown to be altered in n-3 PUFA deficiency. Rats fed an n-3 PUFA-supplemented diet possessed 40% higher levels of dopamine in brain tissues, accompanied by a significant decrease in monoamine oxidase activity in the frontal cortex compared with animals fed a control diet (64). In the case of n-3 PUFA deficiency, endogenous release of vesicle-stored dopamine decreased upon stimulation. Behavioral parameters were also negatively impacted, as evidenced by increased interaction of deficient animals with the environment (65). The authors hypothesized that the low vesicular pool of dopamine reduced the impact of positive reward and

provided greater disruption of learning (66,67). Overall, diet-induced changes in DHA concentration of neuronal membranes can results in structural, functional and behavioral outcomes that can negatively impact learning potential of the organism.

The role of n-3 PUFA in maintaining integrity and function of the plasma membrane is evident, but the impact of these alterations on potential for learning is of high importance in the human infant. Polyunsaturated FA deficiency of the n-3 variety has been shown to impair hippocampal-dependent learning, which includes encoding of spatial information and spatial task memory (68). Although molecular mechanisms behind the impact of DHA deficiency on learning behavior are not fully understood, the role of structural components on learning behavior are evident as the structural content of the hippocampal neuron directly correlates to arborization of hippocampal neurons (11).

Dietary supplementation of DHA has an impact on long-term potentiation (LTP) and long-term depression, which are two forms of synaptic plasticity involved in learning and memory. Depolarization of the post-synaptic membrane, and the subsequent release of neurotransmitters into the synaptic cleft, allows for LTP formation. Post-synaptic release of arachidonic acid *in vivo* following depolarization of the pre-synaptic membrane modifies neurotransmitter release from the pre-synaptic membrane and subsequently amplifies LTP (69). Not only is the intracellular release of DHA crucial for LTP formation, the presence of extracellular DHA *in vitro* has also been observed to block the induction of long-term depression in hippocampal CA1 neurons (70). *In vivo* studies have also shown a negative correlation, with decreased DHA level corresponding to increased total latency in the behavioral task, for mice subjected to diet-induced deficiency of DHA (71). Such evidence, in combination with the presence of smaller hippocampal neurons in DHA-deficient mice, indicates that a period of n-3

FA deficiency in early development may induce structural impairments to irreversibly impact learning behavior in animal models (72).

Although direct assessment of cognitive outcomes is difficult to ascertain in humans, direct measurement of the impact of DHA supplementation on brain activity through functional MRI protocols are available. They have revealed a dose-dependent increase in functional activity in the dorsolateral prefrontal cortex and precentral gyrus during a continuous performance or attention task compared with placebo groups (73), suggesting a modulatory effect of DHA supplementation on functional cortical activity and attention. Prolonged supplementation of DHA along with long chain n-6 FA have been show to alleviate cognitive and behavioral problems in children diagnosed with dyslexia and attention deficit hyperactivity disorder (74). Collectively, these data suggest that DHA has the potential to impact learning at a fundamental level and ameliorate symptoms associated with neurological disorders impacting learning and behavior.

Incorporation of Polyunsaturated Fatty Acids into Neural Tissue

Lipid Components of the Neural Membrane

The lipid-rich neural membrane comes second only to adipose tissue in terms of its incorporation of a complex variety of lipid species. These molecules include neutral lipids, phospholipids, and other lipid fractions, in total representing approximately 50-60% of total brain mass. The neutral lipid fraction alone includes cholesterol, cholesterol esters, FFA, MAG, DAG, and TAG. The phospholipid subset includes glycerophospholipids, the most abundant of which include phosphatidylcholine (PCH); phosphatidylethanolamine (PE); phosphatidylserine (PS); and phosphatidylinositol (PINS), along with sphingomyelin, and phosphatidic acid. The remaining lipid fraction incorporates cardiolipins, cerebrosides and gangliosides (75). In

neuronal tissue, DHA is primarily incorporated in the synaptosomal glycerophospholipids of the plasma membrane, with the largest proportion being integrated into PS and PE (76–78). Docosahexaenoic acid, along with other LCPUFA, are found primarily esterified to the sn-2 chain of the glycerol backbone of glycerophospholipids, while the sn-1 position is often occupied by a saturated FA, such as palmitic or stearic acids. The positional distribution of these PUFA enable the neuron to maintain structural integrity, membrane fluidity, and thereby allow for optimal function of receptors, membrane bound proteins and ion channels.

Turnover and Biosynthesis of DHA in Neural Tissue

Polyunsaturated FA, including DHA, are critical structural components of neuronal and glial cell membranes. Primarily esterified to the phospholipids of neuronal tissue, DHA experiences rapid diurnal turnover (79). Despite rapid regeneration, a predominant fraction of DHA is recycled back into phospholipids with the aid of a variety of enzymes including multiple isoforms of phospholipase A2. The cerebral endothelium and astrocytes interact to generate DHA from precursors including eicosapentaenoic acid, docosapentaenoic acid and ALA, and release the converted compounds to the extracellular medium. Incapable of *in vivo* synthesis, neuronal cells rely on the cohesive action of endothelial cells and astrocytes to generate and dispense DHA into the extracellular medium, from where it is ultimately obtained by neurons (13). Uptake of precursors or pre-formed DHA from circulation is regulated by the neuronal endothelium, also known as the blood brain barrier (BBB).

Model for Transport of FA in to Neurons

Multiple models of fatty acid transport across the selectively-permeable BBB have been outlined in the literature (80,81). Circulating FA are generally found in the following forms: unesterified, esterified to PL, cholesterol, and TAG components of lipoproteins, or covalently

bound to erythrocytes and platelets. Fatty acids with 22 carbons or less are primarily (~99%) bound to albumin, while FA of longer chain lengths are preferentially bound to lipoproteins (79). The role of albumin-mediated transport of DHA into the brain is generally agreed upon, yet the question of whether simple diffusion or protein-mediated transport regulates the entry of FA into the endothelium remains a topic of debate (81,82). Although a small amount of lipoprotein hydrolysis occurs in the capillaries, uptake of whole lipoproteins into the brain does not occur, therefore lipolysis and generation of unbound FA is the first step in lipid absorption in the brain (83). Considering approximately 5% of albumin-bound FA is "stripped" in a single passage, a unifying model of transmembrane movement of FA incorporation into the brain is often proposed (80,84). Diffusion and protein-mediated transport is combined in this model, with FA binding to the luminal surface of the endothelial membrane and unionized forms of FA diffusing across the endothelial cytoplasm. Because BBB cells are narrow (~0.1 μm), the flip-flop process of diffusion repeats, thereby allowing FA diffusion across the transluminal membrane of the endothelium and into the brain. Selective esterification mediated by FATP traps the optimal variety of FA inside the neuron, and allows for further downstream processing (80). Other models of transmembrane movement of FA suggest that selective discrimination for preferred FA occurs directly within the endothelial cell. In this model, receptor-mediated absorption of whole lipoproteins are followed by intracellular lipolysis and protein-mediated transport of FA into the brain. Proposed transporter proteins include monocarboxylic acid transporters (MCT) and FATP to mediate the selective transluminal transport of FA into adjacent astrocytes (82). Due to possible regulation at multiple points, including lipoprotein hydrolysis and protein synthesis, the latter model is less consistent with the rapid incorporation of circulating FA. However, it does account for the high selectivity observed in FA incorporation into the brain.

Once absorbed into the brain, unesterified FA are converted into fatty acyl-CoA (FA-CoA) in order to retain these FA within the cell. Through the action of acyltransferases, FA are then predominantly incorporated into phospholipids, which are considered the most stable lipid fraction. A smaller portion are shuttled to an alternate pathway, and undergo β-oxidation to maintain energy requirements of the brain (**Figure 2.3**) (79). Approximately 65% of radiolabeled DHA is maintained in the phospholipid fraction with 37% being attached to the sn-2 position of PE (84), suggesting a greater role of n-3 PUFA in structural components of the brain, rather than in energy maintenance.

Nutritional Influences on Gastrointestinal Development

Structural Development of the Intestinal Epithelium

The intestinal epithelium is a critical interface between the gut lumen and intestinal tissue that regulates the absorption of dietary nutrients and macromolecules necessary to support rapid brain development in early life. Macro- and micronutrients, along with non-nutritive bioactive factors found in BM, are not only absorbed through the intestinal epithelium, but also facilitate further development of this organ system in preparation for weaning, immunological development and establishment of normal gastrointestinal (GI) function. The intestinal epithelium consists of finger-like villi and crypts from which enterocytes that line the villi originate. Varying forms of early-life nutrition can impact development of the structural components of the intestine. Infants who are predominantly breast-fed have smaller villi and crypts, but experience higher levels of crypt fission or division when compared to their formula-fed counterparts (85). Similar to the morphology observed in the intestinal epithelium of weaned subjects, hyperplasia of existing crypts are the principal mode of gut maturation seen with formula feeding (85). The crypt fission model of intestinal development is associated with

growth of the small intestine and may be responsible for laying the foundation for maximum generation of feeder crypts to be present before hyperplasia and further development begin.

Impact of Early Life Nutrition on Intestinal Structure and Function

A classic measure of intestinal maturity in neonates is the development of standard patterns of disaccharidase activity. Differences in extent of structural and functional aspects of gut maturity may profoundly impact absorption, transport and delivery of essential glucose and lipids to the brain, ultimately resulting in alterations in customary patterns of brain development. There are two primary classes of disaccharides which include β-glycosidase (i.e., lactase) and α-glucosidases (e.g., sucrase-isomaltase, maltase-glucoamylase, and trehalase) (86). In addition to the differences in structure, functional characteristics of intestinal development including disaccharidase activity are impacted by varying forms of infant nutrition. Evidence in alterations of functional growth can be seen in rat studies in which pups fed rat milk substitute exhibiting sucrase activity that were 20 to 45 times greater than dam-raised, control animals (87). In an effort to accurately compare the impact of experimental diets on brain maturation, the impact of both artificial formula and BM on disaccharidase activity must be assessed.

Dietary fats, yielding the greatest number of calories per unit mass, are a major energy source for the animal, but they are also an important component for establishing cell membrane integrity in the brain (88). Long chain PUFA, namely ARA and DHA, constitute nearly 30% of the total FA in grey matter of the developing brain, and serve as essential components of neuron myelination and neuron outgrowth (89,90). Considering importance of the lipid fraction in energy maintenance and physiological development, it is no surprise that upwards of 90% of total dietary fat is absorbed in a term infant (36). In neonatal piglets, supplementation of n-3 PUFA alters the mucosal architecture with a 38% decrease in intestinal villi length, bringing the

developing gut in line with morphology observed in organisms that are breast-fed (91). In addition, postnatal n-3 LCPUFA supplementation of DHA and EPA enhances the expression of GLUT-2 in the jejunum, allowing for greater glucose absorption (92). Such alterations in the architecture of the mucosal epithelium suggest the possibility of suboptimal whole-body and neural development as a result of consuming maternal milk substitutes not supplemented with n-3 FA. It also presents an opportunity for further research into nutrient-based strategies to alter the lipid matrix of infant formula, allowing for optimal absorption of these beneficial LCPUFA.

Patterns of Brain Development of the Term Infant

Establishment of the Central Nervous System

Neurodevelopment commences during gestation with the establishment of the neural tube, followed by emergence of the 3 primitive brain regions possessing functional specificity in the adult brain. The most rostral part of the neural tube evolves into the prosencephalon, which later develops in to the cortex, basal ganglia, limbic system, thalamus and hypothalamus, while the mesencephalon, or the mid brain, develops from the mid part of the neural tube. The most caudal region of the neural tube develops in to the rhombencephalon, or hindbrain, which contains the cerebellum, pons, and medulla of the adult brain (93). Following primary neurulation, further development of the central nervous system (CNS) continues with neuronal proliferation, migration, differentiation, synaptogenesis, organization, and myelination of axonal tracts (93,94). Although this developmental process is presented as a sequence of individual events, they actually overlap and extend into postnatal life. The latter period of postnatal neurodevelopment consist of dendrite development, lengthening of axons, elaboration of synaptic density and myelination (95). These critical neurodevelopmental events increase brain volume at a rapid rate in the days and months following birth, with overall brain volume

increasing to 64% of adult brain weight by 3 months of age (96). Considering the rapid rate and scope of these processes, infants are particularly vulnerable to nutritional insults during this sensitive period of early neurodevelopment.

Postnatal Neurodevelopment

Neuronal development in the months following birth consists of a diverse number of events including dendritic and axonal growth, synaptogenesis, differentiation and proliferation of glial cells, and subsequent myelination of axonal tracts. These events coincide with synaptic pruning and apoptosis, generating an interplay of progressive and regressive events that establish the neuronal network of the infant brain. Dendritic development accelerates in the last trimester of pregnancy and continues to be highly active up to the first year of postnatal life (97). In the first 6 months of life, axonal and dendrite length increases up to 10-fold (95) and dendritic arborization makes significant strides in laying the foundation for increases in synaptic density. Synaptic density increases at a variable rate depending on the functional hierarchy of needs of the infant. For example, the auditory and visual cortexes experience maximum synaptic density at approximately 3 months of age, while the prefrontal cortex reaches maximum density at 15 months of age (98,99). The expedited rate of development in the visual and auditory areas speak to the importance of establishing the ability to see and hear, while the delay in the prefrontal cortex indicates that higher level thinking and decision making processes are less important in these early stages of development. Synaptogenesis and pruning precedes myelination, which is considered one of the classic neurodevelopmental events of postnatal life.

The myelin sheath is composed of tightly packed plasma membrane of the glial subtype, namely oligodendrocytes in the CNS. It encloses axons to insulate electrical signals and to maximize their conduction velocity, and allows for saltatory conduction of action potentials. Of

the two forms of glial cells that originate from the neuroepithelial cells of the neural tube, the microglial subset gives way to the oligodendrocytes that form the myelin sheath and astrocytes that are hypothesized to aid in the transport of myelin progenitors to their destination (100). Myelination of the central nervous system begins at approximately 25 weeks *in utero* and proliferates at high intensity in the first 6 months of postnatal life, continuing well into adulthood (101). The mature oligodendrocyte, which generates the complex structure of myelin, wraps around axonal tracts. It encompasses myriad proteins, including myelin basic proteins (MBP), proteo-lipid proteins , myelin associated glycoproteins and lipids including cholesterol, phospholipids, galactocerebrosides, and others (102). The mechanisms that initiate or regulate myelination are still under investigation, but the process has revealed itself to be highly ordered (94). It begins with the generation of oligodendrocyte precursors from the neural tube and their subsequent migration to the areas undergoing white matter development (103). Upon reaching their destinations, pre-oligodendrocytes proliferate extensively in white matter, and mature in the myelination phenotype. Myelination in the brain follows a predictable caudorostral directionality, and follows 5 general rules in regard to the order of pathway development: 1) proximal before distal, 2) sensory before motor, 3) projection before associative, 4) central sites before cerebral poles, and 5) occipital poles before frontal and temporal poles (94). Mature myelin forms in the motor tracts by 3 months of postnatal life, in frontal lobes by 5-6 months, in the paracentral regions and occipital poles by 15 months, and in the temporal regions by 23 months of postnatal life (104). Due to the pervasive nature and rapid generation during early life, myelination represents an area of neurodevelopment that is highly vulnerable to nutritional insults (105).

Unlike most biological membranes, myelin is composed of predominantly lipids (70-85%) with a lower concentration of proteins (15-30%), resulting in a lipid-enriched membrane (106). Myelin is enriched in a variety of lipid moieties, the most prominent of which include cholesterol, phospholipids and galactolipids at a ratio ranging from 4:3:2 to 4:4:2 (106,107). Myelin is particularly enriched in cerebrosides (a type of galactolipid), which contain a ceramide core that is rich in LCPUFA of chain lengths greater than 20 carbons (108). Cerebrosides showed a significant increase in LCPUFA incorporation (3 mg/d) between 3 and 11 d of age, and a continued increase in LCPUFA incorporation through 6 months of age. In addition, PE is a significant component of myelin membranes, as this phospholipid increases 15-fold from infancy to adulthood (75). Considering these data, it is evident that incorporating of LCPUFA such as DHA in the infant diet is imperative in this period of rapid neurodevelopment and elevated vulnerability to nutrient deficiencies.

Magnetic Resonance Imaging Techniques to Assess Brain Development

Introduction

Magnetic resonance (MR) imaging (MRI) techniques allow for characterization of neurodevelopmental patterns and timelines *in vivo*. It permits the collection of quantifiable information on the macrostructure and microstructure, nutrient and neurotransmitter concentrations, and metabolism of the developing brain. Magnetic resonance imaging also allows for discrimination between white matter (WM), grey matter (GM), and cerebrospinal fluid (CSF), all of which serve as markers of neurodevelopment.

Magnetic Resonance Imaging

Magnetic resonance imaging relies on the magnetic properties of hydrogen atoms found in abundance in biological tissues. Protons of an atom possess a natural spin or precess, resulting

in an electrical current that in turn generates a magnetic field. The magnetic field generated by the precessing proton can be broken down in to x, y and z components with vectors representing the magnitude and direction of the magnetic field. When exposed to an external magnetic field, the intrinsic angular momentum of the nuclei will align in parallel and in anti-parallel with the external magnetic field. The parallel and antiparallel spins neutralize the field in the x and y components, but the magnetic field in the z direction sums in the direction of the external magnetic field to generate longitudinal magnetization (109). During excitation, the protons jump to a higher energy state, the longitudinal magnetization (z component) decreases, and transverse magnetization (x-y component) increases. During the relaxation phase, electromagnetic energy is retransmitted and is thus dubbed the nuclear MR signal. The time required for longitudinal magnetization to recover post-excitation is called longitudinal relaxation time, or T1, while the time required for transverse magnetization to disappear is referred to as transversal relaxation time, or T2 (109). The contrast mechanisms in MRI rely on the manipulations of T1 and T2 phases. An additional parameter manipulated for image quality is repetition time (TR) of the excitatory radio frequency (RF) pulses, and the echo time (TE), which refer to the time period between excitation and data acquisition (110). For images acquired in the T1 phase, manipulations of TR allow for a gradient in the intensity of the resulting image. For example, a short TR image with a short T1 is highly sensitive to fat and brain tissue vs. CSF, and is highly useful in clinical setting where tissue masses (such as a tumor) need to be visualized. T2-weighted images are manipulated by TE and allows for fluid such as CSF or edemas to be expressed at highest intensity. For our purposes, T1-weighted sequences are used to generate macrostructural datasets, while T2-weighted sequences are employed to image microstructural and neurochemical datasets.

Diffusion Tensor Imaging

Diffusion tensor imaging (DTI) is an MRI modality that characterizes the organization and structural integrity of the axonal tracts of the brain. It originates from diffusion weighted imaging (DWI), which assesses the rate of diffusion of water molecules in the axonal microenvironment (111). Diffusion properties associated with DWI rely on Brownian motion of water molecules characterized by randomized, isotropic movement of free water molecules (112). Due to the presence of cell and organ structures, molecular level diffusion in biological tissues does not experience the same arbitrary movement observed in room temperature water. Changes in tissue composition can impact the rate and directionality of water diffusion, ultimately providing contrasts in MR images that allows for quantitative assessment of development. For instance, with increasing myelination of neuronal tissue, the diffusion of water molecules are restrained down the length of the white matter tracts rather than across them (104). Diffusion tensor imaging measures this diffusion of water and its directionality with respect to the axonal tract, allowing for an indirect measure of the level of myelination present in a given voxel.

There are four quantitative measures used in DTI to assess free water diffusion in WM, and these measures collectively indicate the degree of WM development and myelination. Mean diffusivity (MD), axial diffusivity (AD), radial diffusivity (RD), and fractional anisotropy (FA) all provide distinct information regarding WM integrity, and these complementary measures are interdependent in accurately assessing brain development (111). Apparent diffusion is obtained from the calculated apparent diffusion coefficient (ADC) of free water molecules in the voxels, or 3-dimensional (3D) pixels, which comprise the MR image. In an ADC map, the intensity of each voxel reflects the level of resistance experienced by the free water, with higher ADC values

reflecting water movement down the organ structure and lower ADC values suggesting greater resistance due to a physical barriers (113). Mean diffusivity is an account of the averaged ADC from 6-30 orientations within axonal tracts, and represents a holistic picture of water diffusivity in the brain (111). Axial diffusivity and RD diffusion rates represent diffusion along and across a fiber orientation, respectively, as components of MD. Fractional anisotropy values quantify directionality of randomly moving water molecules in numerical values ranging from 0-1 (113,114). Values closer to 1 indicate anisotropic movement and greater insulation of free water molecules, and provides an indirect, yet sensitive, means of assessing WM development (115). Although these values are powerful tools individually, they are more often used jointly. When combined with high FA and AD values, lower ADC values are often associated with an increase in cell density, indicating dense axonal packing, large axonal diameter and high myelination; all which correlate with mature WM.

Magnetization-Prepared Rapid Gradient Echo

Magnetization-prepared rapid gradient echo (MPRAGE) is a T1-weighted, 3D sequence of the gradient echo imaging technique, and provides macrostructural and anatomical information of the developing brain. This sequence can generate greater contrast between WM, GM and CSF in the brain and other organ systems than preceding T1-weighted spin-echo sequences (116,117). Structural sequences take advantage of the differences in T1 and T2 relaxation periods of WM, GM and CSF to obtain variations in signal intensities which ultimately allows for the segmentation of these components. Generally, tissues with a rapid recovering T1 phase are depicted at higher intensity in structural datasets and slower recovering tissues having a lower intensity, and therefore possess a darker color. Typically, T1 relaxation times follow the following trend: fat > brain tissue, WM > GM, GM > CSF (**Figure 2.3**) (110).

Voxel-based morphometry (VBM) analysis of GM and WM volumes on a voxel-by-voxel basis are also obtained from the MPRAGE sequence. The potential for VBM data is immense as it can be tabulated or represented visually to outline GM and WM volume differences across the brain on a voxel-by-voxel basis, rather than pre-defined structural comparisons (118). In addition to VBM, region-specific volumes can be calculated from the MPRAGE sequence after warping individual datasets against a standardized atlas, and quantifying the variations due to treatment using an inverse warping sequence (119). Recent developments have allowed for the generation of a brain atlas that characterize the automated segmentation of MRI data sets for the emerging biomedical piglet model (119).

Magnetic Resonance Spectroscopy

Markers of structural integrity, metabolic efficiency and energy status can be assessed *in vivo* through magnetic resonance spectroscopy (MRS) (120). Unlike the MPRAGE sequence, which provides morphometric and anatomical information, MRS generates a representation of the chemical makeup of the developing brain (121). Magnetic resonance spectroscopy provides a frequency analysis, or a fourier transform, of the signal detected. The line spectra provides frequency of a given metabolite in parts per million (PPM) and the strength of the signal as indicated by the height of the peak (**Figure 2.4**) (122). Whole-brain or single-voxel spectroscopy (SVS) measures can be attained, but the latter is region-specific and suppresses the signal from outside areas. Suppression of the water peak is another practice used to obtain a more refined and clear depiction of the neurochemicals that are detected with MRS (122). Most commonly reported metabolites include N-acetylaspartate (NAA), myo-inositol (INS), choline-containing compounds [i.e., acetylcholine (ACH), free choline (CHO), glycerophosphocholine (GPC) and phosphochoine (PCH), phosphatidylcholine (PC)], glutamine (GLN), glutamate (GLU), and

creatine-containing compounds [i.e., creatine (CR) and phosphocreatine (PCR)]. The physiological roles of these metabolites are integral in normal function and development of the brain.

The Piglet as a Biomedical Model for the Human Infant

Introduction

Animal models serve as invaluable tools to assess the impact of nutrition on physiological development. Generally, rodents predominate in biomedical research, but small mammals, pigs, companion animals and non-human primates are also used. Physiological similarities to the human, ethical concerns and cost of upkeep are often evaluated when establishing the model for any type of research. In the field of nutritional neuroscience, evidence suggests the piglet may be the most appropriate species due to its status as a precocial "agrimedical" model, and due to its similarities in anatomy, physiology and metabolism as compared with the human (123,124). Parallels in neurodevelopmental patterns to the human infant, and the ability to be trained in behavioral tasks, allow for the neonatal piglet to be an appropriate model in assessing the impact of early-life nutrition on neurodevelopment.

The piglet has been used as a model for areas of nutritional research including LCPUFA metabolism, pre- and probiotic presence for intestinal health, and macro- and micronutrient deficiencies, all of which possess the potential to impact neurodevelopment and behavior (4,92,125,126). Considering the similarities between the pig and human, and its potential as a translational model for human nutrition, it is important to characterize the natural form of piglet nutrition, sow milk. Characterization of sow milk with respect to human BM and infant formula allows for alterations of human infant formula to fit the nutrient requirements of the pig, and subsequently permits for the assessment of dietary lipid metabolism on neurodevelopment. The

macronutrient composition of mature sow milk is higher when compared with human milk, with the exception of lactose (3,127). The energy content of sow milk is also higher, with sow milk providing 114 kcal/dL and human milk providing 68 kcal/dL. Lipid concentrations of sow milk are also higher at approximately 7.1 g/dL while human BM concentrations are approximately 3.5 g/dL (123). Despite this difference in quantity, approximately 50% of total energy is provided from the lipid fraction of milk in both species, with a majority (~70%) of the lipid fraction being represented as TAG. Considering this similarity in the percentage of energy derived from fat, and heavy incorporation of TAG in the lipid fraction, the piglet model has been used to study the impact of artificial nutrition. The safety of DHA supplementation in infant formulas, and establishment of DHA as an essential nutrient in physiological and neurodevelopment, was originally conducted using a pig model (34,128). Thus, although the nutrient composition of sow milk is different than human BM, artificial infant formulas can be altered to meet the caloric and nutritive requirements of the pig to directly assess lipid metabolism.

The human infant GI tract is highly mature at birth, while the rodent model experiences majority of GI development postnatally. The rate of GI development that occurs in piglets is intermediate to that of the rodent and the human, and is therefore a more appropriate model for studying human GI development. For species that have relatively mature GI function at birth, the changes occurring in the gut epithelium in perinatal life are important, where development associated with weaning may be most important in rodent species (129). This allows for the pig to be a more appropriate model than rodents for nutritional studies.

The Piglet as a Model for Nutritional Neuroscience

The piglet has been used sparingly as a biomedical model to assess the impact of early-life nutrition on cognitive development. Relative to the rodent model, piglets are highly

precocial, and can therefore be easily reared artificially, allowing for precise assessment of nutrient intake and body tissue accretion (123). The larger size of piglets allows for conventional means of assessing brain development including MRI, and easier sampling of tissues and blood to assess physiological development (124). Moreover, there are strong similarities between postnatal patterns of brain development between pigs and humans. The piglet and human infant have a comparable proportion of adult brain volume established at birth (20-25% of their ultimate weight). The rodent brain only achieves 12% of total brain weight at birth, while the non-human primate (rhesus monkey) is more mature with 75% brain development (130). In addition, structural and functional complexity of the cortical regions increases in perinatal life, and such comparisons from the gyrencephalic brain of the pig are more relevant to the human infant than with the lissencephalic rodent brain. Previous work has also correlated neurodevelopmental timelines in the human, in years of age, to the pig, in months of age, establishing the pig as an accelerated model for studying human brain development (131). Although similarities to the human infant in structural development are important, one of the primary strengths of the pig model is its ability to be trained in behavioral tasks. Examples of these tasks include the eight-arm radial maze and T-maze, which are designed to assess mechanisms of learning and memory (132). For example, the T-maze is designed to assess hippocampal-dependent spatial discrimination ability using visual cues and a food reward (126,133,134). Such behavioral tasks integrate functional learning and memory tasks with nutrition-induced variations in structural development of the infant brain.

Summary and Thesis Objectives

The neonatal brain undergoes a tremendous growth spurt during early post-natal life, characterized by a synchronized interplay of proliferative and regressive processes.

Neurodevelopment in the months following birth incorporate processes such as dendritic and axonal growth, synaptogenesis, differentiation and proliferation of glial cells, and myelination of axonal tracts (94). These neurodevelopmental milestones are particularly sensitive to nutritional insults (135), and can result in alterations from normative patterns of neuro and cognitive development (136). Docosahexaenoic acid is a nutrient of interest that has gained notoriety in recent years due to its abundance in neural membranes. Neural concentrations of this n-3 LCPUFA is susceptible to dietary manipulation (15). A large scale incorporation of this n-3 FA in neural tissue is observed during early post-natal life, and a growing body of work connects DHA to structural development of the infant brain and cognitive abilities in later life (89). Many of these studies have suggested greater incorporation of DHA in breast-fed infants compared with their formula-fed counterparts (4,137). However, characterization of the dietary fat matrix in BM is incomplete, and further research is necessary to identify nutrient-based strategies to allow for optimal metabolism and neural incorporation of DHA. Therefore, the goal of this thesis is to identify the impact of pre-digestion of dietary TAG, as well as incorporation of emulsifiers such as lecithin and cholesterol, on DHA metabolism, as well as structural and functional outcomes related to intestinal and brain development. Our goal is to identify whether these strategies affect the intestinal epithelium that serves as a gateway for FA absorption, as well as identify patterns of DHA circulation and brain development as assessed by MRI techniques.

The piglet has been increasingly used in characterizing the role of multiple nutrients including iron, cholesterol, and LCPUFA on brain development (126,138,139). The piglet is an excellent model to identify the impact of nutrient interventions, particularly that of lipids, on neurodevelopment due to similarities in the rate of brain development and similar patterns of lipid metabolism. In comparison with the rodent model, the piglet brain is more precocial,

allowing for nutrient intervention earlier in life, and offers a longer life-span to assess the impact of dietary intervention on brain development. The larger size of the piglet allows for the use of clinically-applicable tools such as MRI to assess brain development, and yields larger quantities of tissue for molecular analysis in comparison to the rodent model. Overall, the piglet is a highly translatable model that can provide high-quality and novel pre-clinical evidence regarding DHA metabolism and insight into how manipulation of the dietary fat matrix influences brain and intestinal development of the neonate.

Literature Cited

1. Mortensen EL, Michaelsen KF, Sanders SA, Reinisch JM. The association between duration of breastfeeding and adult intelligence. *Am Med Assoc*. 2014;287:2365–72.

2. Anderson JW, Johnstone BM, Remley DT. Breast-feeding and cognitive development: a meta-analysis. *Am J Clin Nutr*. 1999;70:525–35.

3. Ballard O, Morrow AL. Human milk composition: nutrients and bioactive factors. *Pediatr Clin North Am*. Elsevier Inc; 2013;60:49–74.

4. Deoni SCL, Dean DC, Piryatinsky I, O'Muircheartaigh J, Waskiewicz N, Lehman K, Han M, Dirks H. Breastfeeding and early white matter development: A cross-sectional study. *Neuroimage*. Elsevier B.V.; 2013;82:77–86.

5. Reynolds a. Breastfeeding and brain development. *Pediatr Clin North Am*. 2001;48:159–71.

6. Carlson SE. Early determinants of development: a lipid perspective. *Am J Clin Nutr*. 2009;89:1523S–9S.

7. Jensen RG, Hagerty MM, McMahon KE. Lipids of human milk and infant formulas: a review. *Am J Clin Nutr*. 1978;31:990–1016.

8. Bézard J, Blond JP, Bernard A, Clouet P. The metabolism and availability of essential fatty acids in animal and human tissues. *Reprod Nutr Dev*. 1994;34:539–68.

9. Innis SM. Dietary (n-3) fatty acids and brain development. *J Nutr*. 2007;137:855–9.

10. Bjerve K. Omega 3 fatty acid deficiency in man: implications for the requirement of alpha-linolenic acid and long-chain omega 3 fatty acids. *World Rev Nutr Diet*. 1991;133–42.

11. Heaton AE, Meldrum SJ, Foster JK, Prescott SL, Simmer K. Does docosahexaenoic acid supplementation in term infants enhance neurocognitive functioning in infancy? *Front Hum Neurosci*. 2013;7:1–12.

12. Innis SM. Dietary triacylglycerol structure and its role in infant nutrition. *Am Soc Nutr*. 2011;2:275–83.

13. Youdim KA, Martin A, Joseph JA. Essential fatty acids and the brain: possible health implications. *Int J Dev Neurosci*. 2000;18:383–99.

14. Innis SM. Human milk: maternal dietary lipids and infant development. *Proc Nutr Soc*. 2007;66:397–404.

15. Ouellet M, Emond V, Chen CT, Julien C, Bourasset F, Oddo S, LaFerla F, Bazinet RP, Calon F. Diffusion of docosahexaenoic and eicosapentaenoic acids through the blood-brain barrier: An in situ cerebral perfusion study. *Neurochem Int*. 2009;55:476–82.

16. Deoni SCL, Mercure E, Blasi A, Gasston D, Thomson A, Johnson M, Williams SCR, Murphy DGM. Mapping infant brain myelination with magnetic resonance imaging. *J Neurosci*. 2011;31:784–91.

17. Jensen CL, Voigt RG, Prager TC, Zou YL, Fraley JK, Rozelle JC, Turcich MR, Llorente AM, Anderson RE, Heird WC. Effects of maternal docosahexaenoic acid intake on visual function and neurodevelopment in breastfed term infants. *Am J Clin Nutr*. 2005;82:125–32.

18. Birch EE, Garfield S, Hoffman DR, Uauy R, Birch DG. A randomized controlled trial of early dietary supply of long-chain polyunsaturated fatty acids and mental development in term infants. *Dev Med Child Neurol*. 2000;42:174–81.

19. Innis SM, Gilley J, Werker J. Are human milk long-chain polyunsaturated fatty acids related to visual and neural development in breast-fed term infants? *J Pediatr*. 2001;139:532–8.

20. Helland IB, Smith L, Saarem K, Saugstad OD, Drevon CA. Maternal supplementation with very-long-chain n-3 fatty acids during pregnancy and lactation augments children's IQ at 4 years of age. *Pediatrics*. 2003;111:e39–e44.

21. Bazan NG. Cell survival matters: docosahexaenoic acid signaling, neuroprotection and photoreceptors. *Trends Neurosci*. 2006;29:263–71.

22. Chung W-L, Chen J-J, Su H-M. Fish oil supplementation of control and (n-3) fatty acid-deficient male rats enhances reference and working memory performance and increases brain regional docosahexaenoic acid levels. *J Nutr*. 2008;138:1165–71.

23. Sanders TAB, Reddy S. The influence of a vegetarian diet on the fatty acid composition of human milk and the essential fatty acid status of the infant. *J Pediatr*. 1992;120:S71–S77.

24. Innis S. The colostrum-deprived piglet as a model for study of infant lipid nutrition. *J Nutr*. 1993;123:386–90.

25. Yuhas R, Pramuk K, Lein EL. Human milk fatty acid composition from nine countries varies most in DHA. *Lipids*. 2006;41:851–8.

26. Koletzko B, Lien E, Agostoni C, Bohles H, Campoy C, Cetin I, Decsi T. The roles of long-chain polyunsaturated fatty acids in pregnancy, lactation and infancy: review of current knowledge and consensus recommendations. *J Perinat Med*. 2008;36:5–14.

27. Holub BJ. Omega-3 levels in fish: data quality, quantity, and future. 2009. p. 1–35.

28. Cunnane SC, Francescutti V, Brenna JT, Crawford MA. Breast-fed infants achieve a higher rate of brain and whole body docosahexaenoate accumulation than formula-fed infants not consuming dietary docosahexaenoate. *Lipids*. 2000;35:105–11.

29. Su H, Bernardo L, Mirmiran M, Ma X, Corso T, Nathanielsz P, Brenna J. Bioequivalence of dietary alpha linolenic and docosahexaenoic acids as sources of docosahexaenoate accretion in brain and associated organs of neonatal baboons. *Pediatr Res*. 1999;45:87–93.

30. Kennedy K, Fewtrell MS, Morley R, Abbott R, Quinlan PT, Wells JCK, Bindels JG, Lucas A. Double-blind, randomized trial of a synthetic triacylglycerol in formula-fed term infants: effects on stool biochemistry , stool biochemistry, stool characteristics, and bone mineralization. *Am J Clin Nutr*. 1999;70:920–7.

31. Mu H, Hoy CE. The digestion of dietary triacylglycerols. *Prog Lipid Res*. 2004;43:105–33.

32. Liu L, Bartke N, Van Daele H, Lawrence P, Qin X, Park HG, Kothapalli K, Windust A, Bindels J, et al. Higher efficacy of dietary DHA provided as a phospholipid than as a triglyceride for brain DHA accretion in neonatal piglets. *J Lipid Res*. 2014;55:531–9.

33. Carnielli VP, Verlato G, Pederzini F, Luijendijk I, Boerlage A, Pedrotti D, Sauer PJ. Intestinal absorption of long-chain polyunsaturated fatty acids in preterm infants fed breast milk or formula. *Am J Clin Nutr*. 1998;67:97–103.

34. Mathews S a, Oliver WT, Phillips OT, Odle J, Diersen-Schade D a, Harrell RJ. Comparison of triglycerides and phospholipids as supplemental sources of dietary long-chain polyunsaturated fatty acids in piglets. *J Nutr*. 2002;132:3081–9.

35. Hernell O, Bläckberg L. Human milk bile salt-stimulated lipase: functional and molecular aspects. *J Pediatr*. 1994;125:S56–61.

36. Abrahamse E, Minekus M, Aken GA, Heijning B, Knol J, Bartke N, Oozeer R, Beek EM, Ludwig T. Development of the digestive system-experimental challenges and approaches of infant lipid digestion. *Food Dig*. 2012;3:63–77.

37. Lindquist S, Hernell O. Lipid digestion and absorption in early life: an update. *Curr Opin Clin Nutr Metab Care*. 2010;13:314–20.

38. Hamosh M, Scow RO. Lingual lipase and its role in the digestion of dietary lipid. *J Clin Invest* [Internet]. 1973;52:88–95.

39. Hamosh M. Digestion in the newborn. *Clin Perinatol*. 1996;23:191–209.

40. Manson WG, Weaver LT. Fat digestion in the neonate. *Arch Dis Child Fetal Neonatal Ed*. 1997;76:F206–11.

41. Zoppi G, Andreotti G, Pajno-Ferrara F, Njai DM, Gaburro D. Exocrine pancreas function in premature and full term neonates. *Pediatr Res*. 1972;6:880–6.

42. Mansbach II CM, Gorelick F. Development and physiological regulation of intestinal lipid absorption . II . Dietary lipid absorption , complex lipid synthesis , and the intracellular packaging and secretion of chylomicrons. *Am J Physiol Gastrointest Liver Physiol*. 2007;293:G645–50.

43. Kamp F, Guo W, Souto R, Pilch PF, Corkey BE, Hamilton J a. Rapid flip-flop of oleic acid across the plasma membrane of adipocytes. *J Biol Chem*. 2003;278:7988–95.

44. Nassir F, Wilson B, Han X, Gross RW, Abumrad N a. CD36 is important for fatty acid and cholesterol uptake by the proximal but not distal intestine. *J Biol Chem*. 2007;282:19493–501.

45. Poirier H, Degrace P, Niot I, Bernard A, Besnard P. Localization and regulation of the putative membrane fatty-acid transporter (FAT) in the small intestine comparison with fatty acid-binding proteins (FABP). *Eur J Biochem*. 1996;238:368–73.

46. Chen M, Yang Y, Braunstein E, Georgeson KE, Harmon CM. Gut expression and regulation of FAT/CD36: possible role in fatty acid transport in rat enterocytes. *Am J Physiol Endocrinol Metab*. 2001;281:E916–23.

47. Stremmel W, Lotz G, Strohmeyer G, Berk PD. Identification, isolation, and partial characterization of a fatty acid binding protein from rat jejunal microvillous membranes. *J Clin Invest*. 1985;75:1068–76.

48. Stahl a, Hirsch DJ, Gimeno RE, Punreddy S, Ge P, Watson N, Patel S, Kotler M, Raimondi A, et al. Identification of the major intestinal fatty acid transport protein. *Mol Cell*. 1999;4:299–308.

49. Milger K, Herrmann T, Becker C, Gotthardt D, Zickwolf J, Ehehalt R, Watkins P a, Stremmel W, Füllekrug J. Cellular uptake of fatty acids driven by the ER-localized acyl-CoA synthetase FATP4. *J Cell Sci*. 2006;119:4678–88.

50. Phan CT, Tso P. Intestinal lipid absorption and transport. *Front Biosci* [Internet]. 2001;6:D299–319. Available from: http://www.researchgate.net/publication/12101620_Intestinal_lipid_absorption_and_transport

51. Cox N. Lehninger principles of biochemistry. 4th ed. New York, NY: W H Freeman and Company; 2005.

52. Black DD. Development and physiological regulation of intestinal lipid absorption. I. Development of intestinal lipid absorption: cellular events in chylomicron assembly and secretion. *Am J Physiol Gastrointest Liver Physiol*. 2007;293:G519–24.

53. Breslow JL. n-3 fatty acids and cardiovascular disease. *Am J Clin Nutr*. 2006;83:1477–82.

54. Turner N, Else PL, Hulbert a J. Docosahexaenoic acid (DHA) content of membranes determines molecular activity of the sodium pump: implications for disease states and metabolism. *Naturwissenschaften*. 2003;90:521–3.

55. Tomobe YI, Morizawa K, Tsuchida M, Hibino H, Nakano Y, Tanaka Y. Dietary docosahexaenoic acid suppresses inflammation and immunoresponses in contact hypersensitivity reaction in mice. *Lipids*. 2000;35:61–9.

56. Uauy R, Hoffman DR, Mena P, Llanos A, Birch EE. Term infant studies of DHA and ARA supplementation on neurodevelopment: results of randomized controlled trials. *J Pediatr*. 2003;143:S17–25.

57. Kidd PM. Omega-3 DHA and EPA for cognition, behavior, and mood: clinical findings and structural-functional synergies with cell membrane phospholipids. *Altern Med Rev*. 2007;12:207–27.

58. Stillwell W, Shaikh SR, Zerouga M, Siddiqui R, Wassall SR. Docosahexaenoic acid affects cell signaling by altering lipid rafts. *Reprod Nutr Dev*. 2005;45:559–79.

59. Daveloose D, Linard A, Arfi T, Viret J, Christon R. Simultaneous changes in lipid composition, fluidity and enzyme activity in piglet intestinal brush border membrane as affected by dietary polyunsaturated fatty acid deficiency. *Biochim Biophys Acta*. 1993;1166:229–37.

60. Kamada T, Yamashita T, Baba Y, Kai M, Setoyama S, Chuman Y, Otsuji S. Dietary sardine oil increases erythrocyte membrane fluidity in diabetic patients. *Diabetes*. 1986;35:604–11.

61. Treen M, Uauy R, Jameson D, Thomas V, Hoffman D. Effect of docosahexaenoic acid on membrane fluidity and function in intact cultured Y-79 retinoblastoma cells. *Arch Biochem Biophys*. 1992;294:564–70.

62. Salem N, Niebylski C. The nervous system has an absolute molecular species requirements for proper function. *Mol Membr Biol*. 1995;12:131–40.

63. Aïd S, Vancassel S, Poumès-Ballihaut C, Chalon S, Guesnet P, Lavialle M. Effect of a diet-induced n-3 PUFA depletion on cholinergic parameters in the rat hippocampus. *J Lipid Res*. 2003;44:1545–51.

64. Chalon S, Delion-Vancassel S, Belzung C, Guilloteau D, Leguisquet a M, Besnard JC, Durand G. Dietary fish oil affects monoaminergic neurotransmission and behavior in rats. *J Nutr*. 1998;128:2512–9.

65. Zimmer L, Hembert S, Durand G, Breton P, Guilloteau D, Besnard JC, Chalon S. Chronic n-3 polyunsaturated fatty acid diet-deficiency acts on dopamine metabolism in the rat frontal cortex: a microdialysis study. *Neurosci Lett*. 1998;240:177–81.

66. Zimmer L, Delion-Vancassel S, Durand G, Guilloteau D, Bodard S, Besnard JC, Chalon S. Modification of dopamine neurotransmission in the nucleus accumbens of rats deficient in n-3 polyunsaturated fatty acids. *J Lipid Res*. 2000;41:32–40.

67. Horrocks L a, Farooqui A a. Docosahexaenoic acid in the diet: its importance in maintenance and restoration of neural membrane function. *Prostaglandins Leukot Essent Fatty Acids*. 2004;70:361–72.

68. Yoshida S, Yasuda A, Kawazato H, Sakai K, Shimada T, Takeshita M, Yuasa S, Kobayashi T, Watanabe S, Okuyama H. Synaptic vesicle ultrastructural changes in the rat hippocampus induced by a combination of alpha-linolenate deficiency and a learning task. *J Neurochem*. 1997;68:1261–8.

69. McGahon BM, Martin DS, Horrobin DF, Lynch M a. Age-related changes in synaptic function: analysis of the effect of dietary supplementation with omega-3 fatty acids. *Neuroscience*. 1999;94:305–14.

70. Young C, Gean PW, Wu SP, Lin CH, Shen YZ. Cancellation of low-frequency stimulation-induced long-term depression by docosahexaenoic acid in the rat hippocampus. *Neurosci Lett*. 1998;247:198–200.

71. Moriguchi T, Salem N. Recovery of brain docosahexaenoate leads to recovery of spatial task performance. *J Neurochem*. 2003;87:297–309.

72. Ahmad A, Murthy M, Greiner R, Moriguchi T, Salem NJ. A decrease in cell size accompanies a loss of DHA in the rat hippocampus. *Nutr Neurosci*. 2002;5:103–13.

73. Mcnamara RK, Able J, Jandacek R, Rider T, Tso P, Eliassen JC, Alfieri D, Weber W, Jarvis K, et al. Docosahexaenoic acid supplementation increases prefrontal cortex activation during sustained attention in healthy boys : a placebo-controlled , dose-ranging , functional magnetic resonance imaging study. *Am J Clin Nutr*. 2010;91:1060–7.

74. Richardson A, Puri BK. A randomized double-blind, placebo-controlled study of the effects of supplementation with highly unsaturated fatty acids on ADHD-related symptoms in children with specific learning difficulties. *Prog Neuro-Psychopharmacology Biol Psychiatry*. 2002;26:233–9.

75. Odutuga AA, Carey EM, Prout RES. Changes in the lipid and fatty acid composition of developing rabbit brain. *Biochim Biophys Acta - Mol Cell Biol Lipids*. 1973;316:115–23.

76. Salem N, Serpentino P, Puskin JS, Abood LG. Preparation and spectroscopic characterization of molecular species of brain phosphatidylserines. *Chem Phys Lipids*. 1980;27:289–304.

77. Farooqui A, Horrocks L, Farooqui T. Glycerophospholipids in brain: their metabolism, incorporation into membranes, functions, and involvement in neurological disorders. *Chem Phys Lipidspids*. 2000;106:1–29.

78. Breckendirdge WC, Gombos G, Morgan IG. The lipid composition of adult rat brain synaptosomal plasma membranes. *Biochim Biophys Acta - Mol Cell Biol Lipids*. 1972;266:695–707.

79. Rapoport SI. In vivo fatty acid incorporation into brain phosholipids in relation to plasma availability, signal transduction and membrane remodeling. *J Mol Neurosci*. 2001;16:243–62.

80. Hamilton J a., Brunaldi K. A model for fatty acid transport into the brain. *J Mol Neurosci*. 2007;33:12–7.

81. Farooqui A. Transport synthesis and incorporation of n-3 and n-6 fatty acids in brain glycerolipids. Beneficial Effects of Fish Oil on Human Brain. Springer US; 2009.

82. Edmond J. Essential polyunsaturated fatty acids and the barrier to the brain. *J Mol Neurosci*. 2001;16:181–93.

83. Purdon D, Arai T, Rapoport S. No evidence for direct incorporation of esterified palmitic acid from plasma into brain lipids of awake adult rat. *J Lipid Res*. 1997;38:526–30.

84. Rapoport SI, Purdon D, Shetty HU, Grange E, Smith Q, Jones C, Chang MCJ. In vivo imaging of fatty acid incorporation into brain to examine signal transduction and neuroplasticity involving phospholipids. *Ann N Y Acad Sci*. 1997;820:56–73.

85. Cummins a G, Thompson FM. Effect of breast milk and weaning on epithelial growth of the small intestine in humans. *Gut*. 2002;51:748–54.

86. Commare CE, Tappenden K a. Development of the infant intestine: implications for nutrition support. *Nutr Clin Pract*. 2007;22:159–73.

87. Dvorak B, McWilliam DL, Williams CS, Dominguez J a, Machen NW, McCuskey RS, Philipps a F. Artificial formula induces precocious maturation of the small intestine of artificially reared suckling rats. *J Pediatr Gastroenterol Nutr*. 2000;31:162–9.

88. Jacobi SK, Odle J. Nutritional factors influencing intestinal health of the neonate. *Adv Nutr*. 2012;3:687–96.

89. Innis SM. Dietary omega 3 fatty acids and the developing brain. *Brain Res*. 2008;1237:35–43.

90. Yum J. The effects of breast milk versus infant formulae on cognitive development. *J Dev Disabil*. 2007;13:525–35.

91. Boudry G, Douard V, Mourot J, Lalle J, Huerou-luron I. Linseed oil in the maternal diet during gestation and lactation modifies fatty acid composition , mucosal architecture , and mast cell regulation of the ileal barrier in piglets. *J Nutr*. 2009;139:1110–7.

92. Gabler NK, Spencer JD, Webel DM, Spurlock ME. In utero and postnatal exposure to long chain (n-3) PUFA enhances intestinal glucose absorption and energy stores in weanling pigs. *J Nutr*. 2007;137:2351–8.

93. Breedlove MS, Watson N V, Rosenzweig MR. Biological psychology: an introduction to behavioral, cognitive, and clinical neuroscience. 6th ed. 2010.

94. Volpe JJ. Overview: normal and abnormal human brain development. *Ment Retard Dev Disabil Res Rev*. 2000;6:1–5.

95. Graff-Peters V, Hadders-Algra M. Ontogeny of the human central nervous system: what is happening when? *Early Hum Dev*. 2006;82:257–66.

96. Holland D, Chang L, Ernst TM, Curran M, Buchthal SD, Alicata D, Skranes J, Johansen H, Hernandez A, et al. Structural growth trajectories and rates of change in the first 3 months of infant brain development. *JAMA Neurol*. 2014;71:1266–74.

97. Eyre J, Miller S, Clowry G, Conway E, C W. Functional corticospinal projections are established prenatally in the human foetus permitting involvement in the development of spinal motor centres. *Brain*. 2000;123:51–64.

98. Huttenlocher P, Dabholkar A. Regional differences in synaptogenesis in human cerebral cortex. *J Comp Neurol*. 1997;387:167–78.

99. Huttenlocher P. Synapse elimination and plasticity in developing human cerebral cortex. *Am J Ment Defic*. 1984;88:488–96.

100. Bunge RP. Glial cells and the central myelin sheath. *Physiol Rev*. 1968;48:197–251.

101. Lenroot RK, Giedd JN. Brain development in children and adolescents: insights from anatomical magnetic resonance imaging. *Neurosci Biobehav Rev*. 2006;30:718–29.

102. Dubois J, Dehaene-Lambertz G, Kulikova S, Poupon C, Hüppi PS, Hertz-Pannier L. The early development of brain white matter: a review of imaging studies in fetuses, newborns and infants. *Neuroscience*. 2013;276:48–71.

103. Lachapelle F, Duhamel-Clerin E, Gansmuller A, Baron-Van Evercooren A, Villarroya H, Gumpel M. Transplanted transgenically marked oligodendrocytes survive, migrate and myelinate in the normal mouse brain as they do in the shiverer mouse brain. *Eur J Neurosci*. 1994;6:814–24.

104. Cowan FM. Magnetic resonance imaging of the normal infant brain: term to 2 years. MRI of the neonatal brain [Internet]. 2001. Available from: http://www.mrineonatalbrain.com/

105. Georgieff MK. Nutrition and the developing brain: nutrient priorities and measurement. *Am J Clin Nutr*. 2007;85:614S–620S.

106. Quarles RH, Macklin WB, Morell P. Myelin formation, structure and biochemistry. Basic Neurochemistry: Molecular, Cellular and Medical Aspects. Elsevier, Inc; 2006. p. 51–72.

107. Baumann N, Pham-Dinh D. Biology of oligodendrocyte and myelin in the mammalian central nervous system. *Physiol Rev*. 2001;81:871–927.

108. Blass JP. Fatty acid composition of cerebrosides in microsomes and myelin of mouse brain. *J Neurochem*. 1970;17:545–9.

109. Schild HH. MRI made easy. 1st ed. Schering AG; 1990.

110. Noll D. MRI physics 1: spins, excitation, relaxation. 2014.

111. Wang X. Advanced neuroimaging fundamentals and methods. Diffusion MR Imaging of the Brain. 2014. p. 1–8.

112. Moseley E, Wendland F, Kucharczyk J, Tsumuda J. Diffusion weighted MR imaging of anisotropic water diffusion in cat central nervous system. *Radiology*. 1990;176:439–45.

113. Mori S, Zhang J. Principles of diffusion tensor imaging and its applications to basic neuroscience research. *Neuron*. 2006;51:527–39.

114. Dubois J, Hertz-Pannier L, Dehaene-Lambertz G, Cointepas Y, Le Bihan D. Assessment of the early organization and maturation of infants' cerebral white matter fiber bundles: a feasibility study using quantitative diffusion tensor imaging and tractography. *Neuroimage*. 2006;30:1121–32.

115. Wijtenburg S a, McGuire S a, Rowland LM, Sherman PM, Lancaster JL, Tate DF, Hardies LJ, Patel B, Glahn DC, et al. Relationship between fractional anisotropy of cerebral white matter and metabolite concentrations measured using (1)H magnetic resonance spectroscopy in healthy adults. *Neuroimage*. Elsevier Inc.; 2012;66C:161–8.

116. Wetzel SG, Johnson G, Tan AGS, Cha S, Knopp EA, Lee VS, Thomasson D, Rofsky NM. Three-dimensional, T1-weighted gradient-echo imaging of the brain with a volumetric interpolated examination. *AJNR Am J Neuroradiol*. 2002;23:995–1002.

117. Brant-Zawadzki M, Gillan GD. MPRAGE: A three-dimensional, T1-weighted, gradient-echo sequence- initial experience in the brain. *Radiology*. 1992;182:769–75.

118. Ashburner J, Friston KJ. Voxel-based morphometry-the methods. *Neuroimage*. 2000;11:805–21.

119. Conrad MS, Dilger RN, Nickolls A, Johnson RW. Magnetic resonance imaging of the neonatal piglet brain. *Pediatr Res*. 2012;71:179–84.

120. Scavuzzo CJ, Larsen RJ. The use of Magnetic Resonance Spectroscopy for assessing the effect of diet on cognition. Unpublished manuscript.

121. Soares DP, Law M. Magnetic resonance spectroscopy of the brain: review of metabolites and clinical applications. *Clin Radiol*. The Royal College of Radiologists; 2009;64:12–21.

122. Bluml S. Magnetic Resonance Spectroscopy: Basics. In: Blüml S, Panigrahy A, editors. MR Spectroscopy of Pediatric Brain Disorders. New York, NY: Springer New York; 2013. p. 11–24.

123. Odle J, Lin X, Jacobi SK, Kim SW, Stahl CH. The suckling piglet as an agrimedical model for thestudy of pediatric nutrition and metabolism. *Annu Rev Anim Biosci*. 2014;2:419–44.

124. Puiman P, Stoll B. Animal models to study neonatal nutrition in humans. *Curr Opin Clin Nutr Metab Care*. 2008;11:601–6.

125. Bergen WG, Mersmann HJ. Comparative aspects of lipid metabolism : impact on contemporary research and use of animal models. *J Nutr*. 2005;135:2499–502.

126. Rytych JL, Elmore MRP, Burton MD, Conrad MS, Donovan SM, Dilger RN, Johnson RW. Early life iron deficiency impairs spatial cognition in neonatal piglets. *J Nutr*. 2012;142:2050–60.

127. Hansen A, Strathe A, Kebreab E, France J, Theil P. Predicting milk yield and composition in lactating sows: a Bayesian approach. *J Anim Sci*. 2012;90:2285–98.

128. Huang M, Brenna JT, Chao AC, Tschanz C, Diersen-schade DA, Hung H. Differential tissue dose responses of (n-3) and (n-6) PUFA in neonatal piglets fed docosahexaenoate and arachidonate. *J Neurochem*. 2007;137:2049–55.

129. Sangild PT. Experimental biology and medicine gut responses to enteral nutrition in preterm infants and animals. *Exp Biol Med*. 2006;231:1695–711.

130. Dobbing J, Sands J. Comparative aspects of the brain growth spurt. *Early Hum Dev*. 1979;3:79–83.

131. Workman AD, Charvet CJ, Clancy B, Darlington RB, Finlay BL. Modeling transformations of neurodevelopmental sequences across mammalian species. *J Neurosci*. 2013;33:7368–83.

132. Kornum B, Knudsen G. Cognitive testing of pigs (Sus scrofa) in translational biobehavioral research. *Neurosci Biobehav Rev*. 2011;35:437–51.

133. Bolhuis JE, Schouten WGP, de Leeuw J a, Schrama JW, Wiegant VM. Individual coping characteristics, rearing conditions and behavioural flexibility in pigs. *Behav Brain Res*. 2004;152:351–60.

134. Dilger RN, Johnson RW. Behavioral assessment of cognitive function using a translational neonatal piglet model. *Brain, Behav iImunity*. Elsevier Inc.; 2010;24:1156–65.

135. Benton D. The influence of dietary status on the cognitive performance of children. *Mol Nutr Food Res*. 2010;54:457–70.

136. Benton D. The influence of children's diet on their cognition and behavior. *Eur J Nutr*. 2008;47:25–37.

137. Isaacs EB, Fischl BR, Quinn BT, Chong WUIK, Gadian DG, Lucas A. Impact of breast milk on intelligence quotient , brain size , and white matter development. *Pediatr Res*. 2010;67:357–62.

138. Boleman SL, Graf TL, Mersmann HJ, Su DR, Krook LP, Savell JW, Park YW, Pond WG. Pigs fed cholesterol neonatally have increased cerebrum cholesterol as young adults. *J Nutr*. 1998;128:2498–504.

139. Alessandri JM, Goustard B, Durand PGG. Polyunsaturated fatty acids status in blood , heart , liver , intestine , retina and brain of newborn piglets fed either sow milk or a milk replacer diet Polyunsaturated fatty acids status. *Reprod Nutr Dev*. 1995;36:95–109.

Figures

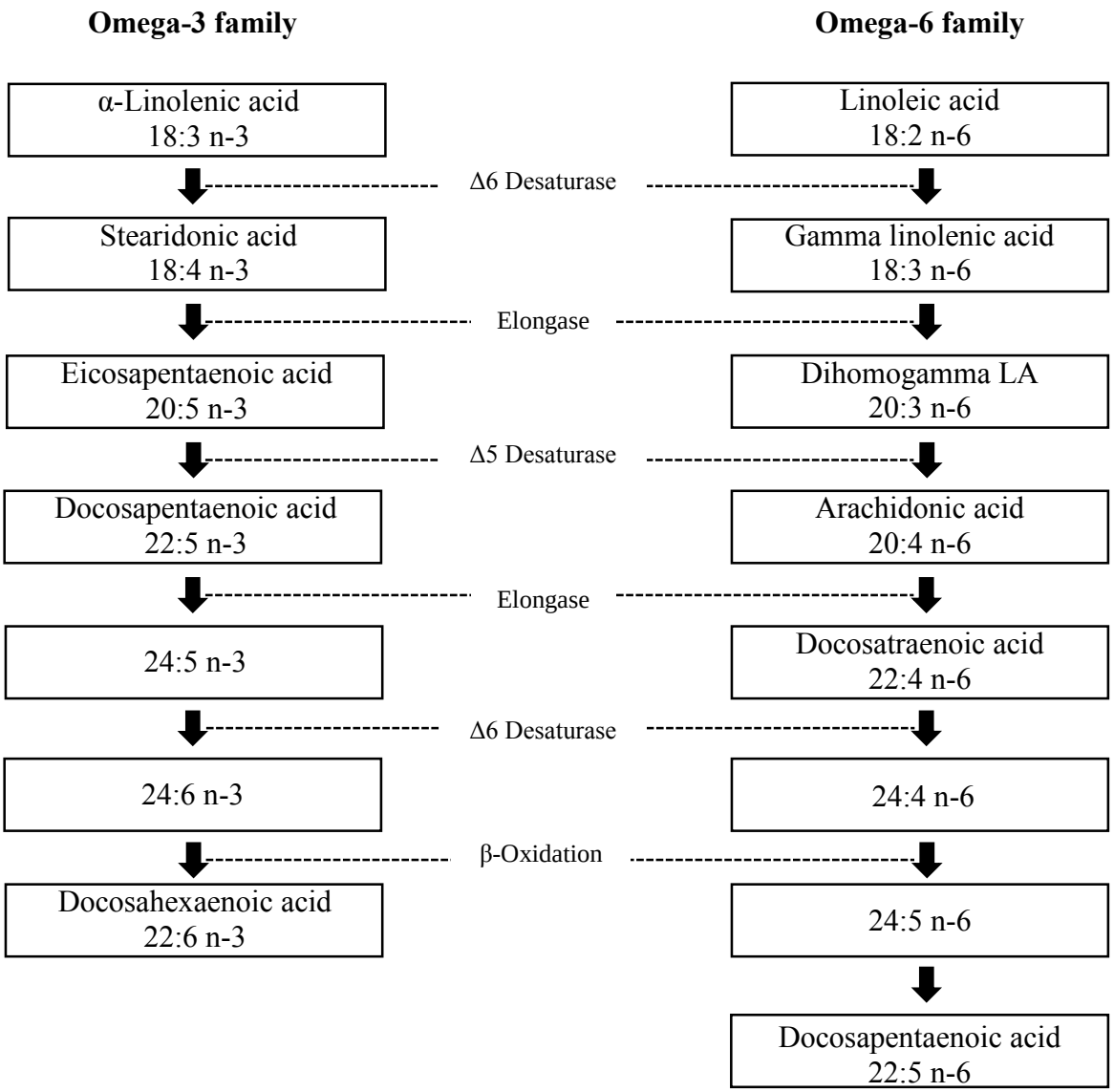

Figure 2.1. The biosynthetic pathway involved in the synthesis of n-6 and n-3 long chain PUFA (9,11).

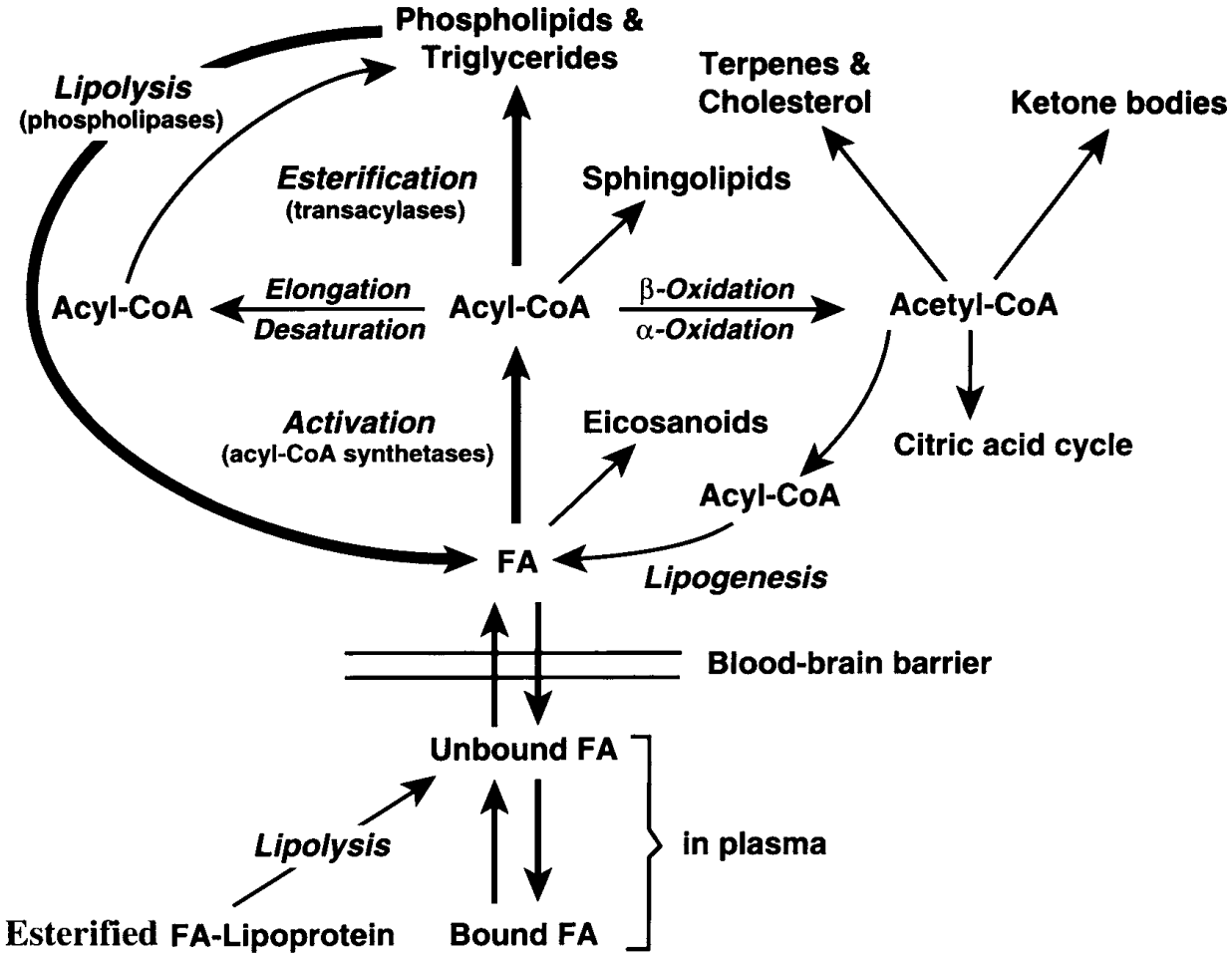

Figure 2.2. Pathways of fatty acid incorporation and metabolism in the brain (adapted from 79).

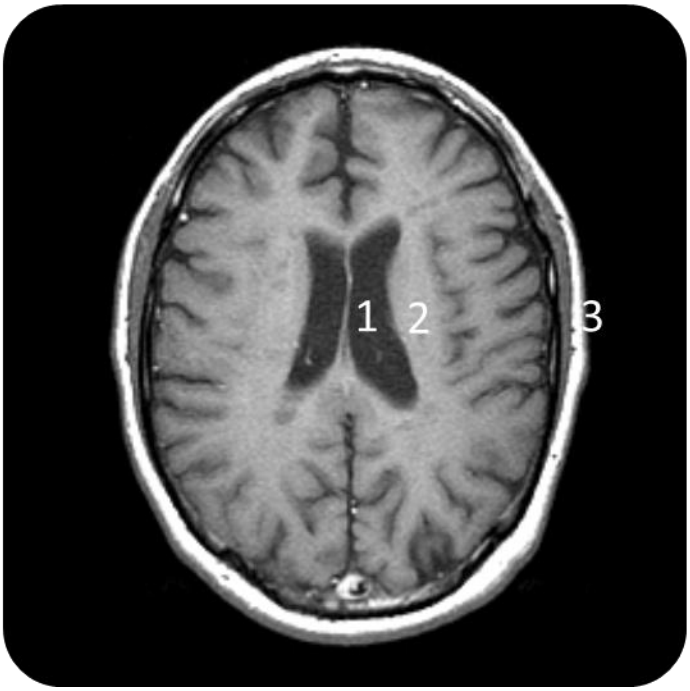

Figure 2.3. Illustration of T1-acquired image with labeled: 1) CSF, 2) WM tracts, and 3) fat (adapted from 110).

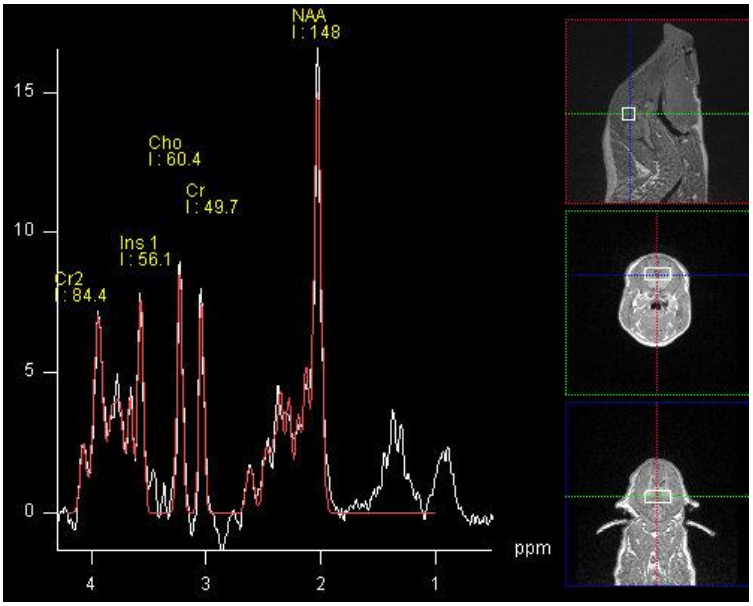

Figure 2.4. Line spectra obtained from MRS indicating hippocampal neurochemical concentrations expressed in PPM.

Chapter 3

IMPACT OF DIETARY LIPID MATRIX ON BRAIN MICROSTRUCTURE OF THE NEONATAL PIG

Abstract

The lipid matrix found in breast milk may benefit cognitive function and neural maturation in neonates. Using the piglet as a pediatric biomedical model, we assessed the impact of dietary fat composition on postnatal neurodevelopment. Over a 25-day study, piglets (n=9-10/treatment, 1.5 ± 0.2 kg initial BW) were subjected to 1 of 3 experimental treatments: T1, artificially-reared (AR) control formula; T2, T1 with 45% of total dietary fat replaced by pre-digested fat (PDF); T3, T2 + 10% lecithin + 0.4% cholesterol. Reference values obtained from sow-reared (SR) animals were not included in the statistical analysis when comparing treatments. Piglets were weighed daily, serum samples were collected at d 0, d14, and d25 of study, and fecal samples were collected, and pooled from d 13-27. At study conclusion, piglets were euthanized and tissues were collected for further analysis. Sow-reared piglets exhibited higher BW gain and heavier extracted whole brain weights compared with AR piglets. Analysis of fecal fat suggested greater ($P < 0.05$) excretion of dietary fat with addition of PDF along with lecithin and cholesterol. Serum lipid profiling at d 14 and d 25 revealed serum concentrations of triacylglycerides (TAG), lipoproteins and cholesterol to be higher in SR animals, with d25 serum cholesterol concentrations being higher ($P < 0.05$) in T3-fed piglets when compared with T1- and T2-fed piglets. Serum TAG concentrations at d14 and d25 remained higher ($P = 0.176$, $P = 0.164$) in T3-fed piglets when compared with T1- and T2 fed piglets. Hippocampal tissue analysis revealed neutral lipid (NL) DHA concentrations were greater ($P < 0.05$) in T3-fed pigs compared with T1-fed and SR pigs. Hippocampal phospholipid (PL) DHA concentrations of T2- or T3-fed pigs were intermediate to T1-fed and SR piglets. Higher fecal fat excretion, partnered

with no differences in serum TAG concentrations compared with SR piglets, suggested higher bioavailability of the PDF, especially when supplemented with lecithin and cholesterol. Replacing part of formula TAG with PDF, and addition of lecithin and cholesterol, may elicit preferential accretion of brain DHA due to compositional manipulations of the dietary lipid matrix.

Introduction

Docosahexaenoic acid [DHA; 22:6 (n-3)] is increasingly promoted as a long-chain polyunsaturated fatty acid (LCPUFA) of critical importance for neural development of the neonate (1). It is the most prevalent n-3 fatty acid (FA) in the central nervous system, and serves as an integral structural component of neural membranes. Docosahexaenoic acid is primarily integrated into glycerophospholipids, including phosphatidylethanolamine (PE) and phosphatidylserine (PS), and its concentration in neural tissue increases substantially in the first year of life (2–4). Dietary supplementation with DHA has been associated with increased brain DHA accretion (5), increased visual acuity (6) and cognitive development (7) in animal models and in the human clinical setting. The predominant sources of infant nutrition in early life are breast milk (BM) and infant formula. An increasing number of studies (8–11) are focusing on the impact of these varying sources of nutrition on brain development, and the role of DHA in structural and cognitive development of breast-fed and formula-fed infants.

An increasing body of clinical neuroimaging studies have revealed a favorable effect of BM on brain development (9,12), and as such, BM has been increasingly promoted as the optimal source of nutrition for the infant. The incorporation of preformed DHA in this medium has been suggested to influence modulations of early life neurodevelopment (12). Differences in DHA accretion between breast-fed and formula-fed infants have been noted as early as 6 months

of age. Consumption of infant formula without DHA supplementation resulted in average daily accretion of brain DHA at approximately half that of levels observed in breast-fed infants (13). Due to its neuro-augmenting nature, DHA was approved as an additive to infant formula in 2002 at concentrations similar to those found in BM (14,15). Supplementation of pre-formed DHA is of critical importance to the developing infant, as the rate of endogenous DHA synthesis from α-linolenic acid [ALA: 18:3 (n-3)] is quite slow, and is suggested to be insufficient to meet requirements of the developing infant (1,16–18). As such, supplementation of preformed DHA in infancy may be the best route to ensure optimal tissue accretion of this LCPUFA.

Although the role of DHA in infant development has obtained notoriety in recent years, few studies have focused on identifying dietary strategies to improve tissue incorporation of DHA at levels similar to those found with BM. Presently, TAG, PL, or ethyl esters are the three primary sources of DHA in infant formula (19). The proportion of fat absorption has been reported to be higher with the incorporation of PUFA found in PL compared with TAG (20), but others have observed no differences in DHA absorption between subjects fed DHA as TAG versus PL (21). As for incorporation of DHA into neural tissue, incorporation into gray matter and synaptosome tissues appear to be higher when DHA is supplemented in TAG form, but DHA accretion in the same brain regions as a proportion of dosage was significantly higher from the PL fraction (provided as phosphatidylcholine) (19). Positional distribution of FA in the dietary TAG may affect pancreatic lipase mediated hydrolysis and subsequent absorption of saturated and polyunsaturated FA. Most saturated FA, such as palmitic acid, is esterified at the sn-2 position in BM. This positional specificity allows for a higher proportion of these FA to be absorbed when compared with cow milk or infant formula, which preferentially esterifies palmitic acid at sn-1 and sn-3 positions (22,23). Pancreatic lipase preferentially cleaves at the sn-

1 and sn-3 positions of TAG, therefore we hypothesize that esterifying saturated FA to the sn-2 position, and predigesting the sn-1 and sn-3 bound LCPUFA will allow for greater availability of DHA.

The piglet has been successfully used human infant nutrition to characterize the role of multiple nutrients including iron (24), cholesterol (25), and PUFA (26) on neurodevelopment. Due to similarities in nutrient requirements, lipid metabolism, and patterns of brain development, the piglet serves as a powerful translational model for human infants (27–29). In addition, the precocial nature and expedited growth rate of the pig when compared with the human infant allows for nutrient intervention immediately following birth, and a rapid timeline on which to observe the influence of early-life nutrition on neurodevelopment.

Using artificially-reared (AR) and sow-reared (SR) piglets as models for the formula-fed and breast-fed infants, respectively, the purpose of this study is to determine whether nutrient-based strategies to manipulate the lipid matrix would allow for greater absorption, transport and incorporation of DHA into the brain. To assess differences between treatments, we outlined three primary objectives for this study: 1) identify whether pre-digestion of sn-1 and sn-3 bound LCPUFA, or the addition of lecithin and cholesterol, allow for improved absorption and tissue incorporation of DHA; 2) assess the impact of varying fat matrices on growth performance and integrity and maturity of the intestinal brush border; and 3) identify whether differences exist for any of the above-mentioned outcomes between AR and SR piglets.

Materials and Methods

All animal experimentation procedures were approved by the Institutional Animal Care and Use Committee at the University of Illinois, and followed guidelines from the National Institute of Health Guidelines for the Care and Use of Laboratory Animals.

Animals, Housing, and Feeding

Naturally-farrowed, vaginally-derived piglets (n=10/treatment, 1.5 ± 0.2 kg initial BW; sourced from 10 sows, n=2/treatment from each sow) were obtained from the Imported Swine Research Laboratory herd located at the University of Illinois. Piglets were allowed access to colostrum for up to 48 h, at which point they were immediately allotted to one of 4 experimental treatments for the duration of a 25-d feeding study (conducted using 5 cohorts of piglets). Piglets were housed individually in stainless steel cages (101.6 cm L x 76.2 cm W x 81.28 cm H), and were provided with a towel and toy (Bio-Serv, Flemington, NJ) for comfort and environmental enrichment. Cages were fitted with vinyl-coated expanded-metal flooring (Tenderfoot/NS^{TM}), which was designed for neonatal piglets, and were also outfitted with a heat lamp and electric heat mat (K&H Manufacturing, Colorado Springs, CO) to maintain home cage temperatures between 23-31°C. A 12-h light/dark cycle was maintained with minimal light provided during dark cycles for the duration of the study.

Artificially-reared animals were fed 1 of 3 isocaloric dietary treatments as follows: T1, AR control formula; T2, T1 with 45% total dietary fat replaced by pre-digested fat (PDF); T3, T2 + 10% lecithin + 0.4% cholesterol. Sow reared animals (T4) remained with their respective mother and litter mates for the duration for the study (**Table 3.1**).

Artificially-reared piglets were fed using an automated feeding system that dispensed a pre-determined volume of formula over a period of 13 ± 2 h based on daily BW of piglets. The diets were replaced twice daily and were dispensed from 6 identical reservoirs that were cleaned and sterilized daily. Piglets were fed 285 ml/kg BW, 300 ml/kg BW, and 325 ml/kg BW from 0-7, 8-16, and 18-25 d on study, respectively.

Per agricultural protocols, all piglets were identified at birth using ear notches, and further, needle teeth were removed to prevent harm to littermates and the sow. Moreover, piglets

received a supplemental iron injection at 1 d of age, but did not undergo other agricultural processing (i.e., tail docking and castrations did not occur). Approximately 5 ml of clostridium perfringens antitoxin C + D (Colorado Serum Company, Denver, CO) was administered subcutaneously as a prophylactic agent at d 2 of age. If piglets developed diarrhea, supplemental water and electrolytes (Pedialyte, Abbott Laboratories, Abbott Park, IL) were provided. Sulfamethoxazole and trimethroprim oral suspension (50 and 8 mg/mL, respectively, Hi-Tech Pharmacal, Amityville, NY) were given if symptoms were not alleviated after 48 h of exhibiting initial symptoms.

Individual piglet body weights were recorded daily to assess growth performance, and blood samples were collected on study d 0, 14, and 25. Blood was collected in to serum tubes (BD Franklin Lakes, NJ, USA), gently inverted and centrifuged at 1300 x g for 15 minutes at 20°C. Serum samples were obtained and processed at all-time points for analysis of serum lipid levels. Serum was obtained and stored at -80°C until further processing. Serum samples were analyzed for HDL, LDL, TAG and cholesterol using established methods (Lipoprotein Composition Laboratory, University of Tennessee, Knoxville, TN). Red blood cells (RBC) were collected on study d 25, and all samples were stored at -80°C pending subsequent analyses. Fecal samples were collected between study d 13-17, and samples were stored at -80°C.

At study conclusion (i.e., d 27 of age), piglets were euthanized for tissue and blood collection. All animals were euthanized in the fed state with respective treatments being provided until an hour before administering anesthesia. Piglets were anesthetized using an intramuscular injection of telazol:ketamine:xylazine administered at 0.022 mL/kg BW. Pain reflex and eye blink response were tested to ensure deep anesthesia before euthanizing animals with an intracardiac injection of 390 mg/mL sodium pentobarbital solution at 1 mL/5 kg BW. Blood was

collected immediately after euthanasia and processed for serum and RBC fractionation. Whole brains were extracted and select brain regions, including the left and right hippocampi, were dissected, snap frozen in liquid nitrogen, and stored at -80°C pending analyses.

The small intestine, spanning from the pyloric sphincter to the ileocecal junction, was dissected and weighed. The intestine was separated from mesentery, and segmented into 10, 75 and 15% of the total length to identify duodenal, jejunal, and ileal sections, respectively (30). The jejunum was folded in half to identify proximal and distal sections of the jejunum. A 25 cm segment was collected from the middle of the proximal part of the jejunum. Approximately 20-cm segment was resected and the luminal surface was exposed for collection of mucosa. The adjacent 5-cm segment was opened longitudinally and stored in 10% neutral buffer formalin for histomorphological analysis of brush border maturity. Samples were submitted to the University of Illinois Veterinary Diagnostic Laboratory where samples were embedded in paraffin, sectioned, and stained with hematoxylin and eosin. Samples were visualized using the Nanozoomer Digital Pathology system at the University of Illinois Institute for Genomic Biology. Villi surface area was calculated from the apical width (d), basal width (c), and villi length (a) using the following formula (c + d)/2*a (31).

Quantification of docosahexaenoic acid in red blood cells and brain

Lipids were extracted from RBC and hippocampal samples using a methanol and chloroform procedure (32,33). Briefly, RBC were added drop-wise into a known amount of cold methanol and agitated in a sonicating water bath. For hippocampal tissue, approximately 0.15 g of tissue was homogenized in cold methanol using a bead homogenizer. In total, a 2:1 ratio of chloroform/methanol was then added to the homogenized solvent, with further agitation to

achieve final ratio of 50:1 solvent to sample. The solution was then filtered through filter paper (Whatman® 541, Sigma Aldrich, St. Louis, MO) to remove precipitated proteins, and the resulting supernatant was dried under a stream of argon. The remaining lipid residue was resuspended in 2 ml of chloroform, and separated into PL and NL fractions using HyperSep™ Silica SPE Cartridges (Thermo Scientific, Waltham, MA) conditioned with 10 ml chloroform. The NL fraction of fatty acids was eluted with 20 ml chloroform, and the PL fraction was eluted with 20 ml methanol. Solutions isolated using these procedures were separately dried under a stream of argon, and all samples were stored at 4°C until processed for methylation (34).

The lipid residue obtained from the extraction process was re-suspended in 1.8 ml hexane, and 0.2 ml of an internal standard (pentacosanoic acid; 25:0, 20.06 µg/ml). The solution was hydrolyzed and methylated using 3 ml of methanolic-HCl and incubated for 1 hour at 100°C, before samples were resuspended in 5 ml of potassium carbonate and 2 ml hexane. Following centrifugation, the resulting upper fraction containing long chain fatty acids was obtained, protected from light, and dried under a stream of argon. The methylated fatty acid residue was transferred to amber vials and fatty acid methyl esters were analyzed by gas chromatography according to established procedures (35). Fatty acids were identified by comparing retention times to known standard mixtures.

Analysis of fecal fat

Fecal samples were collected into sterile sampling bags (Whirl-Pak, Pioneer Container Corp, Cedarburg, WI) and stored at -20°C until further processing. Fecal samples were dried at 57°C in a forced-air oven and ground (Model 4 Wiley Mill; Thomas Scientific, Swedesboro, NJ) using a 2 mm screen. Samples were subsequently analyzed for dry matter (DM), organic matter

(OM), and acid hydrolyzed fat (36,37). To calculate proportion of DM and OM in fecal samples, a minimum of 200 mg sample was dried at 105°C overnight, and subsequently ashed at 600°C. To quantify crude fat content, acid hydrolysis of fecal matter was conducted (36). In brief, a 500 mg sample was saturated with 95% ethanol and hydrolyzed with 10 ml of 25% HCl solution and heated in a water bath at 75.5°C. A regimen of 25 ml ethyl ether and 25 ml petroleum ether, followed by 15 ml ethyl ether and 20 ml petroleum ether, was used to extract crude fat from the fecal samples. The top layer containing ether-bound fat was collected and ether was evaporated in a steam bath. Crude fat weights were obtained prior to drying samples in a 135°C oven. Percent fat was calculated using the following equation:

$$\text{Fat (\%)} = \frac{\text{Fat weight (g)}}{\text{Sample weight on DM basis (g)}} * 100$$

All procedures were completed in duplicate, and the assay was repeated if calculated error exceeded 5%.

Statistical Analysis

Data were subjected to an analysis of variance (ANOVA) using the MIXED procedure of SAS, version 9.4 (SAS Institute Inc., Cary, NC). Replicate of pigs was included as a random variable, and the threshold of significance was set at $P < 0.05$. Data collected from a single time-point were analyzed using a one-way ANOVA, while any measures acquired from the same animal over multiple time-points were analyzed using a repeated-measures ANOVA. Values obtained from SR animals were designated as reference values, and thus were not included in the statistical analysis when comparing treatments.

Results

Growth performance and organ weights

Growth performance of SR piglets was greater than all other treatments **(Table 3.2,)**, with no significant differences between AR groups. However, no differences ($P > 0.05$) were observed in average daily BW gain during the last week of life, indicating a similar growth trajectory for the SR and AR piglets during this period.

Compared with AR piglets, SR piglets had numerically heavier absolute whole-brain weights, and lighter whole-brain weights expressed relative to BW (**Table 3.3**). No differences were detected within AR treatments for absolute or relative whole-brain weights. Sow-reared piglets exhibited numerically smaller absolute and relative small intestine weight and length when compared with AR piglets. No differences were detected within AR treatments in small intestine and length measurements. Intestinal weight, as a percentage of body weight, was greater ($P < 0.05$) in AR female piglets, but no interactive effects of treatment and sex were observed in these measurements. Whole-liver weights were not different between treatments, but liver weights as a percentage of body weight were numerically lighter in SR piglets.

Serum lipids

No differences in any serum lipids were observed at the beginning of the study (**Table 3.4**). At 16 and 27 d of age, serum TAG, HDL, LDL, and cholesterol were all numerically higher in SR piglets compared with all AR treatments. Serum TAG levels at d16 were trending ($P = 0.176$) to be higher in T2 and T3 animals when compared with T1 animals. Similarly, serum LDL levels at were trending ($P = 0.069$) to be highest in T2 animals with in the AR experimental groups. Treatment effects were also noted within AR treatments at 27 d of age for serum TAG, HDL and cholesterol, with serum TAG levels trending ($P = 0.164$) to be highest in T3 animals

when compared with T2 and T1- fed groups. Serum HDL concentrations were higher ($P < 0.05$) in T2 and T3 when compared with T1-fed animals. Circulating serum cholesterol levels were higher ($P < 0.05$) in T3-fed animals when compared with T1-fed animals. No differences in serum cholesterol were observed in piglets fed T1 vs. T2, and T2 vs. T3. Finally, female pigs had higher ($P < 0.05$) HDL concentrations pigs at 27 d of age. This serum lipid measure represents the only outcome in the study where a significant sex effect was observed.

Fatty acid analysis of red blood cells (RBC) and brain

Hippocampal DHA concentrations in the NL fraction were higher ($P < 0.05$) in T3-fed AR piglets when compared with T1, T2 or SR reference animals (**Figure 3.1, Table 3.5**). Within AR groups, a graded increase ($P < 0.05$) in hippocampal neutral lipid DHA concentration was observed in piglets fed T2 vs. T1, and T3 vs. T2, with DHA concentrations of SR animals falling between those of T1 and T2. Phospholipid DHA concentrations of RBC were different ($P < 0.05$) between treatments, with highest concentrations of DHA being present in T2-fed animals. No differences were observed between T1 and T3, or T1 and T2-fed animals. No other differences in hippocampal or RBC DHA concentrations were observed. A numerical increase ($P = 0.240$) in hippocampal DHA concentration was observed in the PL fraction of pigs fed treatments T2 or T3, with highest DHA concentrations observed in T3-fed pigs when compared with either T1 or SR treatments. However, no differences in DHA concentrations due to treatment were observed in hippocampal PL or RBC NL fractions.

Whole-brain DHA was calculated based on hippocampal DHA concentration and absolute whole-brain weights at study conclusion. Although no significant differences in whole-brain DHA accretion were present, a numerical increase ($P = 0.084$) was observed in the NL fraction of pigs fed treatments T3 when compared with T1 and T3. In accordance with

hippocampal PL and NL observations, the highest calculated quantity of whole-brain DHA in PL and NL fraction was present in piglets fed T3.

Fecal fat

Percentage of fecal OM was higher ($P < 0.05$) in piglets receiving T1 compared with T3, and pigs fed T2 exhibited an intermediate response (**Table 3.6**). Percentage of fecal fat, presented on an OM basis, was higher ($P < 0.05$) in T2 and T3 groups compared with T1. No differences due to treatment were observed in fecal DM, but a numerical increase ($P = 0.0582$) was observed in percentage of fecal fat on a DM basis for T2 and T3 compared with T1.

Histological analysis of jejunal tissue samples

Brush border maturity in the jejunum was assessed via outcomes including villi height, villi surface area and crypt depth. Histological analysis of the brush border revealed all variables to be shorter in SR animals when compared with AR treatment groups, with no differences observed between AR treatments (**Figure 3.2**). No significant differences in villi morphology, nor villi surface area, were observed between any treatments.

Discussion

Using the piglet as a biomedical model, this study sought to investigate the impact of manipulating the dietary lipid matrix found in infant formula on the absorption and integration of DHA into neural tissue. Artificially-reared piglets were raised individually and fed 1 of 3 isocaloric dietary treatments, while SR reference animals remained with the dam and littermates for the duration for the study. Our findings indicated improved growth performance and overall elevated serum lipid concentrations in SR piglets compared with AR piglets. Analysis of

hippocampal tissue also indicated that transport of DHA to the brain via the neutral lipid fraction may be a primary route of DHA transport.

Growth performance

Although AR animals never reached the growth trajectory observed in SR animals, average BW gain during the last week on study indicated a similar growth rate between the 2 rearing conditions (data not shown). Established patterns of growth in human infants indicate no consistent differences in weight gain in the first 1-2 months of life between breast-fed and formula-fed infants, but the rate of BW gain is reported to be higher in formula-fed infants from 2 months to 1 year of age (34, 35). Our AR animals did not reach the growth trajectory observed in SR animals, and therefore did not concur with aforementioned patterns of human development, the lack of differences in the rate of BW gain in the third week of life suggest that similar patterns of growth may be present between treatments if animals were brought to 2 or 3 months of life. To further elucidate drivers of BW gain and brain development, we chose to focus our efforts on characterizing the impact of varying lipid profiles of maternal milk and infant formula on overall metabolism.

Serum lipids

As expected, characterization of serum lipids revealed higher HDL, LDL and cholesterol concentrations in SR animals compared with their AR counterparts. Of particular interest were the elevated levels of serum cholesterol at d 16 and d 27 of age in SR animals when compared with AR treatments. Similar to our observations, breast-fed infants exhibit higher serum cholesterol levels when compared with formula-fed infants, which is likely due to the elevated cholesterol content of human milk (90-150 mg/L) as compared with most cow milk-based

formulas (10-40 mg/L) (40). Although a 2-4-fold increase of serum cholesterol during breast-feeding coincides with an period of substantial cholesterol accretion and white matter maturation within the CNS (41), most current evidence suggests a primary dependence on endogenously synthesized cholesterol to meet neurodevelopmental requirements. Approximately 95% of cholesterol required for processes such as myelination is synthesized within the glial cells of the central nervous system (41,42). However, ^{3}H labeling of unbound cholesterol has revealed low levels of its transport in the capillary endothelium of rodents (5), and minimal incorporation of hexadeuterium-labeled cholesterol from circulation into the cerebrum and cerebellum in the adult guinea pig (43). Therefore, elevated levels of circulating cholesterol as seen in T3 can result in an increase in cerebral cholesterol concentrations. It is plausible that a small, but critical, amount of circulating cholesterol may be transported through tight junctions of the blood brain barrier (BBB). The expression of bidirectional transporters such as LDL receptor (LDLR), scavenger receptor class B type 1 (SRB1), and unesterified cholesterol transporters such as ABCA1 (41) could provide the missing link between high serum cholesterol of the breast-fed infant, and high level of brain cholesterol accretion that mediates white matter maturation.

As a separate component of this study, magnetic resonance imaging (MRI) techniques were used to assess white matter maturation in the developing piglet brain. Overall, our MRI results suggested greater myelination of white matter tracts in the SR animal when compared with AR piglets. Cholesterol is an essential component of myelin, therefore we were interested in characterizing any existing correlations between supplementation of dietary cholesterol and MRI outcomes. As previously suggested, there is minimal, yet impactful incorporation of circulating cholesterol in to the cerebrum. As such, The higher levels of myelination observed in the SR animal as compared with AR animals can be due to the elevated levels of circulating cholesterol.

In support of this hypothesis, we observed a 20% increase in serum cholesterol in T3-fed pigs when compared with T1-fed pigs at 27 d of age. Although we did not observe outcomes indicating greater myelination on a whole-brain level with the addition of lecithin and cholesterol to the PDF system, region specific assessment of internal capsule (IC) myelination indicated similar trajectory for white matter development between T3 and SR reference animals. The IC is a white matter-rich region that experiences early maturation relative to the cortices (44). Considering the lack of differences in the IC, partnered with the highest level of serum cholesterol observed in T3-fed piglets when compared with all other AR groups, this suggests an impact of supplementation of dietary cholesterol on brain cholesterol accretion. Although these interpretations are purely speculative, uptake of dietary cholesterol at rates too low to be detected by current methods may be present. Such incorporation of dietary cholesterol could provide means for supplementing the in situ generation of brain cholesterol. However, further investigation, including the expression of cholesterol transporter proteins in the BBB and radiolabeling of dietary cholesterol, is warranted to elucidate the extent to which dietary cholesterol is incorporated into the brain during perinatal neurodevelopment.

Fatty acid analysis of hippocampal tissue and red blood cells

Data from our study suggest that hippocampal accretion of DHA is primarily occurring through the NL fraction. In addition, these results suggest greater incorporation of DHA due to the novel lipid strategies that were employed. Treatments 1 and 2 incorporated 140 mg/kg of DHA, while T3 included DHA at 150 mg/kg. The 7% increase in DHA incorporation in T3-fed pigs allowed for a 17% increase in hippocampal NL DHA when compared with T2-fed pigs, and a 30% increase when compared with T1-fed pigs. This increase in hippocampal DHA suggests that the PDF + lecithin + cholesterol fat system optimized incorporation of DHA into the NL

fraction of hippocampal tissue. Although not statistically significant, hippocampal PL DHA concentration increased by 1.2-fold with the addition of PDF, and 2.2-fold with the PDF + lecithin + cholesterol fat system compared with the control formula (T1).

Lysophosphatidylcholine (lysoPC, i.e., lysolecithin) has been suggested as a preferred carrier of DHA to the brain and erythrocytes (45). It is generally accepted that the transport of DHA into the brain is bound to albumin (46), but serum albumin also binds lysoPC. Previous studies have revealed that ^{14}C-labeled lysoPC-bound DHA (47), ARA, linoleic and oleic acids (48) are taken up by the rat brain at 5-to-10-fold greater efficiency when compared with the non-esterified forms. Thus, greater incorporation of PL DHA in the hippocampus may be due to the preferential transport of albumin-associated, lysoPC-bound DHA across the BBB. Our study did not support the preferential incorporation of DHA via lysoPC into the erythrocyte, as the concentration of RBC PL DHA decreased in pigs fed the PDF + lecithin + cholesterol fat system when compared with the PDF fat system alone. However, the dietary lipid profiles of our artificial formulas were successful in increasing the concentration of PL bound DHA in RBC as a percentage of DHA present, when compared with SR piglets.

Martin et al. suggests that DHA is first incorporated into NL fraction upon uptake within cerebral tissues, and only then fractioned into glycerophospholipids such as PE and PC (49). Such sequential release of FA from NL to PL allow for storage of DHA in NL such as TAG, and provides a possible explanation for the increase in the NL fraction of hippocampal DHA with the PDF + lecithin + cholesterol fat system. Although not significant, we observed a similar graded increase in the PL fraction when comparing T2 vs. T1 and T3 vs. T2. If our data follows the hypothesis put forward by Martin et al. (47), it is plausible that lecithin-bound DHA exhibits preferential transport across the BBB as compared with the non-esterified DHA. Such PL-

mediated transport may help to explain the reduction of PL-bound RBC DHA concentrations in T3 when compared with T2.

Although the relationship between RBC and brain DHA is not fully elucidated, our data suggest that pre-digestion of dietary lipids allow for greater absorption of DHA across the intestinal endothelium. However, it could be the addition of lecithin that allows for preferential incorporation of DHA into nervous tissue subsequent to transport across the BBB. Perfusion studies have shown that addition of bovine serum albumin to unesterified DHA decreased the brain transport coefficient (5) of PUFA, further supporting the notion that albumin as a preferential transporter of DHA in the blood. Albumin-bound DHA should be further investigated to verify that the combined action of PDF and lecithin is in fact responsible for greater levels of DHA observed in erythrocytes and brain tissue. In addition, Ouellet et al., and others (46) suggest a preferential and passive incorporation of unesterified PUFA across the BBB, with lipolysis occurring at the neural endothelium. As such, quantifying albumin-bound DHA as well as lipase activity at the BBB may provide insights into the combined activity of PDF and lecithin on the transport of DHA into neural tissue.

Fecal fat

Percentage of fecal fat excretion was highest in piglets provided with the PDF and PDF + lecithin + cholesterol fat systems. These data are surprising because these diets were formulated to reflect fat content of sow milk with reported values of 5.5% w/w (55 g/L) (50) to 6.2% w/w (51) under standard dietary conditions. Incorporation of mostly unsaturated and monounsaturated fat sources at ~10% yielded fecal fat excretion ranging from approximately 14-22% (52). Considering that artificial formulas used in this study incorporated between 66-73 g/L of fat, the fecal fat excretion ranging from 35 to 50% is over 2-fold higher than expected. We anticipated

the PDF fat system would reduce fecal fat excretion as supplementation of PUFA have previously been demonstrated to induce a reduction in total fatty acid excretion on a wt. % basis (53). Addition of egg yolk PL has also been demonstrated to have favorable effects of fat emulsification, and thereby reduce fecal fat excretion (54), but again, we did not observe a reduction in fat excretion in T3-fed pigs when compared with T1- or T2-fed animals. Despite an increase in fecal fat excretion, serum TAG concentrations at both sampling points (d 14 and d 25 of study) were most similar between T3 and SR animals. These results suggest that although a lower proportion of T3 dietary lipids were absorbed, inclusion of lecithin as an emulsifier may have mediated more efficient incorporation of dietary TAG into circulation.

Histological Analysis of proximal jejunum

Postnatal development of the intestinal epithelium is not well characterized in humans, but animal studies have indicated a hypertrophic effect of formula-feeding on small intestine morphology. Previous studies on neonatal piglets and humans, respectively, have revealed similar patterns as those observed in our results, with an increased weight of the intestine (55), and up to 30% increase in crypt depth (56). In our study, histological analysis of the proximal jejunum revealed a reduction in crypt depth, and a trend indicating lower villi surface area in SR than in any AR treatment groups. Previous studies in rodents have suggested a reductive effect of n-3 PUFA on epithelial cell proliferation partnered with increased apoptotic levels (57). Moreover, modulation of mucosal architecture, characterized by shorter villi and crypt depth, were also reported in piglets supplemented with linseed oil high in n-3 PUFA (58). Our results are in consensus with these observations, as our data indicate shorter crypt depth and an incremental, numerical decrease in villi length in T2- and T3-fed animals compared with control pigs (T1). These results suggest that greater availability of PUFA in the diet, due to pre-digestion

of fatty acids, as well as the addition of lecithin and cholesterol, elicits intestinal morphology most closely similar to that of maternally-reared subjects.

Conclusion

Our findings indicate that the primary route of DHA accretion in hippocampal tissue occurs through the NL fraction. Incremental addition of lecithin and cholesterol with the PDF system appears to positively modulate DHA incorporation within this predominantly white matter-rich brain region. Although not statistically significant, we see similar trends in PL bound DHA accretion, indicating a need for further research in this area. Overall, further quantification of DHA in grey matter-rich regions, such as cerebral cortex or cerebellum, is required before extrapolating the impact of the applied dietary fat systems on whole brain DHA accretion.

Literature Cited

1. Innis SM. Dietary omega 3 fatty acids and the developing brain. *Brain Res*. 2008;1237:35–43.

2. Martinez M. Tissue levels of polyunsaturated fatty acids during early human development. *J Pediatr*. 1992;120:S129–138.

3. Innis SM, Gilley J, Werker J. Are human milk long-chain polyunsaturated fatty acids related to visual and neural development in breast-fed term infants? *J Pediatr*. 2001;139:532–8.

4. Farooqui A, Horrocks L, Farooqui T. Glycerophospholipids in brain: their metabolism, incorporation into membranes, functions, and involvement in neurological disorders. *Chem Phys Lipidspids*. 2000;106:1–29.

5. Ouellet M, Emond V, Chen CT, Julien C, Bourasset F, Oddo S, LaFerla F, Bazinet RP, Calon F. Diffusion of docosahexaenoic and eicosapentaenoic acids through the blood-brain barrier: An in situ cerebral perfusion study. *Neurochem Int*. 2009;55:476–82.

6. Hoffman DR, Birch EE, Castaneda YS, Fawcett SL, Wheaton DH, Birch DG, Uauy R. Visual function in breast-fed term infants weaned to formula with our with out LCPUFA at 4 to 6 months: A randomized clinical trial. *J Pediatr*. 2003;142:669–77.

7. Birch EE, Garfield S, Hoffman DR, Uauy R, Birch DG. A randomized controlled trial of early dietary supply of long-chain polyunsaturated fatty acids and mental development in term infants. *Dev Med Child Neurol*. 2000;42:174–81.

8. Mcnamara RK, Able J, Jandacek R, Rider T, Tso P, Eliassen JC, Alfieri D, Weber W, Jarvis K, et al. Docosahexaenoic acid supplementation increases prefrontal cortex activation during sustained attention in healthy boys : a placebo-controlled , dose-ranging , functional magnetic resonance imaging study. *Am J Clin Nutr*. 2010;91:1060–7.

9. Isaacs EB, Fischl BR, Quinn BT, Chong WUIK, Gadian DG, Lucas A. Impact of breast milk on intelligence quotient , brain size , and white matter development. *Pediatr Res*. 2010;67:357–62.

10. Reynolds a. Breastfeeding and brain development. *Pediatr Clin North Am*. 2001;48:159–71.

11. Anderson JW, Johnstone BM, Remley DT. Breast-feeding and cognitive development: a meta-analysis. *Am J Clin Nutr*. 1999;70:525–35.

12. Deoni SCL, Dean DC, Piryatinsky I, O'Muircheartaigh J, Waskiewicz N, Lehman K, Han M, Dirks H. Breastfeeding and early white matter development: A cross-sectional study. *Neuroimage*. Elsevier B.V.; 2013;82:77–86.

13. Cunnane SC, Francescutti V, Brenna JT, Crawford MA. Breast-fed infants achieve a higher rate of brain and whole body docosahexaenoate accumulation than formula-fed infants not consuming dietary docosahexaenoate. *Lipids*. 2000;35:105–11.

14. Jacobi SK, Odle J. Nutritional factors influencing intestinal health of the neonate. *Adv Nutr*. 2012;3:687–96.

15. Koletzko B, Lien E, Agostoni C, Bohles H, Campoy C, Cetin I, Decsi T. The roles of long-chain polyunsaturated fatty acids in pregnancy, lactation and infancy: review of current knowledge and consensus recommendations. *J Perinat Med*. 2008;36:5–14.

16. Goyens PLL, Spilker ME, Zock PL, Katan MB, Mensink RP. Compartmental modeling to quantify alpha-linolenic acid conversion after longer term intake of multiple tracer boluses. *J Lipid Res*. 2005;46:1474–83.

17. Burdge GC, Jones AE, Wootton SA. Eicosapentaenoic and docosapentaenoic acids are the principal products of α-linolenic acid metabolism in young men. *Br J Nutr*. 2002;88:355–63.

18. Bradbury J. Docosahexaenoic acid (DHA): an ancient nutrient for the modern human brain. *Nutrients*. 2011;3:529–54.

19. Liu L, Bartke N, Van Daele H, Lawrence P, Qin X, Park HG, Kothapalli K, Windust A, Bindels J, et al. Higher efficacy of dietary DHA provided as a phospholipid than as a triglyceride for brain DHA accretion in neonatal piglets. *J Lipid Res*. 2014;55:531–9.

20. Carnielli VP, Verlato G, Pederzini F, Luijendijk I, Boerlage A, Pedrotti D, Sauer PJ. Intestinal absorption of long-chain polyunsaturated fatty acids in preterm infants fed breast milk or formula. *Am J Clin Nutr*. 1998;67:97–103.

21. Mathews S a, Oliver WT, Phillips OT, Odle J, Diersen-Schade D a, Harrell RJ. Comparison of triglycerides and phospholipids as supplemental sources of dietary long-chain polyunsaturated fatty acids in piglets. *J Nutr*. 2002;132:3081–9.

22. Jensen RG, Hagerty MM, McMahon KE. Lipids of human milk and infant formulas: a review. *Am J Clin Nutr*. 1978;31:990–1016.

23. Kennedy K, Fewtrell MS, Morley R, Abbott R, Quinlan PT, Wells JCK, Bindels JG, Lucas A. Double-blind, randomized trial of a synthetic triacylglycerol in formula-fed term infants: effects on stool biochemistry , stool biochemistry, stool characteristics, and bone mineralization. *Am J Clin Nutr*. 1999;70:920–7.

24. Rytych JL, Elmore MRP, Burton MD, Conrad MS, Donovan SM, Dilger RN, Johnson RW. Early life iron deficiency impairs spatial cognition in neonatal piglets. *J Nutr*. 2012;142:2050–60.

25. Boleman SL, Graf TL, Mersmann HJ, Su DR, Krook LP, Savell JW, Park YW, Pond WG. Pigs fed cholesterol neonatally have increased cerebrum cholesterol as young adults. *J Nutr*. 1998;128:2498–504.

26. Alessandri JM, Goustard B, Durand PGG. Polyunsaturated fatty acids status in blood , heart , liver , intestine , retina and brain of newborn piglets fed either sow milk or a milk replacer diet Polyunsaturated fatty acids status. *Reprod Nutr Dev*. 1995;36:95–109.

27. Odle J, Lin X, Jacobi SK, Kim SW, Stahl CH. The suckling piglet as an agrimedical model for thestudy of pediatric nutrition and metabolism. *Annu Rev Anim Biosci*. 2014;2:419–44.

28. Dobbing J, Sands J. Comparative aspects of the brain growth spurt. *Early Hum Dev*. 1979;3:79–83.

29. Amate L, Gil A. Feeding Infant Piglets Formula with Long-Chain Polyunsaturated Fatty Acids as Triacylglycerols or Phospholipids Influences the Distribution of These Fatty Acids in Plasma Lipoprotein Fractions 1. *J Nutr*. 2001;1250–5.

30. Houle V, Schroeder E, Odle J, Donovan S. Small intestinal disaccharidase activity and ileal villus height are increased in piglets consuming formula containing recombinant human insulin-like growth factor-I. *Pediatr Res*. 1997;42:78–86.

31. Iji P a, Saki A, Tivey DR. Body and intestinal growth of broiler chicks on a commercial starter diet. 1. Intestinal weight and mucosal development. *Br Poult Sci*. 2001;42:505–13.

32. Campbell JM, Fahey GC, Lichtensteiger C a, Demichele SJ, Garleb K a. An enteral formula containing fish oil, indigestible oligosaccharides, gum arabic and antioxidants affects plasma and colonic phospholipid fatty acid and prostaglandin profiles in pigs. *J Nutr*. 1997;127:137–45.

33. *AOAC: official methods of analysis*. (1984). Arlington, VA. Retrieved from http://archive.org/stream/gov.law.aoac.methods.1.1990/aoac.methods.1.1990_djvu.txt

34. Lepage G, Roy CC. Direct transesterification of all classes of lipids in one-step reaction. *J Lipid Res*. 1986;27:114–20.

35. Sukhija PS, Palmquist DL. Rapid method for determination of total fatty acid content and composition of feedstuffs and feces. *J Agric Food Chem*. 1988;36:1202–6.

36. Budde E. The determination of fat in baked biscuit type of dog foods. *J assoc agric chem*. 1952;35:799–805.

37. *AOAC: official methods of analysis*. (2002). Retrieved from http://archive.org/stream/gov.law.aoac.methods.1.1990/aoac.methods.1.1990_djvu.txt

38. Ziegler EE. Growth of Breast-Fed and Formula-Fed Infants. 2006 p. 51–63.

39. Dewey K. Growth characteristics of breast-fed compared to formula-fed infants. *Biol Neonate*. 1998;74:94–105.

40. Demmers T a, Jones PJH, Wang Y, Krug S, Creutzinger V, Heubi JE. Effects of early cholesterol intake on cholesterol biosynthesis and plasma lipids among infants until 18 months of age. *Pediatrics*. 2005;115:1594–601.

41. Dietschy JM, Turley SD. Thematic review series: brain Lipids. Cholesterol metabolism in the central nervous system during early development and in the mature animal. *J Lipid Res*. 2004;45:1375–97.

42. Saher G, Brügger B, Lappe-Siefke C, Möbius W, Tozawa R, Wehr MC, Wieland F, Ishibashi S, Nave K-A. High cholesterol level is essential for myelin membrane growth. *Nat Neurosci* [Internet]. 2005 [cited 2014 Dec 10];8:468–75. Available from: http://www.ncbi.nlm.nih.gov/pubmed/15793579.

43. Lütjohann D, Stroick M, Bertsch T, Kühl S, Lindenthal B, Thelen K, Andersson U, Björkhem I, Bergmann Kv K Von, Fassbender K. High doses of simvastatin, pravastatin, and cholesterol reduce brain cholesterol synthesis in guinea pigs. *Steroids*. 2004;69:431–8.

44. Cowan FM. Magnetic resonance imaging of the normal infant brain: term to 2 years. MRI of Neonatal Brain. 1st ed. 2002.

45. Brossard N, Croset M, Normand S, Pousin J, Lecerf J, Ladle M, Tayot JL, Laennec FDMR, Modclisation L De. Human plasma albumin transports DHA in two lipid forms to blood cells. *J Lipid Res*. 1997;38:1571–82.

46. Rapoport SI. In vivo fatty acid incorporation into brain phosholipids in relation to plasma availability, signal transduction and membrane remodeling. *J Mol Neurosci*. 2001;16:243–62.

47. Thies F, Pillon C, Moliere P, Lagarde M, Lecerf J. Preferential incorporation of sn-2 lysoPC DHA over unesterified DHA in the young rat brain. *Am J Physiol Endocrinol Metab*. 1994;267:R1273–R1279.

48. Thies F, Delachambre MC, Bentejac M, Lagarde M, Lecerf J. Unsaturated fatty acids esterified in 2-acyl-1-lysophosphatidylcholine bound to albumin are more efficiently taken up by the young rat brain than the unesterified form. *J Neurochem*. 1992;59:1110–6.

49. Martin RE, Wickham JQ, Om A, Sanders J, Ceballos N. Uptake and Incorporation of Docosahexaenoic Acid (DHA) into Neuronal Cell Body and Neurite / Nerve Growth Cone Lipids : Evidence of Compartmental DHA Metabolism in Nerve Growth Factor-Differentiated PC12 Cells. *Neurochem Res*. 2000;25:715–23.

50. Foote D, Mackinnon J, Innis M. Brain synaptosomal, liver, plasma and red blood cell lipids in piglets fed exclusively on a vegetable-oil-containing formula with and without fish-oil supplements. *Am J Clin Nutr*. 1990;51:1001–6.

51. DeMan JM, Bowland J. Fatty acid composition of sow ' s colostrum, milk and body fat as determined by gas-liquid chromatography. *J Dairy Res*. 1963;30:339–43.

52. Hamilton RMG, McDonald BE. Effect of dietary fat source on the apparent digestibility of fat and the composition of fecal lipids of the young pig. *J Nutr*. 1968;97:33–41.

53. Morgan C, Davies L, Corcoran F, Stammers J, Colley J, Spencer SA, Hull D. Fatty acid balance studies in term infants fed formula milk containing long-chain polyunsaturated fatty acids. *Acta Paediatr*. 1998;87:136–42.

54. Watkins J. Lipid digestion and absorption. *Pediatrics*. 1985;75:151–6.

55. Le Huërou-Luron I, Blat S, Boudry G. Breast- v. formula-feeding: impacts on the digestive tract and immediate and long-term health effects. *Nutr Res Rev*. 2010;23:23–36.

56. Thompson F, Catto-Smith A, Moorde D, Davidson G, Cummins A. Epithelial growth of the small intestine in human infants. *J Pediatr Gastroenterol Nutr*. 1998;26:506–12.

57. Calviello G, Palozza P, Maggiano N, Piccioni E, Franceschelli P, Frattucci A, Di Nicuolo F, Bartoli GM. Cell proliferation, differentiation, and apoptosis are modified by n-3 polyunsaturated fatty acids in normal colonic mucosa. *Lipids*. 1999;34:599–604.

58. Boudry G, Douard V, Mourot J, Lalle J, Huerou-luron I. Linseed oil in the maternal diet during gestation and lactation modifies fatty acid composition , mucosal architecture , and mast cell regulation of the ileal barrier in piglets. *J Nutr*. 2009;139:1110–7.

Tables

Table 3.1 Nutrient composition of experimental artificial formulas and reference sow milk values

	Experimental Treatment[1]						
	per kg of DM			per L of formula			per L of sow milk
	T1	T2	T3	T1	T2	T3	Reference[2]
Proximate analysis							
Energy, kcal	1179	1197	1154	1129	1143	1102	1000
Density, g	5.11	5.03	5.07	-	-	-	-
Total solids, %	-	-	-	20.45	20.83	20.67	-
Protein, g	249.6	251.2	256.2	53.3	54.8	55.5	55
Crude fat, g	329.6	337.5	306.7	70.4	73.6	66.4	55
Ash, g	47.92	55.21	56.12	10.23	12.04	12.15	-
Lipid profile							
Linoleic acid, g	72.03	58.76	65.55	15.38	12.82	14.20	0.715
α-Linolenic acid, g	7.78	4.61	6.29	1.66	1.01	1.36	0.033
Arachidonic acid, g	1.467	1.488	1.548	0.313	0.325	0.335	0.061
Docosahexaenoic acid, g	0.685	0.672	0.726	0.146	0.147	0.157	0.006
Cholesterol, mg	-	-	-	-	-	280	-
Lecithin, g	-	-	-	-	-	7.3	-
Minerals							
Calcium, g	7.29	9.79	10.06	1.56	2.14	2.18	-
Chloride, g	5037	4945	4935	1076	1078	1069	-
Copper, mg	5.38	5.42	5.32	1.15	1.18	1.15	-
Iodide, µg	1614	2208	2177	344.6	481.6	471.5	-
Iodine, µg	2748	2252	2240	586.9	491.0	485.1	-
Iron, mg	109.05	115.70	111.76	23.29	25.23	24.20	-
Magnesium, mg	899.76	868.94	899.85	192.15	189.51	194.87	-
Manganese, mg	0.83	0.89	0.98	0.18	0.19	0.21	-

Table 3.1 Nutrient composition of experimental artificial formulas and reference sow milk values continued

Molybdenum, µg	295.8	274.6	306.7	63.2	59.9	66.4	-
Phosphorus, g	4.45	4.48	4.80	0.95	0.98	1.04	-
Potassium, g	10.32	10.95	10.93	2.20	2.39	2.37	-
Selenium, µg	333.5	347.6	336.7	71.2	75.8	72.9	-
Sodium, g	3.89	3.78	3.88	0.831	0.824	0.841	-
Zinc, mg	50.86	54.25	52.73	10.86	11.83	11.42	-
Vitamins							
A, IU	32910	27796	35704	7028	6062	7732	-
D_3, IU	6210.3	5760.9	6628.0	1326.3	1256.4	1435.4	-
E, mg	113.45	100.82	112.72	32.95	29.90	33.20	-
K, µg	1535.45	1137.78	1369.13	327.91	248.14	296.50	-
B1,Thiamine, mg	11.59	11.38	11.51	2.47	2.48	2.49	-
B2, Riboflavin, mg	13.64	13.35	13.26	2.91	2.91	2.87	-
B3, Niacinamide, mg	72.86	72.97	71.60	15.56	15.91	15.51	-
B5, Pantothenic Acid, mg	49.88	51.37	48.38	10.65	11.20	10.48	-
B6, Pyridoxine, mg	3.69	3.73	3.70	0.79	0.81	0.80	-
B7, Biotin, µg	567.24	528.08	532.17	121.14	115.17	115.25	-
B9, Folic Acid, µg	1633.3	1517.0	1412.7	348.8	330.9	305.9	-
B12, µg	60.64	53.29	58.54	12.95	11.62	12.68	-
C, mg	1100.24	921.75	1146.59	234.97	201.02	248.30	-
Choline, mg	1545.23	1445.03	2186.74	330.00	315.15	473.56	-
Lutein, µg	4.16	4.37	5.22	890.00	950.00	1130.00	-

[1]Experimental treatments include T1, artificially-reared control; T2, PDF; T3, PDF + lecithin + cholesterol.
[2] Reference values obtained from Foote et al., 1990.

Table 3.2 Growth performance of artificially-reared (AR) and sow-reared piglets (SR)[1]

	Experimental Treatment[2]				*P*-value	
Variable[3]	**T1**	**T2**	**T3**	**SR Reference**	**Treatment**	**Sex**
n	9	10	10	10		
Initial BW (d 2), kg	1.51 ± 0.10	1.49 ± 0.09	1.51 ± 0.09	1.59 ± 0.10	0.965	0.159
Final BW (d 27), kg	5.12 ± 0.32	5.08 ± 0.31	5.46 ± 0.31	8.47 ± 0.47	0.582	0.277
Overall BW gain, kg	3.60 ± 0.28	3.58 ± 0.27	3.96 ± 0.27	6.91 ± 0.43	0.482	0.340
Week 1	36.80 ± 9.26	50.46 ± 8.83	47.74 ± 8.83	199.10 ± 13.76	0.542	0.818
Week 2	123.80 ± 14.33	116.60 ± 13.91	138.90 ± 13.91	290.50 ± 18.07	0.317	0.862
Week 3	227.90 ± 15.84	224.90 ± 15.11	246.60 ± 15.11	235.20 ± 18.74	0.558	0.497
Overall	144.05 ± 11.05	143.39 ± 10.71	158.26 ± 10.69	276.88 ± 16.00	0.482	0.340

[a-b]Means within a row lacking a common superscript letter differ ($P < 0.05$).
[1]Values are presented as means ± SEM.
[2]Experimental treatments include AR (T1-T3) and SR groups. T1, AR control; T2, PDF; T3, PDF + lecithin + cholesterol. Reference values obtained from SR piglets were not included in the statistical analysis when comparing treatments.
[3]Abbreviations: BW, body weight.

Table 3.3 Organ growth of artificially-reared (AR) and sow-reared (SR) piglets[1]

	Experimental Treatment[2]				*P-value*	
Response variable[3]	**T1**	**T2**	**T3**	**SR Reference**	**Treatment**	**Sex**
n	9	10	10	10		
Absolute brain weight, g	41.79 ± 1.345	40.38 ± 1.293	40.76 ± 1.293	46.17 ± 1.328	0.680	0.92
Relative brain weight, %[4]	0.84 ± 0.055	0.82 ± 0.052	0.75 ± 0.052	0.59 ± 0.056	0.448	0.11
GIT weight, g	342.64 ± 31.351	343.76 ± 30.690	384.74 ± 30.690	284.20 ± 31.588	0.226	0.07
GIT weight, %[4,5]	6.75 ± 0.454	6.68 ± 0.450	7.01 ± 0.450	3.41 ± 0.376	0.376	0.05
GIT length, m	7.67 ± 0.575	7.88 ± 0.567	7.48 ± 0.567	6.59 ± 0.527	0.621	0.90
GIT length, %[4]	0.16 ± 0.009	0.16 ± 0.009	0.14 ± 0.009	0.08 ± 0.009	0.178	0.18
n	7	8	8	8		
Liver weight, g	226.44 ± 26.094	224.63 ± 24.877	254.80 ± 25.047	249.99 ± 23.126	0.491	0.54
Liver weight, %[4]	4.49 ± 0.217	4.37 ± 0.208	4.61 ± 0.209	2.68 ± 0.187	0.569	0.94

[1]Values are presented as means ± SEM with threshold for significance set at $P < 0.05$.
[2]Experimental treatments include AR (T1-T3) groups. T1, AR control; T2, PDF; T3, PDF + lecithin + cholesterol. Reference values obtained from SR piglets were not included in the statistical analysis when comparing treatments.
[3]Abbreviations: GIT, gastrointestinal tract.
[4]Expressed relative to body weight at d27 of age.
[5]Relative GIT weight was greater ($P < 0.05$) in female piglets when compared with male pigs.

Table 3.4 Serum lipid concentrations (mg/dL) in artificially-reared (AR) and sow-reared (SR) piglets [1]

	Experimental Treatment[2]				*P*-value	
Response Variable[3]	**T1**	**T2**	**T3**	**SR Reference**	**Treatment**	**Sex**
Day 0[4]						
n	9	10	10	10		
TAG, mg/dl	113.6 ± 30.35	92.7 ± 29.48	130.2 ± 29.48	134.3 ± 31.12	0.481	0.839
HDL, mg/dl	26.4 ± 3.78	23.4 ± 3.70	24.4 ± 3.70	29.4 ± 4.33	0.646	0.990
LDL, mg/dl	36.8 ± 5.78	35.1 ± 5.65	30.3 ± 5.65	40.9 ± 7.00	0.424	0.557
Cholesterol, mg/dl	85.6 ± 13.16	76.9 ± 12.99	80.9 ± 12.99	97.2 ± 15.40	0.635	0.678
Day 14[4]						
n	9	10	10	10		
TAG, mg/dl	64.8 ± 11.88	91.1 ± 11.33	93.8 ± 11.33	119.4 ± 10.72	0.176	0.572
HDL, mg/dl	45.6 ± 4.23	44.3 ± 4.06	45.2 ± 4.06	75.7 ± 3.80	0.968	0.809
LDL, mg/dl	17.2 ± 2.37	24.4 ± 2.28	20.7 ± 2.28	86.9 ± 6.70	0.069	0.549
Cholesterol, mg/dl	75.6 ± 5.73	87.1 ± 5.46	84.5 ± 5.46	186.5 ± 8.30	0.339	0.723
Day 25[4]						
n	8	10	8	9		
TAG, mg/dl	44.9 ± 12.43	40.0 ± 12.10	55.7 ± 12.43	71.4 ± 12.03	0.164	0.510
HDL, mg/dl[5]	30.8 ± 2.83[b]	38.7 ± 2.65[a]	41.2 ± 2.83[a]	69.4 ± 3.51	0.005	0.057
LDL, mg/dl	29.8 ± 3.46	32.5 ± 3.18	34.3 ± 3.46	96.3 ± 5.50	0.548	0.867
Cholesterol, mg/dl	69.0 ± 6.91[b]	76.0 ± 6.60[ab]	86.2 ± 6.91[a]	180.3 ± 7.02	0.031	0.108

[a-b] Means within a row lacking a common superscript letter differ ($P < 0.05$).

[1]Values are presented as means ± SEM.

[2]Experimental treatments include AR (T1-T3) groups. T1, AR control; T2, PDF; T3, PDF + lecithin + cholesterol. Reference values obtained from SR piglets were not included in the statistical analysis when comparing treatments.

[3]Abbreviations: TAG, triacylglycerol; HDL, high-density lipoprotein; LDL, low-density lipoprotein; CHOL, cholesterol.

[4]Serum samples were collected on d0, d14 and d25 of study which coincides with d1, d16, and d27 of life.

[5]D27 serum HDL concentrations (mg/dL) were higher in female piglets when compared with male piglets.

Table 3.5 Hippocampi and red blood cell (RBC) concentrations of DHA in artificially-reared (AR) and sow-reared (SR) piglets[1]

	Experimental Treatment[2]				*P*-value	
Sample Type[3]	**T1**	**T2**	**T3**	**SR Reference**	**Treatment**	**Sex**
n	8	10	10	10		
RBC PL	9.4 ± 2.71[ab]	13.0 ± 2.73[a]	7.3 ± 2.78[b]	4.2 ± 2.81	0.052	0.902
RBC NL	4.8 ± 1.32	5.1 ± 1.12	4.1 ± 1.41	4.3 ± 0.88	0.849	0.727
HP PL	125.5 ± 83.05	138.6 ± 76.77	263.9 ± 76.77	116.1 ± 75.88	0.240	0.074
HP NL	20.9 ± 3.39[b]	24.7 ± 3.17[ab]	30.1 ± 3.17[a]	23.0 ± 3.09	0.041	0.966
Brain accretion, PL[4]	5359 ± 3582.5	6078 ± 3324.2	10706 ± 3324.2	5556 ± 3364.9	0.310	0.073
Brain accretion, NL[4]	868 ± 131.2[b]	997 ± 120.5[ab]	1215 ± 120.5[a]	1053 ± 120.5	0.084	0.813
RBC PL[5]	92.94	93.26	94.97	95.49	-	-
RBC NL[5]	7.06	6.74	5.03	4.51	-	-
HP PL[5]	28.45	24.82	28.44	37.61	-	-
HP NL[5]	71.55	75.18	71.56	62.39	-	-

[a-b] Means within a row lacking a common superscript letter differ ($P < 0.05$).

[1]Phospholipid and neutral lipid concentrations (µg/g tissue) of DHA from hippocampal tissue and RBC. Data are presented as mean ± SEM.

[2]Experimental treatments include AR (T1-T3) groups. T1, AR control; T2, PDF; T3, PDF + lecithin + cholesterol. Reference values obtained from SR piglets were not included in the statistical analysis when comparing treatments.

[3]Abbreviations: RBC, red blood cell; HP, hippocampus; PL, phospholipid; NL, neutral lipid.

[4]Brain accretion calculated from µg/g tissue * absolute whole brain weight (g) at 27 d of age.

[5]Values depict percentage of DHA accretion in the PL and NL fractions as a proportion of DHA present in both fractions combined.

Table 3.6 Percentage of fat in fecal samples from artificially-reared (AR) and sow-reared (SR) piglets[1]

	Experimental Treatment[2]				*P*-value	
Item	**T1**	**T2**	**T3**	**SR Reference[3]**	**Treatment**	**Sex**
n	5	10	10	8		
Fecal dry matter, %	38.5 ± 3.50	40.6 ± 2.73	38.3 ± 2.73	54.3 ± 1.33	0.813	0.539
Fecal organic matter, %	88.2 ± 1.08[a]	86.0 ± 0.89[ab]	85.1 ± 0.89[b]	88.4 ± 0.58	0.037	0.929
Fecal fat, % DM	35.8 ± 4.89	47.6 ± 3.66	49.2 ± 3.66	68.1 ± 2.52	0.058	0.298
Fecal fat, % OM	40.5 ± 5.35[b]	55.3 ± 3.96[a]	57.7 ± 3.96[a]	77.2 ± 3.19	0.029	0.303

[a-b] Means within a row lacking a common superscript letter differ ($P < 0.05$).

[1]Percentage of acid-hydrolyzed fat and organic matter (OM) in fecal matter. Samples were collected from d 13-17 of study and pooled for all analyses. Data are presented on a dry matter (DM) basis as means ± SEM.

[2]Experimental treatments include AR (T1-T3) groups. T1, AR control; T2, PDF; T3, PDF + lecithin + cholesterol. Reference values obtained from SR piglets were not included in the statistical analysis when comparing treatments.

[3]Reference values obtained from sow-reared animals that were not part of this study.

Figures

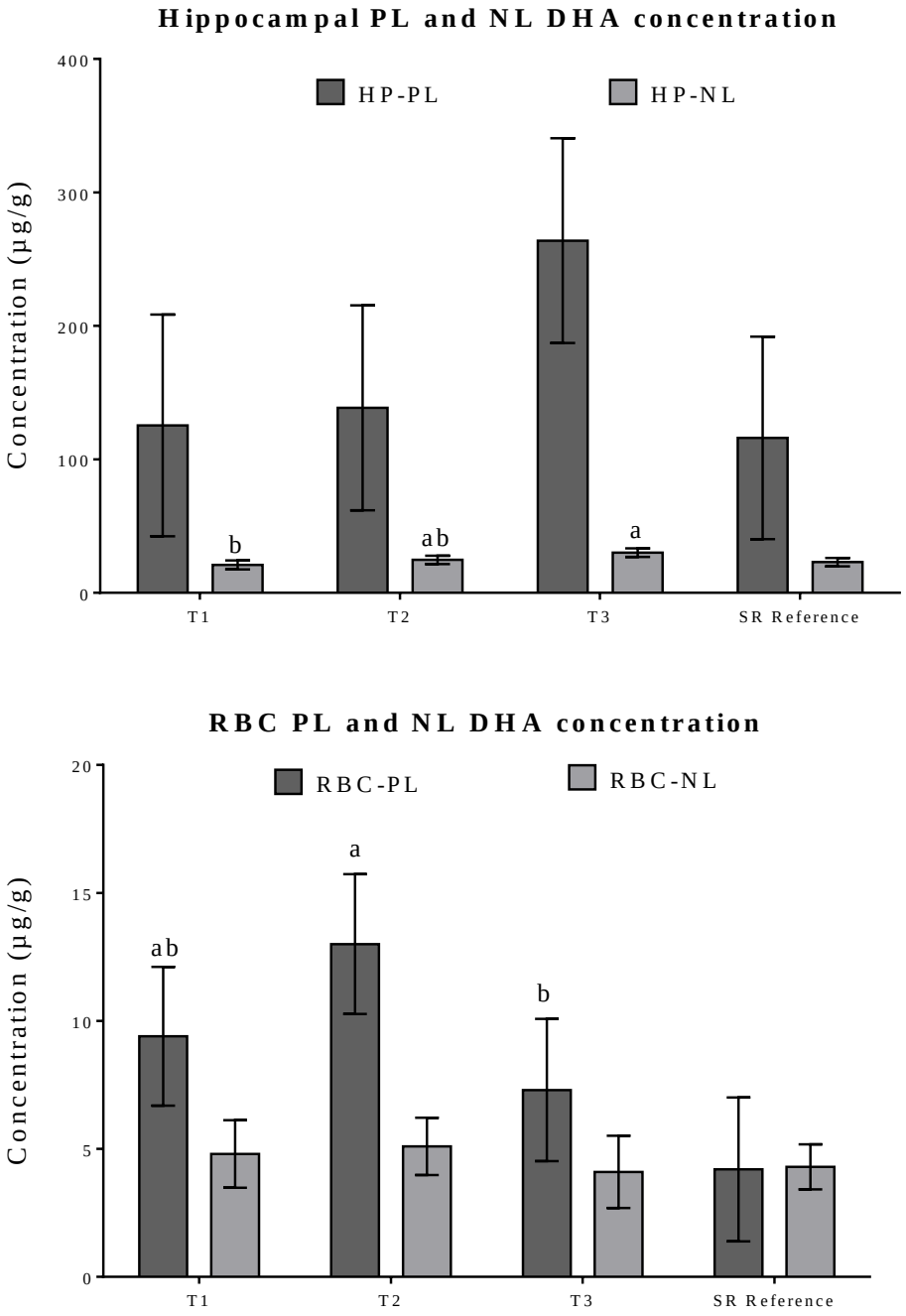

Figure 3.1 Concentration of hippocampal (HP) and red blood cell (RBC) DHA in the phospholipid (PL) and neutral lipid (NL) fractions are presented. Phospholipid bound DHA concentrations in RBC were not different ($P > 0.05$) between T1 v T2 and T1 v T3. Neutral lipid bound DHA in hippocamapal tissue were not different ($P > 0.05$) between T1 and T2, but DHA concentrations were higher in T2 and T3. Experimental treatment groups include artificially-reared piglets fed T1, Control; T2, PDF; T3, PDF + Lecithin + Cholesterol. Reference values obtained from sow-reared (SR) piglets were not included in the statistical analysis when comparing treatments.

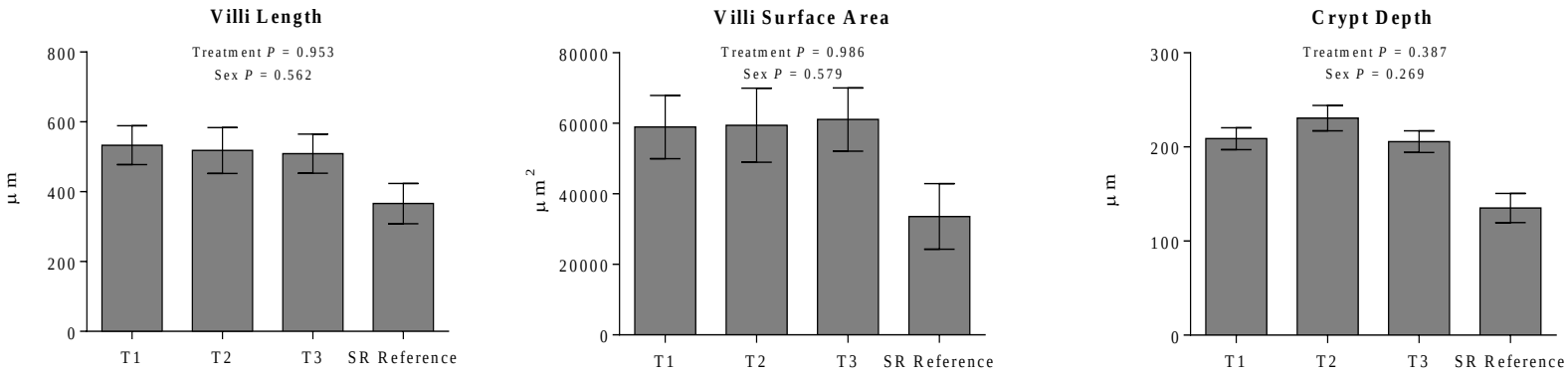

Figure 3.2 Histological analysis of brush border development, as assessed by villi length, surface area, and crypt length, revealed shorter ($P < 0.05$) crypt depth depth in T4 piglets when compared with T1-T3 fed piglets. Experimental treatment groups include artificially-reared piglets fed T1, Control; T2, PDF; T3, PDF + Lecithin + Cholesterol. Sow-reared (SR) reference piglets were not included in statistical analysis when comparing treatments.

Chapter 4

COMPARISON OF BRAIN DEVELOPMENT IN SOW-REARED AND ARTIFICIALLY-REARED PIGLETS

Abstract

Provision of nutrients immediately following birth is critical for proper growth and development of the neonate, but the impact of nutritional composition of breast milk on neural maturation has yet to be determined. Using the piglet as a model for the human infant, our objective was to compare maternal sow's milk with artificial formula on postnatal neurodevelopmental patterns. Over a 25-day feeding study, piglets (n=9-10 per treatment, 1.5 ± 0.2 kg initial BW) were either sow-reared (SR) with *ad libitum* intake, or artificially-reared (AR) receiving 1 of 3 milk replacers modified to mimic the nutritional profile and intake pattern of sow's milk. Our AR treatments included: T1, artificially-reared (AR) control formula; T2, T1 + 45% total dietary fat replaced with pre-digested fat (PDF); T3, T2 + 10% lecithin + 0.4% cholesterol. At study conclusion, piglets were subjected to a standardized set of magnetic resonance imaging (MRI) procedures to quantify structure and composition of the brain. Diffusion tensor imaging, an MRI sequence that characterizes brain microstructure, revealed that SR piglets had greater ($P < 0.05$) average whole-brain fractional anisotropy (FA) values compared with AR piglets, suggesting differences in white matter organization. Although global analysis did not reveal differences within AR treatments for DTI outcomes, FA values of the internal capsule were not different between SR and T3-fed piglets, suggesting a modulatory effect of PDF + lecithin + cholesterol fat system on white matter maturation. Voxel-based morphometric analysis, a measure of white and grey matter volumes, revealed differences ($P < 0.05$) in bilateral development of grey matter clusters in the cortical brain regions of the AR piglets compared with SR piglets. Region of interest (ROI) analysis revealed larger ($P < 0.05$)

whole brain volumes in SR animals compared with AR, and subcortical regions to be larger ($P < 0.05$) as a percentage of whole-brain volume in AR piglets compared with SR animals. Quantification of brain metabolites using magnetic resonance spectroscopy revealed SR piglets had higher ($P < 0.05$) concentrations of myo-inositol, N-acetylasparate + N-acetylaspartylglutamate, glycerophosphocholine + phosphocholine, and creatine + phosphocreatine compared with AR piglets. Overall, increases in these metabolite concentrations, coupled with greater FA values in white matter tracts and volume differences in grey matter of specific brain regions, suggest greater myelin development and cell proliferation in SR vs. AR piglets.

Introduction

Early-life nutrition, whether provided as breast milk, infant formula, or the combination, may influence structural development, as well as cognitive and behavioral development of the child. Epidemiological findings suggest a positive impact of breastfeeding on motor, problem solving and personal-social outcomes when controlling for confounding variables (1). An increasing number of neuroimaging and cognitive studies positively correlate consumption of breast milk (BM) and duration of breastfeeding with macro- and microstructural maturation of the infant brain, along with improved performance on cognitive testing in adolescence (2,3). The brain is only second to adipose tissue in lipid content, hence the high concentration of n-3 long chain polyunsaturated fatty acids (LCPUFA) in breast milk is considered to be highly influential in infant brain development (4). Specifically, docosahexaenoic acid (DHA) is a notable n-3 LCPUFA hypothesized to drive the enhanced impact of BM on the structural integrity and cognitive development of the infant brain. As a structural component of the neuronal plasma membrane, DHA is highly incorporated into glycerophospholipids, and may play a role in

maintaining integrity of electrical activity within the neuron. Concentration of BM DHA varies according to maternal diet, but an average concentration of 0.2-0.3 g of DHA/100 g of total fatty acids has been noted in North American, European and Australian women (5,6). Due to its neuro-augmenting nature, DHA was approved as an additive to infant formula in 2002 at concentrations similar to those found in BM (7,8). Despite the length of time DHA has been supplemented in infant formulas, it is surprising that the impact of added DHA on infant brain development is not yet fully understood.

Neuroimaging techniques employed to assess brain development include diffusion tensor imaging (DTI), magnetization prepared rapid gradient-echo (MPRAGE) sampling, and magnetic resonance spectroscopy (MRS). Diffusion tensor imaging is a noninvasive method to assess spatial organization and degree of myelination of white matter tracts in the infant brain. The four quantitative measures used in DTI to assess free water diffusion include mean diffusivity (MD), axial diffusivity (AD), radial diffusivity (RD), and fractional anisotropy (FA). Mean diffusivity represents a holistic picture of water diffusivity in the brain (9). Fractional anisotropy assesses the rate and directionality of water diffusivity with in the axonal microenvironment (10). Additionally, AD and RD rates represent diffusion along and across a fiber orientation, respectively, as averaged components of MD. Structural MRI (i.e., MPRAGE) sequences allow for quantification of not only regional volumes, but also grey and white matter volumes, on a voxel-by-voxel basis (11). Lastly, MRS generates a representation of the chemical makeup of the developing brain (12). Each of these measures provides distinct information including neuronal maturation, structural development, and the metabolic profile of the developing brain.

The AR piglet has previously been established in the field of nutritional neuroscience as a relevant translational model for the human infant (13–16). However, to our knowledge,

normative brain development in the SR animal has yet to be characterized. Human neuroimaging research is well ahead of biomedical research in this sense, where the maternally-fed infant has long been identified as the normative standard for brain development against which all other developmental trajectories are measured. Due to the lack of a similar standard in piglet research, a primary objective of this study was to establish the neurodevelopmental trajectory of the SR piglet. Characterization of a normative standard for neurodevelopment in SR piglet will strengthen the model, thereby allowing for current and future conspecific comparisons for structural, functional and cognitive processes. As a secondary objective, nutritional strategies designed to align the lipid composition of human infant formula with that of sow's milk were tested.

Overall, using the piglet as a translational model for the human infant, this study aims to use clinically-relevant MRI techniques to assess the impact of maternal milk and artificial formula on brain development. Three groups of AR piglets consuming human infant formulas modified for the piglet, each with a novel lipid product, were compared with SR piglets.

Materials and Methods

Animals, Housing, and Feeding

Naturally-farrowed piglets (n=10/treatment, 1.5 ± 0.2 kg initial BW; sourced from 10 sows, n=2/treatment from each sow) were obtained from the Imported Swine Research Laboratory herd located at the University of Illinois. Piglets were allowed access to colostrum for up to 48 h, at which point they were allotted to one of 4 experimental treatments for the duration of a 25-d feeding study (conducted using 5 cohorts of piglets). Piglets were housed individually in stainless steel cages (101.6 cm L x 76.2 cm W x 81.28 cm H), and were provided

with a towel and toy (Bio-Serv, Flemington, NJ) for comfort and environmental enrichment. Cages were fitted with vinyl-coated expanded-metal flooring (Tenderfoot/NS^{TM}), which was designed for neonatal piglets, and were also outfitted with a heat lamp and electric heat mat (K&H Manufacturing, Colorado Springs, CO) to maintain home cage temperatures between 23-31°C. A 12-h light/dark cycle was maintained with minimal light provided during dark cycles for the duration of the study.

Artificially-reared animals were fed 1 of 3 isocaloric dietary treatments as follows: T1, AR control formula; T2, T1 + 45% total dietary fat replaced with pre-digested fat (PDF); T3, T2 + 10% lecithin + 0.4% cholesterol. Sow reared animals (T4) remained with their respective mother and litter mates for the duration for the study (**Table 3.1**). Artificially-reared piglets were fed using an automated feeding system that dispensed a pre-determined volume of formula over a period of 13 ± 2 h based on daily BW of piglets. The diets were replaced twice daily and were dispensed from 6 identical reservoirs that were cleaned and sterilized daily. Piglets were fed 285 ml/kg BW, 300 ml/kg BW, and 325 ml/kg BW from 0-7, 8-16, and 18-25 d on study, respectively.

Per agricultural protocols, all piglets were identified at birth using ear notches, needle teeth were removed to prevent harm to littermates and the sow. Moreover, piglets received a supplemental iron injection at 1 d of age, but did not undergo other agricultural processing (i.e., tail docking and castrations). Approximately 5 ml of clostridium perfringens antitoxin C + D (Colorado Serum Company, Denver, CO) was administered subcutaneously as a prophylactic agent at d 2 of age. If piglets developed diarrhea, supplemental water and electrolytes (Pedialyte, Abbott Laboratories, Abbott Park, IL) were provided. Sulfamethoxazole and trimethroprim oral

suspension (50 and 8 mg/mL, respectively, Hi-Tech Pharmacal, Amityville, NY) were given if symptoms were not alleviated after 48 h of exhibiting initial symptoms.

Magnetic Resonance Imaging

Magnetic Resonance Imaging and Anesthesia Overview

All piglets underwent magnetic resonance imaging (MRI) procedures at 21 ± 2 d of age at the Beckman Institute Biomedical Imaging Center using a MAGNETOM Trio 3 Tesla magnet with a Siemens 12-channel head coil. These sequences included magnetization prepared rapid gradient-echo (MPRAGE) and diffusion tensor imaging (DTI) to assess brain macrostructure and microstructure, respectively, as well as magnetic resonance spectroscopy (MRS) to obtain brain metabolite concentrations. In preparation for MRI procedures, anesthesia was induced using an intramuscular injection of telazol:ketamine:xylazine administered at 0.022 mL/kg BW, and maintained with inhalation of isoflurane (98% O_2, 2% isoflurane). Piglets were immobilized during all MRI procedures. Visual observation of a subject's well-being, as well as observations of heart rate, PO_2 and percent of isoflurane were recorded every 5 minutes during the procedure, and every 10 minutes post-procedure until animals recovered. Total scan time for each pig was approximately 60 minutes.

Structural MRI Acquisition and Analysis

A T1-weighted MPRAGE sequence was used to obtain anatomic images of the piglet brain. Three repetitions were acquired using the following parameters: repetition time (TR) = 1900 ms; echo time (TE) = 2.49 ms; inversion time= 900 ms; flip angle = 9°; matrix= 256 x 256; slices = 224; slice thickness = 0.7mm; voxel size=0.7mm x 0.7mm x 0.7mm. Three MPRAGE

data sets from each animal were averaged, and brains were manually extracted using FMRIB Software Library (FSL) (FMRIB Centre, Oxford, UK). Images were realigned using an affine transformation to the same stereotactic space using SPM8 in MATLAB 8.3 with a publically available, population-averaged piglet brain atlas generated by Conrad et al., (www.pigmri.illinois.edu). This process minimized mean square differences between the template and individual sample brains, and aligned position and size of individual images to the atlas.

To complete morphometric analysis of grey and white matter volumes on a voxel-by-voxel basis, GM, WM and cerebrospinal fluid (CSF) were segmented using a tissue probability mask established by the piglet brain atlas. Using a diffeomorphic anatomical registration through exponentiated lie algebra (DARTEL) toolbox in SPM8, an average of all individual brains was obtained to generate an initial study-specific template brain used for registration and spatial normalization of individual brains. Spatial normalization refers to a registration method which allows for warping of images from multiple subjects into the same standard space. This process essentially allows for signal averaging across subjects and corrects for global differences in overall brain shape. Changes from default include a bounding box of -30.1 to 30.1, -35 to 44.8, -28 to 31.5; and a voxel size of 0.7 mm^3. A linear bend energy was used as a cost function, and a 4-mm full-width half maximum (FWHM) smoothing operation was then imposed on the modulated data.

The statistical non-parametric methods (SnPM) toolbox was used to compare modulated grey and white matter data between treatment groups. A designation of 5000 non-parametric permutations were used with a 7-mm FWHW for variance smoothing; ANCOVA was used for global normalization and a mean voxel value was used for global calculation. No covariates were

used, and all other default options were employed. A cluster-level threshold of at least 20 voxels was set, and voxel clusters at the edge of the brain were excluded. Grey and white matter volume differences between treatments were presented in tabulated form with pseudo-t values indicating level of significance, with estimated anatomic regions, as well as the Cartesian coordinate system, indicating an estimated center of significant voxel clusters. Data are also presented as heat maps with corresponding pseudo-t-values. Specific anatomic regions were estimated based on the Saikali atlas of the adult pig, which employed histology to identify individual brain regions (17).

Flow fields generated during the DARTEL procedure were converted to warp fields. The inverse of these warp fields represented a quantifiable amount of shrinkage or expansion of an individual subject's brain in comparison to the study-specific atlas. The inverse warp fields were applied to individual brains to estimate structural volumes for 19 regions of interest. Inverse warps were applied to the region of interest (ROI) maps previously established with the piglet brain atlas, and used brain region volumes in FSL stats.

Diffusion Tensor Imaging Acquisition and Analysis

Diffusion tensor imaging (DTI) was used to assess white matter maturation and axonal tract integrity. Specifically, a diffusion-weighted, echo-planar imaging (DW-EPI) sequence was used with the following parameters: repetition time (TR) = 5000 ms; echo time (TE) = 91 ms; average = 3; diffusion weightings = 2; b value = 1000 s/mm^2 across 30 directions, two images with b-value of 0 s/mm^2; slices = 40, slice thickness = 2.0 mm; final voxel size = 2.0 mm isotropic.

Diffusion-weighted EPI images were assessed in FSL for fractional anisotropy (FA), mean diffusivity (MD), axial diffusivity (AD), and radial diffusivity (RD). Diffusion tensor imaging datasets were manually extracted using standardized procedures. Next, masks for all ROI from the piglet atlas were non-linearly transformed into the subject's MPRAGE space. These ROI were then brought into the DTI space using a linear transformation procedure, and a threshold of 0.15 applied to correct for expansion caused by interpolation. A threshold of 0.5 was applied to known WM segmentation from the MPRAGE sequence and the entire dataset was dilated twice. Average FA values were obtained for these regions with threshold of 0.2 to ensure that only WM was included in the analysis.

Magnetic Resonance Spectroscopy Acquisition and Analysis

Magnetic resonance spectroscopy was used to non-invasively quantify metabolites in both hippocampi, and in intervening tissue. The MRS spin-echo chemical shift sequence was used with the following parameters: repetition time (TR) = 3000 ms; echo time (TE) = 30 ms; average = 128; voxel size = 12 mm x 25 mm x 12 mm centered over the left and right dorsal hippocampi. Both water-suppressed and non-water-suppressed data were collected in institutional units, and all MRS data were analyzed using LC Model (version 6.3). There were two limits placed on MRS data for inclusion in the statistical analysis. Cramer-Tao lower bounds (i.e., % standard deviation) were calculated using the LC Model, and only metabolites with standard deviation less than 20% were considered to have reliable quantitative results of absolute levels. In addition, metabolites included in the analysis were identified in at least 4 subjects per treatment. Metabolite concentrations were expressed in absolute and as a proportion of creatine values, but absolute concentrations were used for statistical analysis as creatine levels fluctuated over treatment groups.

Statistical Analysis

Overall, numerical data obtained from DTI and MRS sequences were subjected to an analysis of variance (ANOVA) using the MIXED procedure in SAS v 9.4. Replicate cohort of pigs was included as a random variable, and the threshold of significance was set at $P < 0.05$. Data collected from a single time-point were analyzed using a one-way ANOVA, and two-sample permutation t-tests were performed to assess differences in MRI outcomes between individual treatments when appropriate. Two-sample permutation t-tests were performed on a voxel-by-voxel basis for grey and white matter volume differences between all AR and SR animals with an uncorrected $P < 0.001$, and between individual AR treatments with an uncorrected $P < 0.01$. Data analysis of ROI volume, DTI components, and metabolite concentrations estimations for effect of treatment and sex were conducted using a two-way ANOVA in MIXED procedure of SAS 9.4. Data are presented as means ± standard error of the mean (SEM) with significance accepted at $P < 0.05$.

Results

Details regarding growth performance, metabolic and intestinal development outcomes associated with this study have previously been discussed (**Figures 3.1-3.3, Tables 3.1-3.6**).

Magnetization-Prepared Rapid Acquisition Gradient Echo

Voxel-based morphometry

Voxel-based morphometric analysis largely revealed effects due to rearing environments. Of the significant voxel clusters identified, those located in the right and left cortex with pseudo-t values of 7.98, 6.54 and 5.33 were estimated in accordance with given x, y and z coordinates to be located in the insular cortex **(Figure 4.1, Table 4.1**). In contrast, WM volume comparison of

SR > AR treatments showed pseudo-t values to be highest in regions located in the olfactory bulbs of the right and left cortices. The following intra-treatment comparisons between AR piglets were also conducted for GM and WM volumes with threshold for statistical significance set at P = 0.01: T1 vs. T2 (**Figure 4.2, Table 4.2**), T1 vs. T3 (**Figure 4.3, Table 4.3**) and T2 vs. T3 (**Figure 4.4, Table 4.4**).

Estimated ROI volumes

Estimation of absolute whole-brain volumes were higher ($P < 0.001$) in SR animals compared to their AR counterparts (**Table 4.6**). However, the incidence at which ROI differed between AR and SR groups decreased, and effects due to sex were more frequently significant, when ROI volumes were expressed as a percent of total brain volume (TBV) (**Table 4.7**). Overall, as a percent of TBV, total hippocampal volume, as well as left and right hippocampal volumes expressed separately, were smaller ($P < 0.05$) in SR piglets compared to their AR counterparts. Ventricular system components including the cerebral aqueduct, fourth ventricle, lateral ventricle and third ventricle were also smaller ($P < 0.05$) as a percent of TBV in SR piglets, with no significant difference in fourth ventricle volume between T3-fed AR piglets and SR piglets. Other ROI including caudate, midbrain and pons were smaller ($P < 0.05$) as a percent of TBV in AR piglets when compared with SR piglets. Volumes of specific ROI including GM, WM, left/right cortex, corpus callosum, caudate, hypothalamus, internal capsule, olfactory bulb, putamen and thalamus were larger ($P < 0.05$) as a percent of TBV in female piglets when compared with males.

Diffusion Tensor Imaging

Average FA values of whole-brain, WM, internal capsule (IC), and right cortex were higher ($P < 0.05$) in SR piglets compared with AR piglets, with no significant differences between AR treatments (**Table 4.8**). Fractional anisotropy of the IC was higher ($P < 0.05$) in SR animals when compared with AR piglets fed either T1 or T2, but no differences were observed between T3 and SR piglets. Average hippocampal FA of female piglets was higher ($P < 0.05$) when compared with their male counterparts. Whole brain MD (**Table 4.10**) and RD (**Table 4.11**) values were lower ($P < 0.05$) in SR animals when compared with AR animals, with no differences observed between AR treatments. Axial diffusivity (**Table 4.9**) of whole-brain was lower ($P < 0.05$) in SR piglets when compared with AR piglets, and higher ($P < 0.05$) in the IC for SR piglets when compared with AR piglets fed T2. A main effect of sex was detected in the right hippocampus, with female piglets exhibiting higher ($P < 0.05$) AD and MD values compared with male piglets.

Magnetic Resonance Spectroscopy

Absolute concentrations of nine metabolites were quantified, with creatine + phosphocreatine (CR-PCR), glycerophosphocholine + phosphocholine (GPC-PCH), myo-inositol (INS), and N-acetylaspartate + N-acetylaspartylglutamate (NAA-NAAG) affected ($P < 0.05$) by treatment (**Table 4.12**). Concentrations of CR-PCR were higher ($P < 0.05$) in SR animals when compared with all AR treatments, with no differences detected between AR treatments. Absolute concentrations of GPC-PCH were higher in SR animals compared with AR piglets, with higher GPC-PCH concentrations detected in T3- vs. T2-fed piglets. Piglets fed T3 exhibited INS concentrations that were not different from SR animals, with the highest values

present in SR piglets and no differences between animals fed T1 or T2. Finally, concentrations of NAA-NAAG were higher ($P < 0.05$) in T3- vs. T2- and T1-fed animals, and there were no differences present between T1- and T2-fed AR piglets, nor T1 and SR animals.

Discussion

Using the piglet as a biomedical model, this study sought to investigate the impact of manipulating the dietary fat matrix found in infant formula on macro- and micro-structural development of the neonatal piglet brain. Artificially-reared animals were raised individually and fed 1 of 3 isocaloric dietary treatments, while SR animals remained with the dam and littermates for duration for the study. Global analysis indicated a steeper neurodevelopmental trajectory in SR animals as characterized by larger whole-brain volumes, higher FA values (indicating greater white matter maturation and myelination of axonal tracts), as well as elevated concentration of metabolites linked to myelin synthesis. Similarities in diffusion characteristics were observed between SR and T3-fed piglets in early-maturing regions, such as the internal capsule, indicating a modulatory effect of the PDF, lecithin and cholesterol fat system on white matter maturation. Furthermore, subcortical region volumes, expressed as proportion of whole-brain volume, were higher in AR animals, suggesting that subcortical regions are preferentially developing in the formula-fed animals at 3 weeks of age.

Region of Interest Volumes

Assessment of absolute brain volumes suggested larger brains in SR vs. AR piglets, with little evidence of sexually-dimorphic effects. Because previous studies have revealed variations in brain development in male and female piglets of this age group (18), we chose to express ROI volumes relative to whole-brain volume. As a percentage of TBV, AR piglets possessed 10 ROI volumes that were different compared with SR piglets. Regions of interest including the left and

right hippocampi, caudate, midbrain, pons, cerebral aqueduct, as well as the fourth, lateral and third ventricles were all proportionally smaller in SR animals when compared with AR animals. When totaled and averaged over all AR treatments, these ROI volumes were 5.81 percentage units larger, as a proportion of TBV, in the AR piglet than in the SR animal. Primarily localized to the subcortical regions, these ROI were mainly sequestered to the limbic system and brain stem, where they are responsible for regulating the most fundamental physiological processes within the brain. Considering that functional hierarchy determines preference for structural development in the neonatal brain (19), we propose that despite a deficit in whole-brain volumes, we still see conserved development of these subcortical regions in piglets fed artificial formula as compared to the SR piglets. Considering whole-brain volumes were considerably smaller in AR animals, compared with their SR counterparts, we expected a decrease in cortical size as a percentage of TBV, but no differences between AR treatments were observed in cortical development. Furthermore, cortical volumes as a proportion of whole-brain volume remained numerically higher in AR animals. This leads us to believe that the volume dedicated to cerebrospinal fluid (CSF) may be smaller in AR animals compared with SR piglets, but this finding has yet to be corroborated.

Typical patterns of postnatal neurodevelopment in healthy infants follow a predictable trajectory, which include competitive elimination of neurons and myelination of axonal tracts (20). Pruning or competitive elimination refers to environmentally regulated changes in the density of synapses per unit of dendritic length, as well as axonal pruning (21). Pruning seems to facilitate higher order functioning in humans (22), and typical patterns of neurodevelopment dictates that large scale synaptogenesis, followed by pruning of non-established connections, occurs before large scale myelination (22). In our study, relative whole-brain GM volume was

numerically lower in SR animals when compared with AR piglets. However, whole-brain FA of SR animals remained higher despite this reduction in GM volume. Such correlation between a reduction in GM volume and increase in FA may indicate greater levels of myelination of the axons in the SR animal. Our interpretation of these data remains speculative, however, as we did not directly assess pruning in our study, and our observations do not fall in line with biological timelines of pruning observed in humans (18,23).

Voxel-based Morphometry

Voxel-based morphometric analysis revealed volumetric differences in both GM and WM between SR and AR groups. Overall, we observed highly-significant differences in GM volume in the frontal-cortical regions of AR animals, while greater WM volumes were revealed in the olfactory areas of SR animals. Most significant GM clusters observed in AR piglets were located bilaterally in the rostral part of the brain. The Saikali atlas estimates that these clusters are localized to the insular cortex (17). The anterior insular cortex is described as an "integrative hub" which processes and directs incoming physiological signals, and is considered a juncture for cognitive and emotional processes (24). Moreover, this region may influence response inhibition of the pre-frontal cortex and activation of the striatum during reward anticipation (25). Similar trends were observed in WM volume of the insular cortex of the left cortex in piglets. As such, the combined higher GM and WM volumes of the insular cortex may indicate greater structural maturity of these regions in AR animals compared with SR piglets.

In SR animals, evidence of highest WM maturation appeared to be localized to the right cortex in the piglet atlas, however, significance was also observed in the somatosensory association cortex, geniculate nuclei, and premotor cortex of the piglet brain based on the Saikali atlas. The somatosensory association cortices integrate somatosensory and visual inputs and

allow improved processing of tactile information (26). Integration of multiple sensory modalities (i.e., touch and sight, or touch and hearing), as well as projections to brain regions in the medial temporal lobe, including the entorhinal and perirhinal cortices and hippocampus, are facilitated by the somatosensory association cortex (27). An increase in WM in this region may suggest a more mature neural network, but such assessments are not fully possible without functional or behavioral outcomes as corroborative evidence.

Diffusion tensor imaging

Diffusion tensor imaging was used to characterize the organization and structural integrity of axonal tracts in the piglet brain. Fractional anisotropy, MD, AD and RD values obtained through DTI techniques provide distinct information regarding WM integrity, and these complementary measures are interdependent in accurately quantifying brain development. Higher FA values of the whole brain, WM, internal capsule, and right cortex of piglets suggested that axonal tract maturity and degree of myelination was highest in SR animals compared with their AR counterparts. These data are consistent with the human literature, which suggests a positive relationship between breastfeeding and development of early-maturing WM regions such as the corpus callosum, internal capsule, corticospinal tract, cerebellum and left optic radiation (2). Extended breast-feeding has also been shown to correlate with myelination in regions associated with language acquisition, sensory motor development, and motor control (2).

In human infant studies, both transverse and parallel diffusivity of free water in early-maturing fiber bundles, such as those found in the internal capsule, are low and accompanied by higher FA values compared with those found in late-maturing subcortical projection and association tracts (28). An increase in FA, partnered with a reduction in free water diffusivity, indicate increased axonal density, pre-myelination, and myelination of established axonal tracts

(29). Of the regions of interest assessed in our study, FA values of the internal capsule were highest, indicating a similar pattern of preferential commissural WM tract development in the piglet when compared with the human infant. In the human infant, myelination is visible in the internal capsule by approximately 3 months of age (30), which correlates with the approximate age at which the piglets underwent MRI. These data further support previously established neurodevelopmental trajectories between the two species (18,23). In addition, the lack of difference in internal capsule FA values between T3-fed and SR animals may suggest the diet directly influences incorporation of LCPUFA in the brain, which may subsequently alter WM maturation.

Magnetic Resonance Spectroscopy

Magnetic resonance spectroscopy provides a measurement of brain metabolites that serve as biomarkers for metabolic efficiency, energy storage, inflammation, structural integrity, and brain integrity (31). Our data reveal CR-PCR concentrations to be higher in SR piglets when compared with AR piglets, and unbound CR concentrations to be numerically lower in T1 and T4 piglets, compared to T2 and T3 piglets. However, it is only in SR piglets that the decrease in unbound CR is compensated for through an increase in phosphate bound CR. The primary role for CR-PCR consist of storing and distributing phosphate-bound energy and serving as a buffer system during low ATP:ADP status (31). During a low energy state, phosphate-bound PCR is paired with ADP, and a phosphate is transferred to ADP to generate CR and ATP. In high energy states, the reverse reaction occurs. Higher levels of phosphate bound CR, when partnered with trends for lower free CR, may indicate higher energy stores in the SR piglets when compared with AR piglets.

N-acetylaspartate is the most abundant metabolite present in the brain, and is heavily involved in oxidative metabolism and myelination. Precursors of NAA are abundantly present when the energy requirements of the cell are met, indicating stability in ATP production and metabolic efficiency(31). N-acetylaspartate is also used to generate myelin precursors in the neuron, and higher concentrations of NAA have been correlated with higher FA values, indicating improved axonal tract integrity, an indirect measure of myelination (31,32). Although our data suggests differences between treatments in NAA-NAAG concentrations, the lack of differences in hippocampal FA values precludes us from correlating NAA concentrations with myelination of hippocampal axons. Myo-inositol cannot cross the blood brain barrier and is primarily synthesized in glial cells, and is therefore considered to be a marker of glial cell proliferation and size (33). No differences in myo-inositol were detected between SR and T3-fed animals, suggesting a similar rate of astrocyte proliferation in these treatment groups.

The substantial role of DHA in maintaining the structural integrity of neuronal plasma membranes (34) lead us to assess whether accretion of DHA within neural tissue correlate with comparable developmental patterns of cortical and subcortical regions in AR and SR animals. Although differences in subcortical ROI volumes as a percentage of TBV were discussed in detail, neither the impact of predigestion of dietary fat, nor the supplementation of lecithin and cholesterol on these outcomes have yet to be discussed. Resistance to dietary nutrient deprivation in hippocampal accretion of PUFA, particularly that of DHA, has been observed in rodents (35). As a separate component of this study, DHA accretion in the hippocampus is higher in piglets fed the PDF system supplemented with lecithin and cholesterol. Animals fed T3 also express lowest numerical variations from subcortical ROI volumes, as percent of TBV, observed in SR animals. Similarities are present in T3 and T4-fed piglets in white matter maturation of the

internal capsule and in hippocampal NAA+ NAAG concentrations. These results are indicative of a positive effect of PDF + lecithin + cholesterol fat system on overall brain development as assessed by MRI techniques.

To our knowledge, this study is the first of its kind to characterize neurodevelopmental patterns of the SR piglet. Although only a single time-point in the invariably changing neonatal neural network was studied, these data provide a foundation for establishing the SR piglet as a biomedical species for studying nutritional neuroscience. Overall results of this study suggest SR piglets experience greater WM maturation at 3 weeks of age compared with AR counterparts. Behavioral assessments are required to ascertain functional implications of the variations in brain macro and microstructure, these data could lay a foundation for future nutritional neuroscience research using the piglet.

Literature Cited

1. McCrory C, Murray A. The effect of breastfeeding on neuro-development in infancy. *Matern Child Health J*. 2013;17:1680–8.

2. Deoni SCL, Dean DC, Piryatinsky I, O'Muircheartaigh J, Waskiewicz N, Lehman K, Han M, Dirks H. Breastfeeding and early white matter development: A cross-sectional study. *Neuroimage*. Elsevier B.V.; 2013;82:77–86.

3. Isaacs EB, Fischl BR, Quinn BT, Chong WUIK, Gadian DG, Lucas A. Impact of breast milk on intelligence quotient , brain size , and white matter development. *Pediatr Res*. 2010;67:357–62.

4. Luchtman DW, Song C. Cognitive enhancement by omega-3 fatty acids from child-hood to old age: findings from animal and clinical studies. *Neuropharmacology*. Elsevier Ltd; 2013;64:550–65.

5. Jensen RG. Lipids in human milk. *Lipids*. 1999;34:1243–71.

6. Innis SM. Human milk: maternal dietary lipids and infant development. *Proc Nutr Soc*. 2007;66:397–404.

7. Jacobi SK, Odle J. Nutritional factors influencing intestinal health of the neonate. *Adv Nutr*. 2012;3:687–96.

8. Koletzko B, Lien E, Agostoni C, Bohles H, Campoy C, Cetin I, Decsi T. The roles of long-chain polyunsaturated fatty acids in pregnancy, lactation and infancy: review of current knowledge and consensus recommendations. *J Perinat Med*. 2008;36:5–14.

9. Wang X. Advanced neuroimaging fundamentals and methods. Diffusion MR Imaging of the Brain. 2014. p. 1–8.

10. Mori S, Zhang J. Principles of diffusion tensor imaging and its applications to basic neuroscience research. *Neuron*. 2006;51:527–39.

11. Ashburner J, Friston KJ. Voxel-based morphometry-the methods. *Neuroimage*. 2000;11:805–21.

12. Soares DP, Law M. Magnetic resonance spectroscopy of the brain: review of metabolites and clinical applications. *Clin Radiol*. The Royal College of Radiologists; 2009;64:12–21.

13. Conrad MS, Dilger RN, Nickolls A, Johnson RW. Magnetic resonance imaging of the neonatal piglet brain. *Pediatr Res*. 2012;71:179–84.

14. Radlowski EC, Conrad MS, Lezmi S, Dilger RN, Sutton B, Larsen R, Johnson RW. A neonatal piglet model for investigating brain and cognitive development in small for gestational age human infants. *PLoS One*. 2014;9:e91951.

15. Rytych JL, Elmore MRP, Burton MD, Conrad MS, Donovan SM, Dilger RN, Johnson RW. Early life iron deficiency impairs spatial cognition in neonatal piglets. *J Nutr*. 2012;142:2050–60.

16. Odle J, Lin X, Jacobi SK, Kim SW, Stahl CH. The suckling piglet as an agrimedical model for thestudy of pediatric nutrition and metabolism. *Annu Rev Anim Biosci*. 2014;2:419–44.

17. Saikali S, Meurice P, Sauleau P, Eliat P-A, Bellaud P, Randuineau G, Vérin M, Malbert C-H. A three dimensional digital segmented and deformable brain atlas of the domestic pig. *J Neurosci Methods*. 2010;192:102–9.

18. Conrad M, Dilger R, Johnson R. Brain growth of the domestic pig (Sus scrofa) from 2 to 24 weeks of age: A longitudinal MRI study. *Dev Neurosci*. 2013;34:291–8.

19. Cowan FM. Magnetic resonance imaging of the normal infant brain: term to 2 years. MRI of Neonatal Brain. 1st ed. 2002.

20. Lenroot RK, Giedd JN. Brain development in children and adolescents: insights from anatomical magnetic resonance imaging. *Neurosci Biobehav Rev*. 2006;30:718–29.

21. Webb SJ, Monk CS, Charles A. Developmental Neuropsychology Mechanisms of Postnatal Neurobiological Development : Implications for Human Development. *Dev Neuropsychol*. 2001;19:147–71.

22. Kolb B, Gibb R. Brain Plasticity and Behaviour in the Developing Brain. *J Can Acad child Adolesc psychiatry*. 2011;20:265–76.

23. Knickmeyer RC, Gouttard S, Kang C, Evans D, Smith JK, Hamer RM, Lin W, Gerig G, John H. A structural MRI study of human brain development from birth to 2 years. *J Neurosci*. 2010;28:12176–82.

24. Menon V, Uddin LQ. Saliency, switching, attention and control: a network model of insula function. *Brain Struct Funct*. 2010;214:655–67.

25. Smith AR, Steinberg L, Chein J. The role of the anterior insula in adolescent decision making. *Dev Neurosci*. 2014;36:196–209.

26. Iwamura Y. Somatosensory association cortices. *Int Congr Ser*. 2003;1250:3–14.

27. Man K, Kaplan J, Damasio H, Damasio A. Neural convergence and divergence in the mammalian cerebral cortex: from experimental neuroanatomy to functional neuroimaging. *J Comp Neurol*. 2013;521:4097–111.

28. Partridge SC, Mukherjee P, Henry RG, Miller SP, Berman JI, Jin H, Lu Y, Glenn O a, Ferriero DM, et al. Diffusion tensor imaging: serial quantitation of white matter tract maturity in premature newborns. *Neuroimage*. 2004;22:1302–14.

29. Berman JI, Mukherjee P, Partridge SC, Miller SP, Ferriero DM, Barkovich a J, Vigneron DB, Henry RG. Quantitative diffusion tensor MRI fiber tractography of sensorimotor white matter development in premature infants. *Neuroimage*. 2005;27:862–71.

30. Cowan FM. Magnetic resonance imaging of the normal infant brain: term to 2 years. MRI of the neonatal brain [Internet]. 2001. Available from: http://www.mrineonatalbrain.com/.

31. Scavuzzo CJ, Larsen RJ. The use of Magnetic Resonance Spectroscopy for assessing the effect of diet on cognition. Unpublished manuscript.

32. Wijtenburg S a, McGuire S a, Rowland LM, Sherman PM, Lancaster JL, Tate DF, Hardies LJ, Patel B, Glahn DC, et al. Relationship between fractional anisotropy of cerebral white matter and metabolite concentrations measured using (1)H magnetic resonance spectroscopy in healthy adults. *Neuroimage*. Elsevier Inc.; 2012;66C:161–8.

33. Rosen Y, Lenkinski RE. Recent advances in magnetic resonance neurospectroscopy. *Neurother J Am Soc Exp Neurother*. 2007;4:330–45.

34. Horrocks L a, Farooqui A a. Docosahexaenoic acid in the diet: its importance in maintenance and restoration of neural membrane function. *Prostaglandins Leukot Essent Fatty Acids*. 2004;70:361–72.

35. Chung W-L, Chen J-J, Su H-M. Fish oil supplementation of control and (n-3) fatty acid-deficient male rats enhances reference and working memory performance and increases brain regional docosahexaenoic acid levels. *J Nutr*. 2008;138:1165–71.

Tables

Table 4.1. Comparison of white matter cluster volumes between artificially-reared (AR) and sow-reared (SR) piglets[1]

Tissue	Comparison	Anatomic Region	Cluster (voxels)	Cluster level (P-value)	x	y	z	Pseudo-t	Saikali ROI[2]
White Matter	SR>AR	Right cortex [3]	522	0.0008	10	10	15	5.66	
		Right cortex	1211	0.0002	3	34	1	5.45	
		Left cortex	191	0.0006	-10	6	17	4.93	Somatosensory association
		Thalamus	94	0.0004	-8	-1	-1	4.68	Geniculate nuclei
		Olfactory	272	0.0006	4	23	-8	4.34	
		Right cortex	22	0.0008	6	20	15	3.27	Premotor cortex
		Undefined	24	0.0006	1	-27	-8	0.09	
		Total voxels	2336						
	AR>SR	Right cortex	1553	0.0002	17	20	10	6.05	
		Left cortex	1863	0.0002	-15	24	10	5.90	Insular cortex
		Left cortex[4]		0.0002	-7	28	13	3.23	Primary somatosensory
		Cerebellum	80	0.0006	-7	-15	-1	5.37	
		Internal capsule	117	0.0002	7	13	6	5.17	
		Undefined	285	0.0008	-6	15	5	5.00	Caudate nucleus
		Right cortex	348	0.0006	10	9	-5	4.96	
		Right cortex	514	0.0002	14	-18	6	4.39	Crus 2 of the ansiform lobule
		Midbrain	224	0.0002	0	-2	-5	4.11	
		Internal capsule	77	0.0004	10	8	3	4.10	
		Midbrain	79	0.0008	5	-5	3	2.68	
		Right cortex	483	0.0008	13	30	9	2.62	
		Medulla	252	0.0008	2	-12	-17	2.61	
		Undefined	28	0.0006	-4	-4	4	2.41	
		Cerebellum	31	0.0008	-4	-18	4	2.26	Cerebellar lobule VI
		Right cortex	50	0.0008	6	16	19	1.42	Primary motor cortex
		Total voxels	4431						

Clusters > 20 were included in analysis with threshold set at $P < 0.001$.

[1]Experimental Treatments include AR (T1-T3) and SR groups. T1, AR control; T2, PDF; T3, PDF + lecithin + cholesterol; T4, SR control.

[2]References the Saikali pig brain atlas which provides more detailed estimation of structures with in cortical regions (17).

[3]Data in this table should be read as follows: 522 voxels in the left cortex contain greater white matter volume in SR pigs in comparison to AR pigs. The center voxel in cluster is located at coordinated 10, 10, and 15 on the x, y, and z plane. Cluster level P = 0.0008 refers to uncorrected P-value associated with pseudo-t value of 5.66.

[4]Missing cluster value is contiguous with voxel cluster listed immediately above, and represents 1 of 2 continuous voxel clusters with 2 different center voxels.

Table 4.2. Comparison of gray matter cluster volumes between artificially-reared (AR) and sow-reared (SR) piglets[1]

Tissue	Comparison	Anatomic Region	Cluster (voxels)	Cluster level (P-value)	x	y	z	Pseudo-t	Saikali ROI[2]
Gray Matter	SR>AR	Right cortex	657	0.0002	14	3	10	5.44	
		Right cortex		0.0008	10	12	13	3.07	
		Olfactory	417	0.0004	-4	25	-8	5.29	
		Undefined	85	0.0002	-9	8	-4	5.26	
		Right cortex	356	0.0004	10	7	-6	5.26	Hippocampus
		Cerebellum	398	0.0002	2	-23	4	5.20	
		Undefined	1032	0.0008	6	34	-1	5.06	Anterior prefrontal cortex
		Cerebellum	149	0.0008	-7	-20	0	4.18	Lateral cerebellar nucleus
		Left cortex	203	0.0002	-4	24	3	3.96	Caudate nucleus
		Left cortex	164	0.0004	-12	4	10	3.88	
		Undefined	74	0.0006	5	24	4	3.69	Caudate nucleus
		Medulla	60	0.0008	3	-22	-15	3.62	
		Cerebellum	24	0.0008	9	-20	-2	3.03	
		Total voxels	3619						
	AR>SR	Right cortex	2149	0.0002	17	14	10	7.98	Insular cortex
		Left cortex	1619	0.0002	-16	14	10	6.54	Insular cortex
		Left cortex[3]		0.0004	-13	24	8	5.33	Insular cortex
		Caudate	469	0.0008	5	10	7	4.82	
		Left cortex	272	0.0002	-17	-1	-4	4.49	Anterior entorhinal cortex
		Right cortex	148	0.0004	3	24	13	4.29	Dorsal anterior cingulate
		Right cortex	463	0.0008	6	17	17	4.04	Premotor Cortex
		Left cortex	315	0.0002	-4	19	17	4.01	
		Left cortex	97	0.0008	-17	6	14	3.51	Insular cortex
		Left cortex	56	0.0002	1	10	15	3.36	Dorsal posterior cingulate
		Right cortex	90	0.0002	21	-5	5	3.02	
		Undefined	53	0.0004	-10	-2	8	2.88	Third ventricle
		Right cortex	23	0.0008	20	5	13	2.74	
		Total voxels	5754						

Clusters > 20 were included in analysis with threshold set at $P < 0.001$.

[1]Experimental Treatments include AR (T1-T3) and SR groups. T1, AR control; T2, PDF; T3, PDF + lecithin + cholesterol; T4, SR control.

[2]References the Saikali pig brain atlas which provides more detailed estimation of structures with in cortical regions (17).

[3]Missing cluster value is contiguous with voxel cluster listed immediately above, and represents 1 of 2 continuous voxel clusters with 2 different center voxels.

Table 4.3. Comparison of grey matter cluster volumes between piglets fed T1 vs. T2[1]

Tissue	Comparison	Anatomic Region	Cluster (voxels)	Cluster level (P-value)	x	y	z	Pseudo-t	Saikali ROI[2]
Gray Matter	T1 > T2	Right cortex	63	0.0062	13	-2	-7	3.44	Perihinal cortex
		Left cortex	29	0.0044	-20	-1	6	2.75	Inferior temporal gyrus
		Left cortex	38	0.0088	-19	7	6	2.61	Inferior temporal gyrus
		Left cortex	124	0.0078	-8	31	8	2.59	Dorsolateral prefrontal
		Total voxels	254						
	T2 > T1	Left cortex	572	0.0006	-15	2	12	5.04	
		Right cortex	822	0.0002	13	-2	17	4.09	Secondary visual cortex
		Right cortex	28	0.0074	15	3	10	3.83	
		Right cortex	293	0.0004	13	10	2	3.57	Amygdala
		Undefined	351	0.0096	1	15	1	3.17	
		Thalamus[3]		0.0090	1	3	2	2.3	Mediodorsal thalamic
		Undefined	26	0.0096	-10	11	1	2.33	
		Total voxels	2092						
White Matter	T1 > T2	Right cortex	124	0.0042	11	6	20	1.33	Somatosensory association
	T2 > T1	Left cortex	405	0.0006	-13	4	13	3.41	
		Left cortex	890	0.0018	-12	4	-10	3.39	
		Right cortex	340	0.0078	17	10	1	3.22	
		Right cortex	30	0.0072	5	10	17	3.05	Premotor cortex
		Left cortex	86	0.0076	-4	10	16	3.04	Dorsal posterior cingular
		Thalamus	227	0.0032	-8	-3	1	2.73	
		Thalamus	33	0.006	0	2	4	2.22	Third ventricle
		Undefined	33	0.005	10	-3	1	2.17	
		Right cortex	305	0.0076	16	-14	3	2.03	Crus 2 of the ansiform
		Left cortex	68	0.0094	-15	10	1	1.98	Amygdala
		Left cortex[3]		0.0084	-18	1	-6	1.77	Parahippocampal cortex
		Left cortex	101	0.0084	-11	-5	-6	1.7	
		Total voxels	2518						

Clusters > 20 were included in analysis with threshold set at $P < 0.01$.

[1]Experimental Treatments include T1, AR control; T2, PDF.

[2]References the Saikali pig brain atlas which provides more detailed estimation of structures with in cortical regions (17).

[3]Missing cluster value is contiguous with voxel cluster listed immediately above, and represents 1 of 2 continuous voxel clusters with 2 different center voxels.

Table 4.4. Comparison of grey matter cluster volumes between piglets fed T1 vs. T3[1]

Tissue	Comparison	Anatomic Region	Cluster (voxels)	Cluster level (P-value)	x	y	z	Pseudo-t	Saikali ROI[2]
Gray Matter	T1 > T3	Right cortex	20	0.0066	15	22	7	1.73	Insular cortex
		Medulla	37	0.0046	6	-17	-13	1.7	Facial nucleus
		Total voxels	57						
	T3 > T1	Left cortex	36	0.0056	-12	7	13	3.01	
		Right cortex	755	0.0032	16	1	17	2.78	
		Right cortex[3]		0.0098	19	-8	10	2.13	Superior temporal gyrus
		Thalamus	56	0.0090	-3	7	-2	1.36	Ventral anterior thalamic
		Cerebellum	241	0.0092	-11	-19	-1	1.35	
		Undefined	860	0.0092	5	-16	15	1.22	Parahippocampal cortex
		Left cortex	41	0.0080	-16	9	-3	0.89	Amygdala
		Total voxels	1989						
White Matter	T1 > T3	Pons	396	0.0004	-4	-6	-11	4.78	
		Pons	33	0.0078	4	-7	-11	3.54	
		Thalamus	33	0.0078	6	6	1	2.8	Ventral anterior thalamic
		Total voxels	462						
	T3 > T1	Left cortex	602	0.0012	-13	5	13	4.75	
		Left cortex	310	0.0016	-8	22	11	4.47	
		Right cortex	192	0.0084	17	24	10	3.02	Insular cortex
		Midbrain	131	0.0072	8	-1	-4	2.21	
		Right cortex	143	0.0096	18	10	2	1.96	
		Undefined	56	0.0078	-8	-4	1	1.93	Nucleus of the optic tract
		Right cortex	66	0.0098	17	-13	3	0.8	
		Total voxels	1500						

Clusters > 20 were included in analysis with threshold set at $P < 0.01$.

[1]Experimental Treatments include T1, AR control; T3, PDF + lecithin + cholesterol.

[2]References the Saikali pig brain atlas which provides more detailed estimation of structures with in cortical regions (17).

[3]Missing cluster value is contiguous with voxel cluster listed immediately above, and represents 1 of 2 continuous voxel clusters with 2 different center voxels.

Table 4.5. Comparison of grey matter cluster volumes between piglets fed T2 vs. T3[1]

Tissue	Comparison	Anatomic Region	Cluster (voxels)	Cluster level (P-value)	x	y	z	Pseudo-t	Saikali ROI[2]
Gray Matter	T2 > T3	Left cortex	49	0.007	-11	-8	-3	3.93	
	T3 > T2	Right cortex	242	0.0048	13	-3	-8	3.23	
		Left cortex	104	0.0082	-8	29	9	2.81	Dorsolateral prefrontal cortex
		Left cortex	24	0.0082	-19	1	-6	1.71	
		Total voxels	370						
White Matter	T2 > T3	Undefined	21	0.006	-5	-8	-8	2.19	
		Right cortex	23	0.0098	11	-16	6	1.5	Cerebellar lobule VI
		Undefined	47	0.0092	2	-15	-11	1.32	
		Undefined	31	0.0092	-7	10	-8	0.53	
		Total voxels	122						
	T3 > T2	Undefined	37	0.0094	-1	13	-9	0.23	Optic chiasm

Clusters > 20 were included in analysis with threshold set at $P < 0.01$.
[1]Experimental Treatments include T2, PDF; T3, PDF + lecithin + cholesterol.
[2] References the Saikali pig brain atlas which provides more detailed estimation of structures with in cortical regions (17).

Table 4.6. Absolute brain and region-specific volumes (mm^3) for artificially-reared (AR) and sow-reared (SR) piglets[1]

	Experimental Treatment[2]				*P*-value	
ROI[3]	**T1**	**T2**	**T3**	**SR Reference**	**Treatment**	**Sex**
n	9	10	10	10		
WB	58292 ± 3571.1[b]	59019 ± 3498.3[b]	58831± 3498.3[b]	73199 ± 3491.2[a]	<0.001	0.173
GM	29767 ± 967.9[b]	30151 ± 942.7[b]	29116 ± 942.7[b]	34585 ± 940.2[a]	<0.001	0.276
WM	11100 ± 603.0[b]	11235 ± 590.9[b]	11121 ± 590.9[b]	13999 ± 589.7[a]	<0.001	0.136
LC	16309 ± 450.1[b]	16483 ± 440.9[b]	16293 ± 440.9[b]	18504 ± 440.0[a]	<0.001	0.272
RC	15412 ± 406.1[b]	15602 ± 397.5[b]	15414 ± 397.5[b]	17588 ± 396.6[a]	<0.001	0.262
LHP	566.2 ± 15.90[b]	582.4 ± 15.48[b]	573.5 ± 15.48[b]	626.7 ± 15.44[a]	0.002	0.978
RHP	627.7 ± 20.10[b]	635.2 ± 19.57[b]	628.2 ± 19.57[b]	700.2 ± 19.51[a]	0.001	0.884
CA	116.5 ± 3.56	116.7 ± 3.39	116.5 ± 3.39	118.3 ± 3.37	0.975	0.354
CB	4570.0 ± 157.99[b]	4646.8 ± 155.05[b]	4525.1 ± 155.05[b]	5371.7 ± 154.77[a]	<0.001	0.948
CC	1041.0 ± 35.92[b]	1026.6 ± 35.04[b]	1030.6 ± 35.04[b]	1167.2 ± 34.95[a]	<0.001	0.204
CD	510.1 ± 18.04[b]	532.7 ± 17.64[ab]	521.6 ± 17.64[ab]	551.8 ± 17.60[a]	0.078	0.261
FV	137.5 ± 3.79[b]	141.0 ± 3.65[b]	134.0 ± 3.65[b]	151.4 ± 3.63[a]	0.003	0.460
HYP	523.9 ± 16.49[b]	531.3 ± 16.15[b]	531.8 ± 16.15[b]	601.8 ± 16.11[a]	<0.001	0.420
IC	4701.5 ± 195.10[b]	4753.6 ± 191.23[b]	4743.9 ± 191.23[b]	5641.1 ± 190.85[a]	<0.001	0.158
LV	1093.1 ± 34.92	1109.1 ± 33.34	1146.9 ± 33.34	1110.5 ± 33.18	0.685	0.928
MB	2960.0 ± 82.88[b]	2988.0 ± 81.26[b]	2975.0 ± 81.26[b]	3318.0 ± 81.11[a]	<0.001	0.588
MED	2377.4 ± 72.05[b]	2407.0 ± 70.68[b]	2348.8 ± 70.68[b]	2744.0 ± 70.55[a]	<0.001	0.503
OB	2966.4 ± 74.69[b]	2942.3 ± 72.57[b]	2938.9 ± 72.57[b]	3332.5 ± 72.36[a]	<0.001	0.278
PN	845.1 ± 18.78[b]	854.0 ± 18.49[b]	846.7 ± 18.49[b]	918.6 ± 18.46[a]	<0.001	0.539
PUT	1127.5 ± 37.45[b]	1138.0 ± 36.56[b]	1124.4 ± 36.56[b]	1301.0 ± 36.47[a]	<0.001	0.115
TH	2941.9 ± 78.81[b]	2996.3 ± 76.89[b]	2940.2 ± 76.89[b]	3339.6 ± 76.70[a]	<0.001	0.242
TV	199.5 ± 5.59	213.2 ± 5.39	207.6 ± 5.39	215.7 ± 5.37	0.072	0.644

[a-b]Means within a row lacking a common superscript letter differ ($P < 0.05$).

[1]Values are presented as means ± SEM.

[2]Experimental Treatments include AR (T1-T3) and SR groups. T1, AR control; T2, PDF; T3, PDF + lecithin + cholesterol; T4, SR control.

[3]Abbreviations: ROI, region of interest; WB, whole brain; GM, grey matter; WM, white matter; AC, average cortex; LC, left cortex; RC, right cortex; AHP, average hippocampi; LHP, left hippocampus; RHP, right hippocampus; CA, cerebral aqueduct; CB, cerebellum; CC, corpus callosum; CD, caudate; FV, fourth ventricle; HYP, hypothalamus; IC, internal capsule; LV, lateral ventricle; MB, midbrain; MED, medulla; OB, olfactory bulb; PN, pons; PUT, putamen; TH, thalamus; TV, third ventricle.

Table 4.7. Region-specific relative volumes for artificially-reared (AR) and sow-reared (SR) piglets[1]

	% TBV[2]					
	Experimental Treatment[3]				*P*-value	
ROI[4]	**T1**	**T2**	**T3**	**SR Reference**	**Treatment**	**Sex**
n	9	10	10	10		
GM	51.31 ± 1.919	51.75 ± 1.854	49.57 ± 1.854	48.25 ± 1.848	0.326	0.034
WM	19.09 ± 0.764	19.18 ± 0.733	18.94 ± 0.733	19.43 ± 0.730	0.957	0.013
LC	28.16 ± 0.985	28.26 ± 0.956	27.79 ± 0.956	25.80 ± 0.954	0.060	0.028
RC	26.63 ± 0.952	26.75 ± 0.925	26.30 ± 0.925	24.53 ± 0.922	0.089	0.031
LHP	0.98 ± 0.040[a]	1.00 ± 0.039[a]	0.98 ± 0.039[a]	0.87 ± 0.039[b]	0.011	0.240
RHP	1.09 ± 0.044[a]	1.09 ± 0.043[a]	1.07 ± 0.043[a]	0.97 ± 0.043[b]	0.020	0.128
CA	0.20 ± 0.011[a]	0.20 ± 0.011[a]	0.20 ± 0.011[a]	0.17 ± 0.011[b]	<0.001	0.647
CB	7.88 ± 0.262	7.96 ± 0.252	7.71 ± 0.252	7.47 ± 0.251	0.387	0.113
CC	1.80 ± 0.069	1.76 ± 0.067	1.76 ± 0.067	1.62 ± 0.067	0.077	0.019
CD	0.88 ± 0.040[a]	0.92 ± 0.039[a]	0.89 ± 0.039[a]	0.77 ± 0.039[b]	0.002	0.051
FV	0.24 ± 0.012[a]	0.24 ± 0.012[a]	0.23 ± 0.012[ab]	0.21 ± 0.012[b]	0.040	0.520
HYP	0.91 ± 0.039	0.91 ± 0.038	0.91 ± 0.038	0.84 ± 0.038	0.125	0.054
IC	8.10 ± 0.322	8.15 ± 0.310	8.09 ± 0.310	7.85 ± 0.309	0.823	0.026
LV	1.90 ± 0.115[a]	1.91 ± 0.112[a]	1.97 ± 0.112[a]	1.55 ± 0.112[b]	<0.001	0.407
MB	5.12 ± 0.188[a]	5.12 ± 0.183[a]	5.08 ± 0.183[a]	4.62 ± 0.183[b]	0.022	0.070
MED	4.10 ± 0.149	4.13 ± 0.144	4.01 ± 0.144	3.83 ± 0.143	0.271	0.076
OB	5.13 ± 0.176	5.04 ± 0.171	5.01 ± 0.171	4.65 ± 0.170	0.074	0.029
PN	1.46 ± 0.059[a]	1.47 ± 0.058[a]	1.45 ± 0.058[a]	1.29 ± 0.057[b]	0.010	0.116
PUT	1.95 ± 0.081	1.96 ± 0.078	1.92 ± 0.078	1.81 ± 0.078	0.305	0.023
TH	5.09 ± 0.206	5.15 ± 0.200	5.02 ± 0.200	4.66 ± 0.200	0.097	0.051
TV	0.35 ± 0.016[a]	0.37 ± 0.016[a]	0.36 ± 0.016[a]	0.30 ± 0.016[b]	<0.001	0.283

[a-b]Means within a row lacking a common superscript letter differ ($P < 0.05$).

[1]Values are presented as means ± SEM.

[2]Percent total brain volume (% TBV) was calculated by dividing ROI absolute volume by total brain absolute volume.

[3]Experimental Treatments include AR (T1-T3) and SR groups. T1, AR control; T2, PDF; T3, PDF + lecithin + cholesterol; T4, SR control.

[4]Abbreviations: ROI, region of interest; WB, whole brain; GM, grey matter; WM, white matter; AC, average cortex; LC, left cortex; RC, right cortex; AHP, average hippocampi; LHP, left hippocampus; RHP, right hippocampus; CA, cerebral aqueduct; CB, cerebellum; CC, corpus callosum; CD, caudate; FV, fourth ventricle; HYP, hypothalamus; IC, internal capsule; LV, lateral ventricle; MB, midbrain; MED, medulla; OB, olfactory bulb; PN, pons; PUT, putamen; TH, thalamus; TV, third ventricle.

Table 4.8. Average fractional anisotropy (FA) values for artificially-reared (AR) and sow-reared (SR) piglets[1]

	Experimental Treatment[2]				*P*-value	
Brain Region[3]	**T1**	**T2**	**T3**	**SR Reference**	**Treatment**	**Sex**
n	9	10	9	9		
WB	0.299 ± 0.002^{b}	0.301 ± 0.002^{b}	0.300 ± 0.002^{b}	0.308 ± 0.002^{a}	0.008	0.679
WM	0.299 ± 0.002^{b}	0.299 ± 0.002^{b}	0.299 ± 0.002^{b}	0.309 ± 0.002^{a}	0.001	0.451
CC	0.280 ± 0.006	0.274 ± 0.006	0.276 ± 0.006	0.285 ± 0.006	0.573	0.357
IC	0.383 ± 0.008^{b}	0.379 ± 0.007^{b}	0.390 ± 0.008^{ab}	0.412 ± 0.008^{a}	0.021	0.130
TH	0.311 ± 0.005	0.306 ± 0.005	0.313 ± 0.005	0.321 ± 0.005	0.216	0.739
LC	0.299 ± 0.005	0.292 ± 0.005	0.296 ± 0.005	0.311 ± 0.005	0.077	0.775
RC	0.298 ± 0.002^{b}	0.298 ± 0.002^{b}	0.299 ± 0.002^{b}	0.308 ± 0.002^{a}	0.008	0.958
LHP	0.271 ± 0.007	0.269 ± 0.007	0.270 ± 0.007	0.278 ± 0.007	0.759	0.120
RHP	0.264 ± 0.006	0.271 ± 0.006	0.281 ± 0.006	0.273 ± 0.006	0.279	0.077

[a-b]Means within a row lacking a common superscript letter differ ($P < 0.05$).

[1]Values are presented as means ± SEM.

[2]Experimental Treatments include AR (T1-T3) and SR groups. T1, AR control; T2, PDF; T3, PDF + lecithin + cholesterol; T4, SR control.

[3]Abbreviations: WB, whole brain; WM, white matter; CC, corpus callosum; IC, internal capsule; TH, thalamus; AHP, average hippocampi; LC, left cortex; RC, right cortex; LHP, left hippocampus; RHP, right hippocampus.

Table 4.9. Axial diffusivity (AD) values for artificially-reared (AR) and sow-reared (SR) piglets[1]

	Experimental Treatment[2]				*P*-value	
Brain Region[3]	**T1**	**T2**	**T3**	**SR Reference**	**Treatment**	**Sex**
n	9	10	9	9		
WB	1.38 ± 0.024[a]	1.38 ± 0.023[a]	1.38 ± 0.024[a]	1.34 ± 0.024[b]	0.007	0.295
WM	1.34 ± 0.023	1.33 ± 0.023	1.32 ± 0.023	1.31 ± 0.023	0.372	0.836
CC	1.65 ± 0.056	1.61 ± 0.053	1.59 ± 0.056	1.57 ± 0.056	0.754	0.892
IC	1.26 ± 0.011[ab]	1.24 ± 0.011[b]	1.26 ± 0.011[ab]	1.29 ± 0.011[a]	0.032	0.428
TH	1.24 ± 0.026	1.21 ± 0.025	1.22 ± 0.026	1.25 ± 0.026	0.563	0.241
LC	1.35 ± 0.034	1.39 ± 0.032	1.32 ± 0.033	1.32 ± 0.033	0.247	0.487
RC	1.33 ± 0.019	1.31 ± 0.019	1.32 ± 0.019	1.31 ± 0.019	0.328	0.771
LHP	1.46 ± 0.068	1.42 ± 0.066	1.43 ± 0.068	1.42 ± 0.068	0.905	0.893
RHP	1.39 ± 0.059	1.32 ± 0.057	1.38 ± 0.059	1.40 ± 0.059	0.749	0.028

[a-b]Means within a row lacking a common superscript letter differ ($P < 0.05$).

[1]Values are presented as means ± SEM × 1000.

[2]Experimental Treatments include AR (T1-T3) and SR groups. T1, AR control; T2, PDF; T3, PDF + lecithin + cholesterol; T4, SR control.

[3]Abbreviations: WB, whole brain; WM, white matter; CC, corpus callosum; IC, internal capsule; TH, thalamus; AHP, average hippocampi; LC, left cortex; RC, right cortex; LHP, left hippocampus; RHP, right hippocampus.

Table 4.10. Mean diffusivity (MD) values for artificially-reared (AR) and sow-reared (SR) piglets[1]

	Experimental Treatment[2]				*P*-value	
Brain Region[3]	**T1**	**T2**	**T3**	**SR Reference**	**Treatment**	**Sex**
n	9	10	9	9		
WB	1.05 ± 0.020[a]	1.05 ± 0.020[a]	1.04 ± 0.020[a]	1.01 ± 0.020[b]	0.007	0.367
WM	1.01 ± 0.020	1.01 ± 0.019	1.00 ± 0.020	0.98 ± 0.020	0.200	0.743
CC	1.27 ± 0.039	1.25 ± 0.037	1.23 ± 0.039	1.21 ± 0.039	0.698	0.866
IC	0.88 ± 0.006	0.87 ± 0.006	0.87 ± 0.006	0.87 ± 0.006	0.750	0.580
TH	0.92 ± 0.016	0.90 ± 0.015	0.91 ± 0.016	0.92 ± 0.016	0.696	0.231
LC	1.02 ± 0.030	1.07 ± 0.028	1.00 ± 0.030	0.99 ± 0.030	0.200	0.463
RC	1.01 ± 0.016	0.99 ± 0.016	1.00 ± 0.016	0.98 ± 0.016	0.134	0.819
LHP	1.13 ± 0.054	1.10 ± 0.053	1.10 ± 0.054	1.09 ± 0.054	0.876	0.663
RHP	1.07 ± 0.044	1.07 ± 0.042	1.06 ± 0.044	1.08 ± 0.044	0.704	0.049

[a-b]Means within a row lacking a common superscript letter differ ($P < 0.05$).

[1]Values are presented as means ± SEM × 1000.

[2]Experimental Treatments include AR (T1-T3) and SR groups. T1, AR control; T2, PDF; T3, PDF + lecithin + cholesterol; T4, SR control.

[3]Abbreviations: WB, whole brain; WM, white matter; CC, corpus callosum; IC, internal capsule; TH, thalamus; AHP, average hippocampi; LC, left cortex; RC, right cortex; LHP, left hippocampus; RHP, right hippocampus.

Table 4.11. Radial diffusivity (RD) values for artificially-reared (AR) and sow-reared (SR) piglets[1]

	Experimental Treatment[2]				*P*-value	
Brain Region[3]	**T1**	**T2**	**T3**	**SR Reference**	**Treatment**	**Sex**
n	9	10	9	9		
WB	0.88 ± 0.019[a]	0.88 ± 0.019[a]	0.88 ± 0.019[a]	0.84 ± 0.019[b]	0.008	0.421
WM	0.85 ± 0.018	0.85 ± 0.018	0.84 ± 0.018	0.82 ± 0.018	0.129	0.697
CC	1.08 ± 0.031	1.06 ± 0.029	1.05 ± 0.031	1.02 ± 0.031	0.638	0.661
IC	0.69 ± 0.007	0.68 ± 0.007	0.68 ± 0.007	0.66 ± 0.007	0.109	0.164
TH	0.77 ± 0.012	0.75 ± 0.011	0.75 ± 0.012	0.76 ± 0.012	0.701	0.268
LC	0.86 ± 0.028	0.91 ± 0.027	0.84 ± 0.028	0.82 ± 0.028	0.175	0.457
RC	0.85 ± 0.015	0.84 ± 0.015	0.84 ± 0.015	0.82 ± 0.015	0.070	0.849
LHP	0.96 ± 0.048	0.94 ± 0.047	0.94 ± 0.048	0.92 ± 0.048	0.833	0.403
RHP	0.91 ± 0.037	0.87 ± 0.035	0.90 ± 0.037	0.93 ± 0.037	0.665	0.080

[a-b]Means within a row lacking a common superscript letter differ ($P < 0.05$).

[1]Values are presented as means ± SEM × 1000.

[2]Experimental Treatments include AR (T1-T3) and SR groups. T1, AR control; T2, PDF; T3, PDF + lecithin + cholesterol; T4, SR control.

[3]Abbreviations: WB, whole brain; WM, white matter; CC, corpus callosum; IC, internal capsule; TH, thalamus; AHP, average hippocampi; LC, left cortex; RC, right cortex; LHP, left hippocampus; RHP, right hippocampus.

Table 4.12. Absolute hippocampal metabolite concentrations for artificially-reared (AR) and sow-reared (SR) piglets[1]

	Experimental Treatment[2]				*P*-value	
Metabolite[3]	**T1**	**T2**	**T3**	**SR Reference**	**Treatment**	**Sex**
n	5-9	5-10	4-9	5-8		
CR	2.97 ± 0.225	3.24 ± 0.246	3.87 ± 0.296	3.06 ± 0.277	0.142	0.236
CR + PCR	3.32 ± 0.159^{b}	3.40 ± 0.152^{b}	3.68 ± 0.150^{b}	4.23 ± 0.160^{a}	0.002	0.709
GLU	6.06 ± 0.492	5.49 ± 0.459	5.61 ± 0.492	5.30 ± 0.598	0.635	0.006
GLU+ GLN	10.21 ± 0.766	8.97 ± 0.698	9.25 ± 0.728	7.43 ± 0.775	0.074	0.018
GPC + PCH	1.25 ± 0.075^{bc}	1.14 ± 0.068^{c}	1.45 ± 0.071^{b}	1.66 ± 0.076^{a}	<0.001	0.216
GSH	2.04 ± 0.361	2.50 ± 0.377	2.47 ± 0.327	2.31 ± 0.377	0.796	0.531
INS	7.67 ± 0.414^{b}	7.70 ± 0.383^{b}	8.76 ± 0.397^{a}	9.54 ± 0.419^{a}	0.001	0.519
NAA	4.70 ± 0.272	4.51 ± 0.262	5.18 ± 0.259	5.00 ± 0.276	0.224	0.745
NAA + NAAG	5.12 ± 0.206^{bc}	4.91 ± 0.198^{c}	5.78 ± 0.196^{a}	5.69 ± 0.209^{ab}	0.008	0.693

[a-c]Means within a row lacking a common superscript letter differ ($P < 0.05$).

[1]Values are presented as means ± SEM. Single voxel MRS for metabolites met criteria for analysis (less than 20% standard deviation) and were detected in at least 4 pigs per treatment.

[2]Experimental Treatments include AR (T1-T3) and SR groups. T1, AR control; T2, PDF; T3, PDF + lecithin + cholesterol; T4, SR control.

[3]Abbreviations: CR, creatine; CR + PCR, creatine + phosphocreatine; GLU, glutamate; GLU+ GLN, glutamate + glutamine; GPC + PCH, glycerophosphocholine + phosphocholine; GSH, glutothione; INS, myo-inositol; NAA, N-acetylaspartate; NAA + NAAG, N-acetylaspartate + N-acetylaspartylglutamate.

Figures

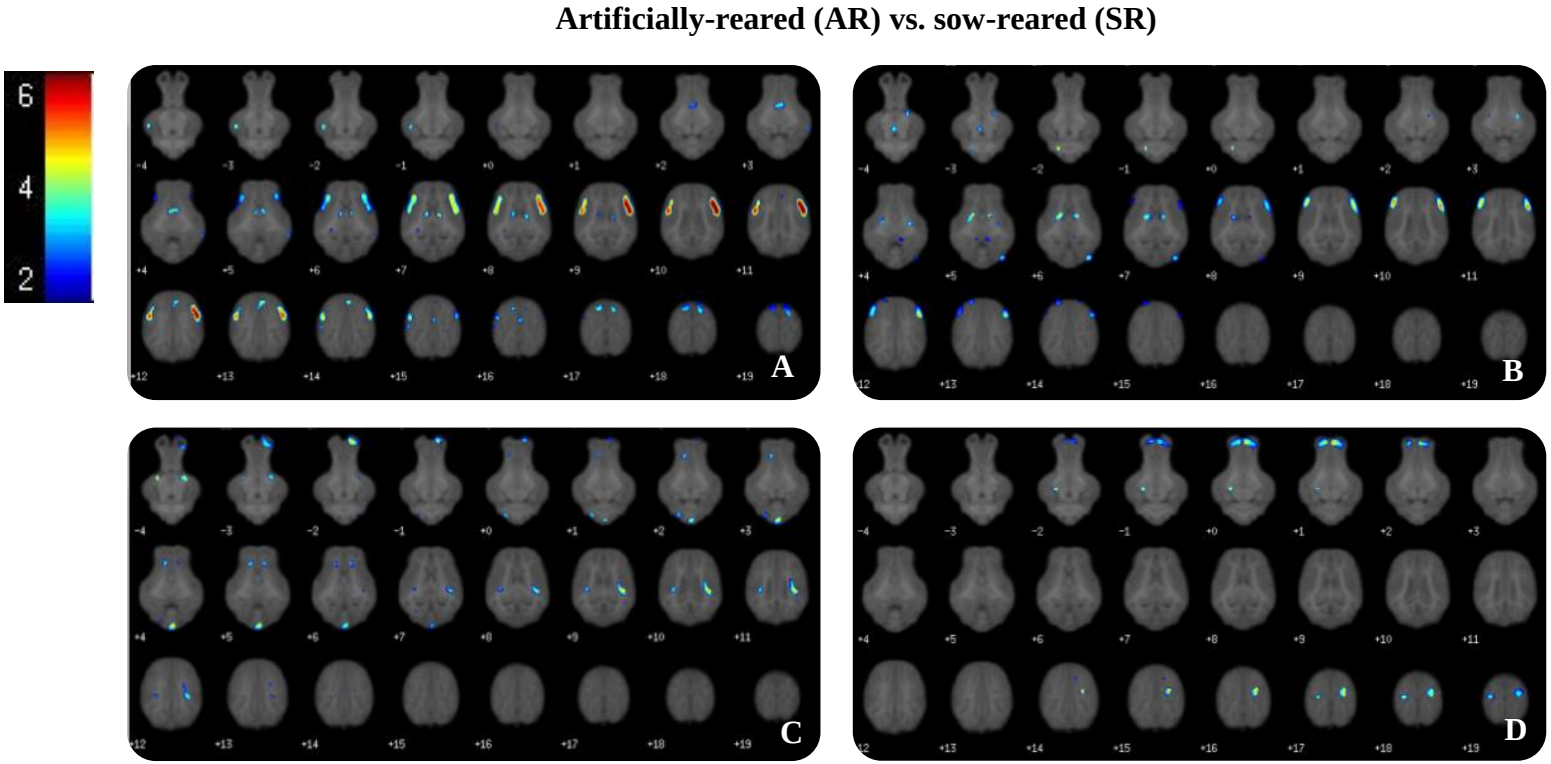

Figure 4.1. Voxel-based morphometric analysis of white and grey matter volume differences between the average of artificially-reared (AR) (T1, T2, and T3) and sow-reared (SR) piglets. Clusters less than 20 voxels and found on the edge of the brain were excluded from the analysis, and height threshold was set at P = 0.001. A) Voxel clusters in which AR > SR in grey matter volume; B) Voxel clusters in which AR > SR in white matters volume C) Voxel clusters in which SR > AR in grey matter volume; D) Voxel clusters in which SR > AR in white matter volume. Experimental Treatments include (n=9-10) T1, AR control; T2, PDF; T3, PDF + lecithin + cholesterol; T4, SR control.

T1 vs. T2

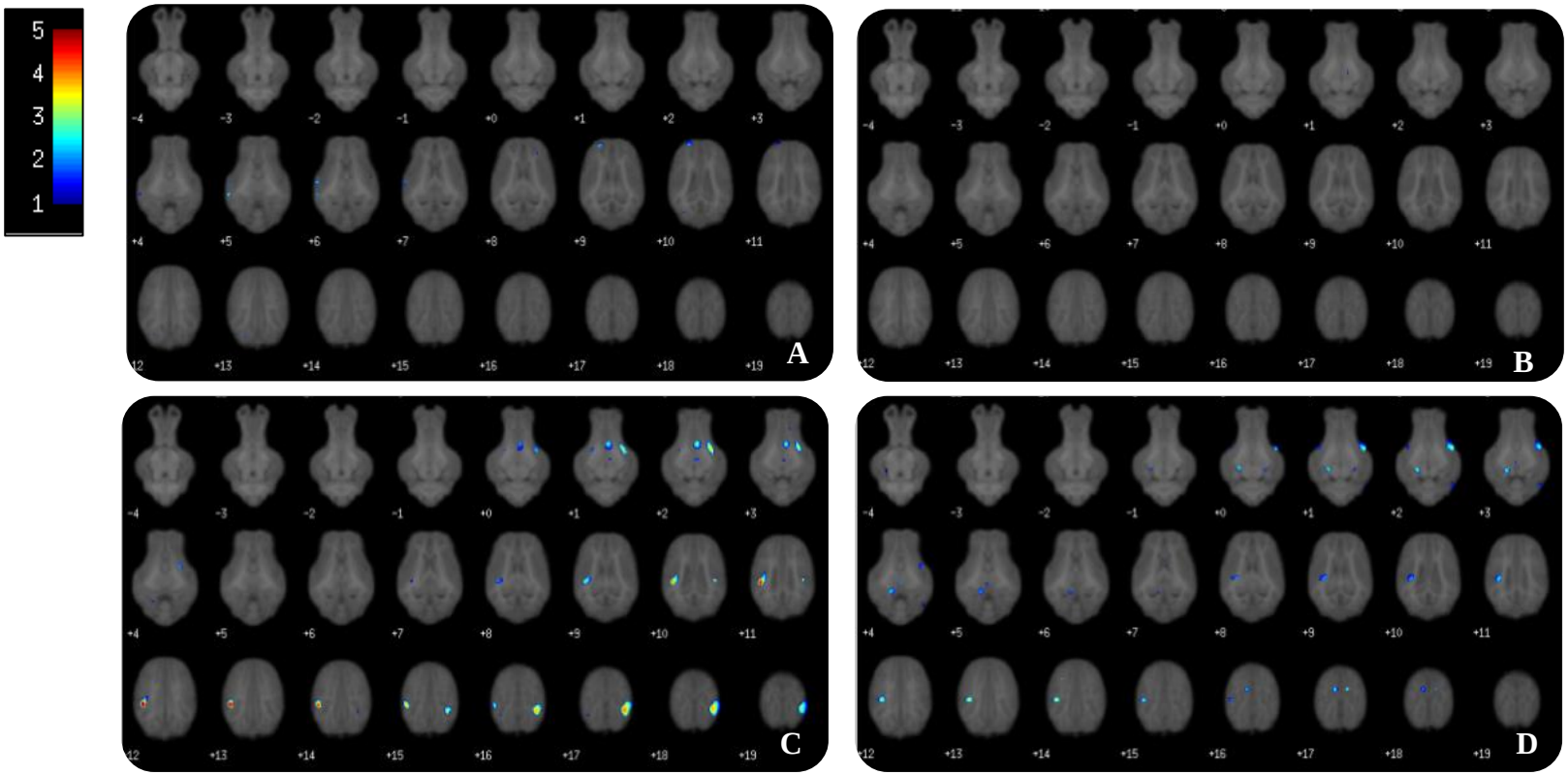

Figure 4.2. Voxel-based morphometric analysis of white and grey matter volume differences between treatments T1 and T2. Voxel clusters < 20 and found on the edge of the brain were removed. Height threshold was set at P = 0.01. A) Voxel clusters in which T1 > T2 in grey matter volume; B) Voxel clusters in which T1 > T2 in white matter volume; C) Voxel clusters in which T2 > T1 in grey matter volume; D) Voxel clusters in which T2 > T1 in white matter volume. Experimental Treatments include (n=9-10) T1, AR control; T2, PDF.

T1 vs. T3

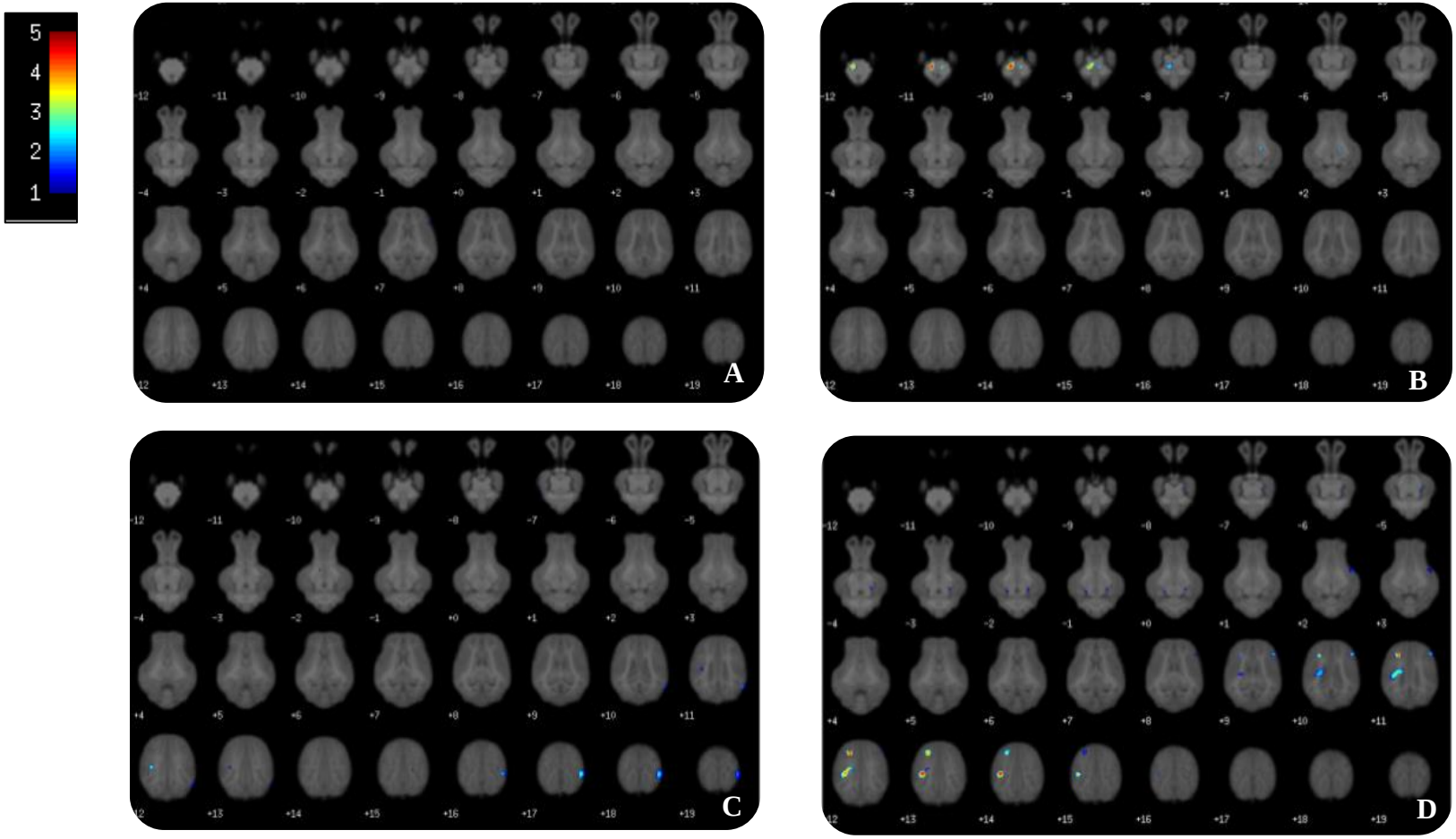

Figure 4.3. Voxel based morphometric analysis of white and grey matter volume differences between treatments T1and T3. Voxel clusters < 20 and found on the edge of the brain were removed. Height threshold was set at P = 0.01. A) Voxel clusters in which T1 > T3 in grey matter volume; B) Voxel clusters in which T1 > T3 in white matter volume; C) Voxel clusters in which T3 > T1 in grey matter volume; D) Voxel clusters in which T3 > T1 in white matter volume. Experimental Treatments include (n=9-10) T1, AR control; T3, PDF + lecithin + cholesterol.

T2 vs. T2

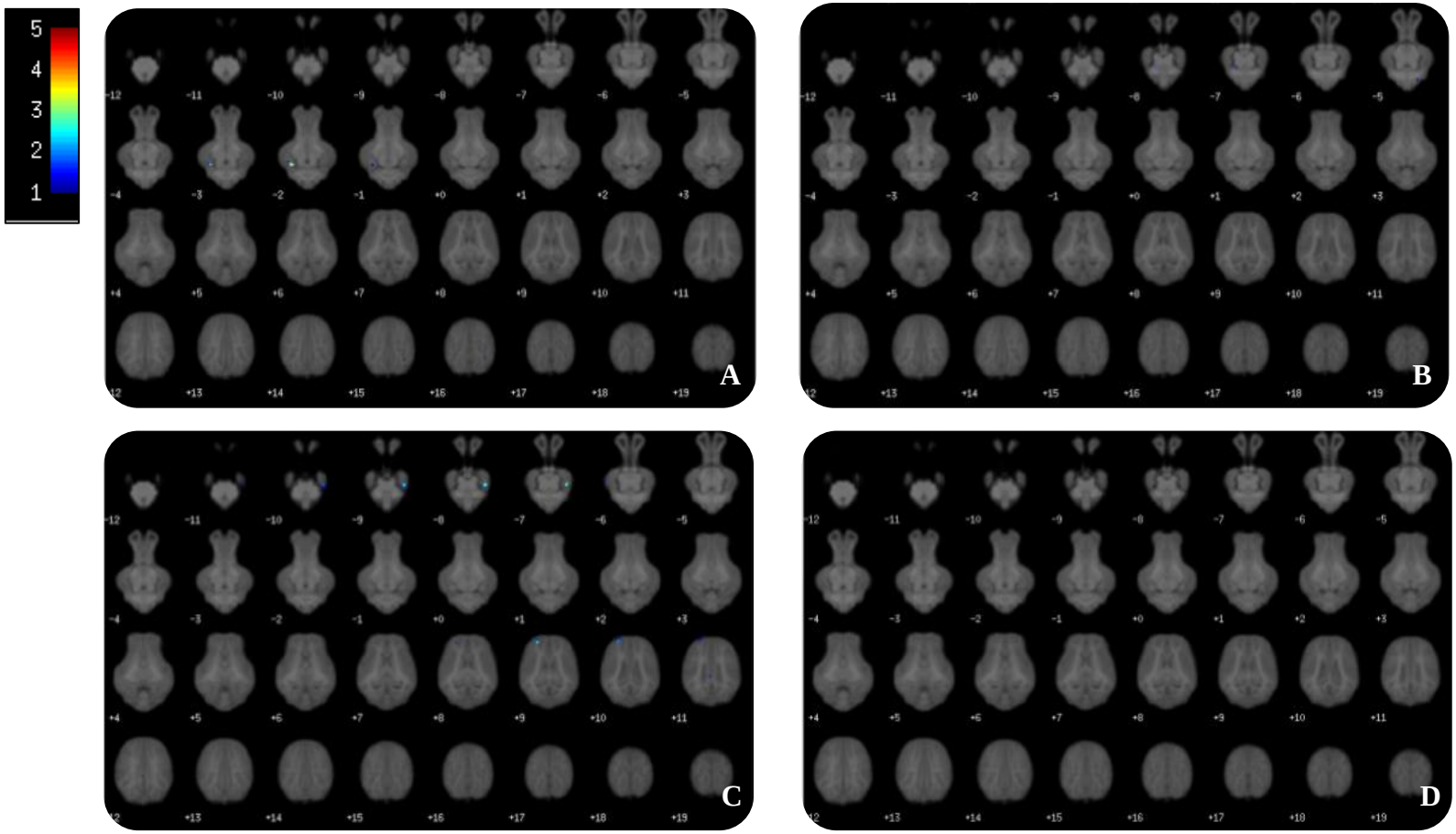

Figure 4.4. Voxel based morphometric analysis of white and grey matter volume differences between treatments T2 and T3. Voxel clusters < 20 and found on the edge of the brain were removed. Height threshold was set at P = 0.01. A) Voxel clusters in which T2 > T3 in grey matter volume; B) Voxel clusters in which T2 > T3 in white matter volume; C) Voxel clusters in which T3 > T2 in grey matter volume; D) Voxel clusters in which T3 > T2 in white matter volume. Experimental Treatments include (n=9-10) T2, PDF; T3, PDF + lecithin + cholesterol.

Chapter 5
SUMMARY AND SIGNIFICANCE

The world health organization recommends up to 6 months of exclusive breast feeding for infants, but there are often circumstances where combined breast and formula feeding or formula feeding alone would be provided to a child. Therefore, it is critical that scientific efforts focus on characterizing the complete composition of maternal milk, and thereby strive to mimic this matrix in infant formula. Of particular interest is docosahexaenoic acid (DHA), an n-3, long chain polyunsaturated fatty acid (LCPUFA) that is naturally enriched in breast milk. Although not considered an essential fatty acid, DHA has been shown to have potent effects in terms of supporting the developing infant brain (1,2). Particularly, DHA is incorporated heavily in glycerophospholipid moieties, which make the up the plasma membrane of neurons and may have notable influence on white matter maturation, signal conduction, and other important processes (3). As dietary triglycerides serves as the primary carrier for essential and non-essential fatty acids in milk, the characterization and supplementation of such fatty acids (FA) has been underway since the 1980s, yet incorporation of DHA into infant formula only began in 2002. Despite the addition of preformed DHA in infant formula, the breast fed infant's ability to absorb dietary lipid remain higher than that of the formula-fed infants (4). Greater absorption of LCPUFA, such as DHA, has often been hypothesized to enhanced brain development and cognitive outcomes in the breast fed infants as compared with their formula-fed counterparts (4,5). This leads us to believe that not only the composition, but the positional specificity with which dietary FA are incorporated into dietary triglycerides, as well as the addition of exogenous emulsifiers, can modulate the absorption, transport and incorporation of these FA into the brain.

Projects contained in this thesis were designed with the broad goal of minimizing the knowledge gap in our understanding of the lipid matrix present in formula and maternal milk. Using the piglet as a model for the human infant, our goal was to assess the impact of altering the lipid matrix found in infant formula on incorporation of DHA into the developing brain, and to characterize any subsequent alterations in neurodevelopment of the neonatal brain, as assessed by magnetic resonance imaging (MRI) techniques. We sought not only to elucidate the impact of varying lipid profiles on brain development in artificially-reared (AR) piglets, but to also generate a conspecific positive control using the sow-reared (SR) piglet. The sow-reared piglet served as an equivalent to the breast-fed infant, while the artificially-reared piglet was considered equivalent to the formula-fed infant. As such, AR piglets were fed 1 of 3 isocaloric dietary treatments as follows: T1, AR control formula; T2, T1 + 45% total dietary fat replaced with pre-digested fat (PDF); T3, T2 + 10% lecithin + 0.4% cholesterol. Sow-reared piglets (T4) remained with their respective mother and litter mates for the duration for the study. Growth performance and metabolic outcomes were also assessed to further understand the impact of modifying the dietary lipid matrix on lipid metabolism and transport of dietary fat into neural tissue. However, we will focus mainly on the correlations between MRI outcomes, serum lipid profiles, as well as quantification of DHA in hippocampal tissue and red blood cells (RBC).

Of the multiple MRI sequences employed to assess neurodevelopment, diffusion tensor imaging (DTI), which assesses brain microstructure, was of particular interest. Importantly, DTI measures the diffusion of free water molecules with the axonal tracts of the developing neuron. Fractional anisotropy (FA) values are calculated from these diffusion outcomes, and provide a numerical range of 0-1 to describe the degree water insulation within the neuronal axon. Fractional anisotropy values that are closer to 1 suggest anisotropic movement of water

molecules, and suggest greater white matter maturation and myelination of axonal tracts. Global assessment of white matter maturity, as assessed by FA values revealed higher FA values in the SR animals as compared with all AR animals, with no differences in whole-brain FA values being present between AR animals. These data suggest that the maternally-reared piglets possessed higher levels of myelination and white matter maturation as compared with the formula-fed piglets. However, region-specific assessment of white matter maturity in the internal capsule (IC) revealed that the addition of lecithin and cholesterol to the PDF system allowed for comparable levels of myelination to be present in T3 and SR piglets. This finding was quite exciting because the IC begins its maturation during gestation, and is therefore one of the primary regions to myelinate early in the postnatal period (6). Considering piglets underwent MRI procedures at a time of rapid brain development, we expected the neurodevelopmental trajectories observed in the IC to be prevalent to the whole-brain, or other regions of interest, as further maturation of the brain occurred.

The role of cholesterol in synthesis of myelin is well established (7). However, few studies have linked the influence of dietary or circulating cholesterol to outcomes related to brain development. In fact, the cerebrum is hypothesized to generate all necessary cholesterol *in situ* (8). However, the correlation between breast feeding and improved myelination of the neonatal brain is undeniable (9). Considering that breast milk is enriched in cholesterol, the literature does acknowledge the possibility of some transport of dietary cholesterol into the brain (10,11). Characterization of serum cholesterol revealed that SR animals possessed higher circulating serum cholesterol. However, the addition of cholesterol and lecithin to the PDF system elicited higher circulating cholesterol concentrations in T3 animals when compared with other artificially-reared treatment groups. These data suggest the PDF system allowed for more

efficacious absorption of dietary lipids, including cholesterol, into circulation. However, it may be the addition of lecithin plus cholesterol to the PDF system that allowed for greater incorporation of dietary cholesterol into the brain, and subsequent improvements in myelination observed in the IC. Verification of this hypothesis requires further analysis of brain cholesterol in the IC, as well as tracking of dietary cholesterol through all stages of digestion, absorption, circulation, and transport.

Quantification of DHA in the phospholipid (PL) and neutral lipid (NL) fractions of tissue revealed that DHA is preferentially incorporated in to the PL fraction. Piglets fed PDF-containing diets experienced a numerical increase in RBC DHA concentration as compared with control animals. However, the addition of lecithin and cholesterol resulted in a reduction of PL bound DHA in RBC to levels similar to that of the SR reference and control treatment. This reduction was unexpected, as RBC bound DHA is often associated with an increase in brain DHA in clinical trials (12). However, we observed that combination of lecithin and cholesterol with the PDF system allowed for greatest incorporation of DHA in hippocampal tissue, thereby achieving levels that were 2-fold higher than were detected in SR reference animals. We hypothesize that the reduction of RBC bound DHA in T3-fed piglets and subsequent increase in hippocampal DHA may be related. The addition of lecithin may be allowing for preferential binding of DHA to transporters (e.g., albumin), which allowed for more efficient transport of these FA beyond the blood brain endothelium. Although we were not able to assess DHA concentrations in the IC directly, the influence of DHA to maintain integrity of neurons and neural tissue has previously been established (1,13,14). Further analysis, including quantification of DHA within the IC of AR and SR animals, is necessary to associate the augmented accretion of DHA in the hippocampus with structural (i.e., maturational) benefits in the brain.

Overall, this project has generated insight into the impact of infant formula and maternal milk on postnatal brain development. As the full representation and replication of maternal milk in formula is far from complete, the data presented in this thesis provide a means to improve the bioavailability of one of the most conditionally essential FA found in infant formula. Our data suggest the addition of lecithin and cholesterol to the PDF system increases serum cholesterol, augments accretion of DHA in the phospholipid fraction of hippocampal tissue, and mediates greater myelination of axonal tracts in the IC as determined by FA values. To our knowledge, this study is also the first of its kind to characterize neurodevelopment of the SR piglet in its effort to establish a conspecific comparison for AR piglets. Suggested future directions for this research include a longer timeline where a subset of the animals are imaged and their tissue sampled at sexual maturity, as well as quantification of cholesterol and DHA in the same brain regions assessed for MRI outcomes. Finally, behavioral assessment to characterize the cognitive benefits of altering the lipid matrix of infant formula is also recommended to extend our findings. Ultimately, the pre-clinical evidence established in this study will pave the way for further clinical applications of these infant formulas, and suggested possibilities for nutrient based strategies to modulate the development of the central nervous system.

Literature Cited

1. Luchtman DW, Song C. Cognitive enhancement by omega-3 fatty acids from child-hood to old age: findings from animal and clinical studies. *Neuropharmacology*. Elsevier Ltd; 2013;64:550–65.

2. Innis SM. Dietary omega 3 fatty acids and the developing brain. *Brain Res*. 2008;1237:35–43.

3. Martinez M, Mougan I. Fatty Acid composition of human brain phospholipids during normal development. *J Neurochem*. 1998;71.

4. Morgan C, Davies L, Corcoran F, Stammers J, Colley J, Spencer SA, Hull D. Fatty acid balance studies in term infants fed formula milk containing long-chain polyunsaturated fatty acids. *Acta Paediatr*. 1998;87:136–42.

5. Kuratko CN, Barrett EC, Nelson EB, Salem N. The relationship of docosahexaenoic acid (DHA) with learning and behavior in healthy children: a review. *Nutrients*. 2013;5:2777–810.

6. Cowan FM. Magnetic resonance imaging of the normal infant brain: term to 2 years. MRI of Neonatal Brain. 1st ed. 2002.

7. Saher G, Brügger B, Lappe-Siefke C, Möbius W, Tozawa R, Wehr MC, Wieland F, Ishibashi S, Nave K-A. High cholesterol level is essential for myelin membrane growth. *Nat Neurosci*. 2005.

8. Jurevics H, Morell P. Cholesterol for synthesis of myelin is made locally, not imported into brain. *J Neurochem*. 1995;64:895–901.

9. Deoni SCL, Dean DC, Piryatinsky I, O'Muircheartaigh J, Waskiewicz N, Lehman K, Han M, Dirks H. Breastfeeding and early white matter development: A cross-sectional study. *Neuroimage*. Elsevier B.V.; 2013;82:77–86.

10. Dietschy JM, Turley SD. Cholesterol metabolism in the brain. *Curr Opin Lipidol*. 2001;12:105–12.

11. Dietschy JM, Turley SD. Thematic review series: brain Lipids. Cholesterol metabolism in the central nervous system during early development and in the mature animal. *J Lipid Res*. 2004;45:1375–97.

12. Uauy R, Hoffman DR, Mena P, Llanos A, Birch EE. Term infant studies of DHA and ARA supplementation on neurodevelopment: results of randomized controlled trials. *J Pediatr*. 2003;143:S17–25.

13. Innis SM. Dietary (n-3) fatty acids and brain development. *J Nutr*. 2007;137:855–9.

14. Carlson SE. Early determinants of development: a lipid perspective. *Am J Clin Nutr*. 2009;89:1523S–9S.